

Pre-Study for conversion of a gas turbine from liquid to gaseous fuel

by
Yueqian Zhang

*Thesis presented in partial fulfilment of the requirements for the degree
of Master of Engineering (Mechanical) in the Faculty of Engineering at
Stellenbosch University*



Supervisor: Prof. T.W. von Backström
Co-supervisor: Mr. R. Haines

March 2016

Declaration

By submitting this thesis electronically, I declare that the entirety of the work contained therein is my own, original work, that I am the sole author thereof (save to the extent explicitly otherwise stated), that reproduction and publication thereof by Stellenbosch University will not infringe any third party rights and that I have not previously in its entirety or in part submitted it for obtaining any qualification.

Date: March 2016

Copyright © 2016 Stellenbosch University

All rights reserved

Abstract

Gaseous fuel has shown its benefits as a promising alternative energy source. In an effort to research the effect of gaseous fuel on gas turbines, a Rover 1S/60 gas turbine was used for the fuel conversion study. This thesis aims to establish a test cell for small gas turbine testing and conduct engine tests with liquid and gaseous fuel. Therefore, a test setup was built from scratch including the fuel supply system, data acquisition system, electronic/mechanical remote control system and emergency shutdown system. The engine used for the test was disassembled and overhauled to study the detailed mechanics of each component so that further modification work could be carried out. After conducting several engine tests with kerosene, it was found the maximum continuous power output decreased from the factory rating of 45 kW to 28.4 kW and many of the measured data did not meet the requirements set by the Rover Company. Therefore, a new operation standard and procedure were set to meet the current condition of the engine. Finally, a newly designed gaseous fuel supply and control system were installed. With a modified gas injector, the engine was successfully converted to operate with LPG, and other gaseous fuels could in principle also be used for further tests.

Opsomming

Gas brandstowwe het verskeie voordele as 'n alternatiewe energie bron. Om die effek van die gebruik van 'n gas brandstof op 'n gasturbine te evalueer, is 'n Rover 1S/60 gas turbine ondersoek. Hierdie studie beoog om 'n toets vir klein gasturbine toetse te vestig en enjintoetse met vloeistof- en gas-brandstowwe uit te voer. Daar is dus 'n eksperimentele opstel gebou wat bestaan uit: 'n brandstof toevoer-, data-versameling- en elektroniese/meganiese afstandbeheer sisteem, so wel as 'n nood-afskakel sisteem. Die gasturbine wat gebruik is in die studie is uit mekaar gehaal, skoongemaak en elke komponent deeglik ondersoek, voordat die gasturbine weer aan mekaar gesit is en die nodige aanpassings gemaak is. Na talle enjintoetslopie met kerosen as verkose brandstof, is daar bevind dat die maksimum onderbroke krag uitset 28.4 kW is, laer as die fabriek-gespesifiseerde waarde van 45 kW. Daar is ook bevind dat verskeie van die gemete waardes nie aan die vereistes, soos gestel deur Rover Company, voldoen nie. Daarom is daar nuwe operasionele standaarde en prosedures in plek gestel om te pas by die huidige toestand van die enjin. Laastens is 'n nuwe gas brandstof toevoer- en beheer stelsel geïnstalleer. Met die aangepaste gas inlaat, is die enjin suksesvol omskep om op LPG te loop, en ander gas brandstowwe kan in toekomstige toetse gebruik word.

Acknowledgements

I would like to express my great appreciation to the following people for their efforts and help:

- My family and Xiaolin Fu for all their support during my stay in South Africa.
- My partner Ruben Luiten who helped me overcome countless problems for more than two years. I cannot tell how much I enjoyed working and laughing with you.
- My supervisors, Prof. T.W. von Backström and Mr. R. Haines for their continuous help and support during my study.
- Mr. Cobus Zietsman, Mr. Ferdi Zietsman, Mr. Julian Stanfliet and the rest of the workshop staff for their assistance, advice and jokes.
- My postgraduate colleagues for their inspirations to my project.

Contents

List of table	ix
List of figures	x
Nomenclature	xiv
1 Introduction	1
2 Literature review	3
2.1 Gas turbines in general	3
2.2 Gas turbine combustion systems	3
2.2.1 Diffuser	4
2.2.2 Combustor liner	5
2.2.3 Fuel preparation and injection	6
2.2.4 Flame and ignition stability	7
2.3 Gas turbine fuels	8
2.3.1 Composition of LPG	10
2.3.2 Density, boiling point and vaporization	11
2.3.3 Flammability limit	13
2.4 Compressible flow for gas injector	13
3 Gas turbine components	17
3.1 Rover gas turbine in general	17
3.2 Air intakes	20
3.3 Compressor	21
3.4 Combustion system	22
3.5 Turbine	24
3.6 Fuel supply system	25
3.6.1 Engine speed regulation	27
3.6.2 Temperature control unit	28
3.7 Starter motor system	28
3.8 Igniter unit	30
4 Test facility design and installation	32
4.1 Test cell overview	32
4.2 Engine and dynamometer	33
4.2.1 Test bench	33
4.2.2 Driveshaft, dynamometer flange and shaft guard	33

4.2.3	Dynamometer setup	35
4.3	Liquid fuel system.....	36
4.3.1	Fuel supply system.....	36
4.3.2	Liquid fuel control system	37
4.4	Exhaust gas system	39
4.5	Gaseous fuel system.....	40
4.5.1	Outdoor LPG supply system.....	40
4.5.2	LPG control system	41
4.5.3	Gas fuel injection	42
4.6	Sensors for measurement	44
4.6.1	Basic measuring sensors layout	44
4.6.2	Engine speed	44
4.6.3	Torque measurement.....	45
4.6.4	Temperature	46
4.6.5	Static pressure	47
4.6.6	Air mass flow rate.....	47
4.6.7	Liquid fuel flow rate	47
4.6.8	Gaseous fuel flow rate	48
4.7	Control cabinet.....	48
5	Testing and results.....	50
5.1	Testing layout overview	50
5.2	Engine starting and performance verification without load.....	50
5.2.1	Engine firing up	51
5.2.2	Performance verification without load	54
5.3	General engine test for setting new operation standard	57
5.3.1	Fuel pressure and engine speed	57
5.3.2	Exhaust gas temperature	61
5.3.3	Air mass flow rate and overall pressure ratio	63
5.3.4	Air inlet and main air casing temperature.....	69
5.3.5	Oil pressure and temperature	71
5.3.6	Needle valve control system test	71
5.3.7	New operation standards.....	71
5.4	Engine test under load.....	72
5.4.1	Engine power check.....	73

5.4.2	Fuel pressure and engine speed under 10 kW load.....	74
5.4.3	Fuel pressure and engine speed under various load.....	75
5.4.4	Engine power and torque curves.....	75
5.5	Engine test using LPG.....	76
5.5.1	Average EGT and engine speed.....	77
5.5.2	Air mass flow rate and overall air/fuel ratio	77
5.5.3	Main air casing temperature and lubrication system condition	78
6	Conclusions and recommendations	80
6.1	Conclusions	80
6.2	Recommendations	81
7	References	82
Appendix A: Standard operating procedure		85
A.1	Standard operating procedure with kerosene	85
A.1.1	Pre-testing procedure	85
A.1.2	Starting procedure	86
A.1.3	Operation standards	86
A.1.4	Load test procedure.....	87
A.1.5	Normal shutdown procedure.....	87
A.1.6	Emergency shutdown procedure.....	88
A.1.7	Post-testing procedure.....	88
A.2	Operating procedure with LPG of the initial test	88
A.2.1	Pre-testing procedure	88
A.2.2	Starting procedure	88
A.2.3	Operation standards for the initial test with 2 mm orifice restricted gas injector.....	89
A.2.4	Normal shutdown procedure.....	89
A.2.5	Emergency shutdown procedure.....	89
A.2.6	Post-testing procedure.....	89
Appendix B: Fuel sprayer test		90
B.1	Function test	91
B.1.1	Mode 1 test.....	91
B.1.2	Mode 2 test.....	92
B.1.3	Mode 3 test.....	93
B.1.4	Mode 4 test.....	94

B.1.5	Mode 5 test.....	94
B.2	Atomization test	95
Appendix C:	Gas injector design and test.....	96
C.1	Flow restriction design of the gas injector	96
C.1.1	Assumption for the design of restriction orifice	96
C.1.2	Restriction orifice test	97
C.2	Pre-mixing holes design	100
C.3	Gas injector caps design.....	102
Appendix D:	Experimental setup.....	103
D.1	Control interface.....	103
D.2	Calibration of the measurement sensors	104
D.3	Air inlet system	105
D.4	Lubrication system of the engine	106
D.5	Dynamometer	108
D.5.1	Dynamometer specifications.....	108
D.5.2	Dynamometer cooling water temperature.....	108
D.5.3	Time lag for the dynamometer.....	109
D.6	Gas flowmeter	111

List of tables

Table 2-1: Typical LHV of gaseous and liquid gas turbine fuels (Meher-Homji et al., 2010)	9
Table 2-2: Purity of Handigas from Afrox	11
Table 2-3: Some physical properties of propane, butane and commercial LPG (Afrox, 2007)	11
Table 2-4: Effect of pressure on flammability limits of LPG (vol. % in air at 100 °C) (Williams & Lom, 1982)	13
Table 3-1: Original Rover1S/60 specifications (Rover Gas Turbine Ltd., 1966)..	20
Table 3-2: Geometries of the compressor section (Quarta, 2012)	22
Table 3-3: Turbine section specification (Quarta, 2012)	25
Table 5-1: Variables for the air mass flow rate calculation (Prinsloo, 2008)	64
Table B-1: Different mode tests on studying fuel sprayer.....	91
Table B-2: Mode 1 test results with fully open shut-off valve and fully closed accumulator.....	92
Table B-3: Mode 2 test results with fully open shut-off valve and 180° rotated accumulator.....	93
Table B-4: Mode 3 test results with accumulator rotating different degrees.....	93
Table B-5: Mode 5 test results with shut-off valve at different position.....	94
Table B-6: Mode 5 test results with exact same condition as Mode 1	94
Table C-1: Test and theory results with orifice diameter of 1 mm	98
Table C-2: Test and theory results with orifice diameter of 2 mm	99
Table D-1: The detailed dimensions of the conical inlet	106
Table D-2: Dynamometer specifications (SCHENCK Pegasus GmbH, 1997) ...	108
Table D-3: Venturi flowmeter test results	113

List of figures

Figure 2-1: Schematic of gas turbine engine components and corresponding thermodynamic states (Massachusetts Institute of Technology, 2006)	3
Figure 2-2: The construction of an annular combustor from CF6-50 (Lefebvre & Ballal, 2010).....	4
Figure 2-3: Main components of a conventional combustor (Lefebvre, 1983)	5
Figure 2-4: Primary zone air flow patterns. (a) Opposed jet. (b) Swirl-stabilised. (c) Combined swirl and opposed jet. (Lefebvre, 1983).....	5
Figure 2-5: Atomizer designs. (a) Simplex pressure-swirl. (b) Dual-orifice (duple). (c) Airblast. (d) Premix-prevaporize. (Lefebvre & Ballal, 2010)	6
Figure 2-6: Typical combustion chamber stability curve and ignition curve (Lefebvre & Ballal, 2010).....	7
Figure 2-7: Effect of pressure on the stability characteristics of a 2.5 cm disk stabiliser (De Zubay, 1950)	8
Figure 2-8: Molecules of propane and two configuration of butane (Williams & Lom, 1982).....	10
Figure 2-9: Vapour pressure of LPG with different mixture (Alternate Energy System, Inc., 2006)	12
Figure 2-10: Gas flow through a converging nozzle with back pressure (Cengel & Cimbala, 2010).....	14
Figure 2-11: The effect of back pressure on the mass flow rate (Cengel & Cimbala, 2010).....	15
Figure 3-1: Section view of Rover 1S/60 gas turbine (Judge, 1960, p.15).....	18
Figure 3-2: Gas flow diagram of Rover 1S/60 gas turbine (Rover Gas Turbine Ltd., 1966)	19
Figure 3-3: Air intake system, designed by Prinsloo (2008)	21
Figure 3-4: The compressor and diffuser of the Rover 1S/60 gas turbine.....	21
Figure 3-5: The combustion chamber construction of the Rover 1S/60 gas turbine (Rover Gas Turbine Limited, 1966) (Judge, 1960, p.213)	23
Figure 3-6: Flame tube of the Rover 1S/60 gas turbine.....	23
Figure 3-7: The turbine disc (left) and the guide vanes (right) of the Rover 1S/60 gas turbine.....	24
Figure 3-8: The construction of the fuel pump body (Rover Gas Turbine Limited, 1972)	26

Figure 3-9: Inner view of the fuel pump	26
Figure 3-10: The fuel pump casing and temperature control unit	27
Figure 3-11: Original relay system for the starter motor	29
Figure 3-12: The original igniter unit	30
Figure 3-13: The construction of the spark plug (Lefebvre & Ballal, 2010).....	30
Figure 3-14: Igniter unit test on 24V	31
Figure 4-1: Test cell layout.....	32
Figure 4-2: Customised driveshaft (top left), dynamometer flange (top right) and shaft guard (bottom).....	34
Figure 4-3: Major part of Schenck LSG2000 dynamometer control unit (shown in the setting for engine testing).....	35
Figure 4-4: Water outlet of the dynamometer	36
Figure 4-5: Fuel tank with level indicator and valves, fuel filter and flow meter .	37
Figure 4-6: Boat throttle (left), fuel sprayer control (right, (Luiten, 2015)).....	38
Figure 4-7: Emergency switch and motor control (left), Needle valve control (right, (Luiten, 2015))	39
Figure 4-8: The exhaust gas system of the engine.....	40
Figure 4-9: LPG supply and outside emergency shut-off valve	41
Figure 4-10: Quick action shut-off valve (left), needle valve control device (right) and data acquisition system (bottom)	42
Figure 4-11: Fuel injector and exchangeable caps.....	43
Figure 4-12: Basic measuring instrument of the engine	44
Figure 4-13: Speed measurement by using a VR speed sensor (SCHENCK Pegasus GmbH, 1997)	45
Figure 4-14: Torque measurement and the load cell (SCHENCK Pegasus GmbH, 1997)	46
Figure 4-15: Main controller and separate modules of the PLC (Luiten, 2015) ...	48
Figure 4-16: Relays and 24 V DC supply.....	49
Figure 5-1: Relationship between the engine speed and the fuel pressure	52
Figure 5-2: Fuel pressure change along with time.....	53
Figure 5-3: Oil pressure and bearing air seal pressure along with time (Run_22)	55
Figure 5-4: The engine speed and the average EGT along with time (Run_22) ...	55
Figure 5-5: Oil temperature and compressor delivery air pressure along with time (Run_22).....	56

Figure 5-6: Fuel pressure and engine speed along with time	57
Figure 5-7: Fuel pressure and engine speed during the starting procedure	59
Figure 5-8: Relationship between the fuel pressure and the engine speed during the starting procedure.....	60
Figure 5-9: Average EGT along with time	61
Figure 5-10: Visible flame during the fuel rich starting procedure	62
Figure 5-11: Typical temperature reading from different measuring points of the exhaust gas (Run_22).....	63
Figure 5-12: Differential air pressure along with time, with and without LPF	65
Figure 5-13: Air mass flow rate along with time from three different tests	65
Figure 5-14: Air mass flow rate along with the engine speed	66
Figure 5-15: Overall pressure ration along with the engine speed	67
Figure 5-16: Overall pressure ratio during the whole engine tests	68
Figure 5-17: Relationship between the air mass flow rate and overall pressure ratio	69
Figure 5-18: Air inlet and main air casing temperature during a complete engine test.....	70
Figure 5-19: The output power and engine speed under different EGT	73
Figure 5-20: Fuel pressure and the engine speed during 10kW load test	74
Figure 5-21: Fuel pressure and the engine speed under different power output....	75
Figure 5-22: Engine power and torque curves.....	76
Figure 5-23: The average EGT and engine speed during LPG test	77
Figure 5-24: The air mass flow rate, the overall air fuel ratio and their trendlines along with time	78
Figure 5-25: Lubrication system condition and the main air casing temperature along with the time	79
Figure B-1: Construction of the early type sprayer	90
Figure B-2: Replacing O-ring and accumulator with position marker	92
Figure B-3: Fuel atomization at high (left) and low pressure condition (right) (processed photos)	95
Figure C-1: Required gaseous fuel flow rate during the starting procedure.....	96
Figure C-2: Test and theory results with orifice diameter of 1 mm	98
Figure C-3: Test and theory results with orifice diameter of 2 mm	99

Figure C-4: Gas flow diagram of the combustor (Rover Gas Turbine Limited, 1966)	100
Figure C-5: Construction of a Bunsen burner (Lim, 2015)	101
Figure C-6: Gas injector test on the separate combustor with low flow rate (left) and high flow rate (right)	102
Figure D-1: ETA user interface for kerosene test	103
Figure D-2: ETA user interface for LPG test	104
Figure D-3: Calibration of the speed sensor	105
Figure D-4: Calibration of the air differential pressure transducer	105
Figure D-5: Geometry of the conical inlet (BS 848, 1997)	106
Figure D-6: Oil spray holes on the engine main shaft	107
Figure D-7: Oil system connections	107
Figure D-8: Dynamometer cooling water temperature during the engine test	109
Figure D-9: Set and real driveshaft speed along with time in “Run_14”	110
Figure D-10: Set and real driveshaft speed along with time in “Run_8”	110
Figure D-11: Construction of the venturi flowmeter (unit in mm)	112

Nomenclature

A	Area	[m ²]
C_d	Discharge coefficient	[-]
c_p	Specific heat at constant pressure	[J/kgK]
c_v	Specific heat at constant volume	[J/kgK]
d	Diameter	[m]
g	Gravitational acceleration	[m/s ²]
I	Current	[A]
k	Specific heat ratio	[-]
L	Length	[m]
\dot{m}	Mass flow rate	[kg/s]
P	Absolute pressure	[Pa]
R	Gas constant	[-]
Re	Reynolds number	[-]
T	Temperature	[K] or [°C]
t	Time	[s]
U	Voltage	[V]
u	Internal energy	[J/kg]
\dot{V}	Volumetric flow rate	[m ³ /s]
v	Velocity	[m/s]
W	Width	[m]

Greek symbols

β	Diameter ratio	[-]
---------	----------------	-----

η	Efficiency	[%]
θ	Angle	[°]
μ	Dynamic viscosity	[kg/m*s]
ρ	Density	[kg/m ³]
τ	Torque	[N*m]
ω	Rotational speed	[RPM]

Superscripts

*	Sonic speed condition
---	-----------------------

Subscripts

a	Dry air
n	Normal
D	Upstream
d	Throat
m	Mean

Acronyms

AC	Alternate Current
APU	Auxiliary Power Unit
bhp	Brake Horsepower
CAD	Computer Aided Design
CAE	Cape Advanced Engineering
CNG	Compressed Natural Gas

CV	Constant Velocity
DC	Direct Current
EGT	Exhaust Gas Temperature
ETA	Engine Test Automation
GmbH	Gesellschaft mit beschränkter Haftung
H.P.	High Pressure
LEL	Lower Explosive Limit
LFL	Lower Flammable Limit
LHV	Lower Heating Value
L.P.	Low Pressure
LPG	Liquefied Petroleum Gas
PLC	Programmable Logic Controller
RPM	Revolution Per Minute
UEL	Upper Explosive Limit
UFL	Upper Flammable Limit
VR	Variable Reluctance

1 Introduction

Gaseous fuel has shown its benefits as a promising alternative energy source compared to fossil fuels. It is cleaner than petrol, diesel and kerosene since it is composed of simple hydro-carbon compounds. Many countries are rich in flammable gas resources such as Russia, Iran, Qatar, Mozambique and Tanzania. Gaseous fuel is an increasingly popular option for gas turbines, especially for heavy duty industrial gas turbines due to its lower environmental impact. The conversion of diesel or kerosene gas turbines to gaseous fuel has been performed with the intention of reducing harmful emissions. Current research on micro turbine generators used in hybrid electric vehicles and other applications are also looking for a cleaner energy resource like liquefied petroleum gas (LPG), compressed natural gas (CNG) or biogas instead of liquid fossil fuels.

In an effort to research alternative fuel, Cape Advanced Engineering (CAE) and Stellenbosch University are sourcing a project involving the conversion of a gas turbine running on kerosene to operate with LPG to simulate biogas. CAE acquired a Rover gas turbine from Stellenbosch University in the 1990s and it was used in investigating the use of a gas turbine for biogas power generation. In the course of the study, the engine was overhauled but never fully converted to run with gaseous fuel due to the time constraints.

To study the impact of the fuel conversion for gas turbines, a small gas turbine test cell has been established to test an original Rover 1S/60 gas turbine. The design of the testing facility includes two sections: hardware (test bench, dynamometer and other mechanical connections) and electronics (control system and sensors). After completing the setup, the engine will be tested with its original fuel injection system. For LPG to be considered as an alternative fuel for the gas turbine, it is necessary to modify and redesign several components, including the gas injection system, ignition system, control system and mixture formation.

In this project, the engine has been overhauled and then tested under different running conditions. During the engine overhaul, some special tools were designed and made to disassemble the engine components. All necessary data was recorded and could be used for further processing. Fault finding was carried out to eliminate all errors from the results. A new performance standard and operating procedure for this particular engine have been established. The fuel supply of the engine was successfully converted to the gaseous fuel and the test facility is capable of running on various gaseous fuels. Finally, the engine has been successfully tested with LPG and the results indicate that the engine can be operated with gaseous fuel.

The objective of this thesis aims to build a test cell for the Rover 1S/60 gas turbine and obtain performance data from the engine tests including operating with liquid and gaseous fuels. Because the gas turbine had not been started for

years, some necessary repair work and performance verification tests were required. The details of the objectives are listed below:

- Build a test facility for the Rover 1S/60 gas turbine with the engine to be controlled from a control room.
- Set up the programmable logic controller (PLC) and control programs including Engine Test Automation (ETA) for the engine testing.
- Design and implement the remote control system, data acquisition system and emergency shutdown system.
- Disassemble the engine and record the detailed mechanism of each component. Overhaul the engine and replace all worn seal and replaceable parts.
- Conduct several engine tests running on kerosene and record all necessary performance data for further analysis.
- Design and build up a permanent gaseous fuel supply system for engine testing.
- Design and modify the engine to operate on gaseous fuel.
- Carry out engine tests while running on gaseous fuel and record all necessary data.

2 Literature review

2.1 Gas turbines in general

Gas turbine cycles can be divided into two groups: shaft power cycles and propulsion cycles (Cohen et al., 1987). The gas turbine engine related to the current project operates on the shaft power cycle and its construction is relatively simple. The Brayton cycle is shown in Figure 2-1.

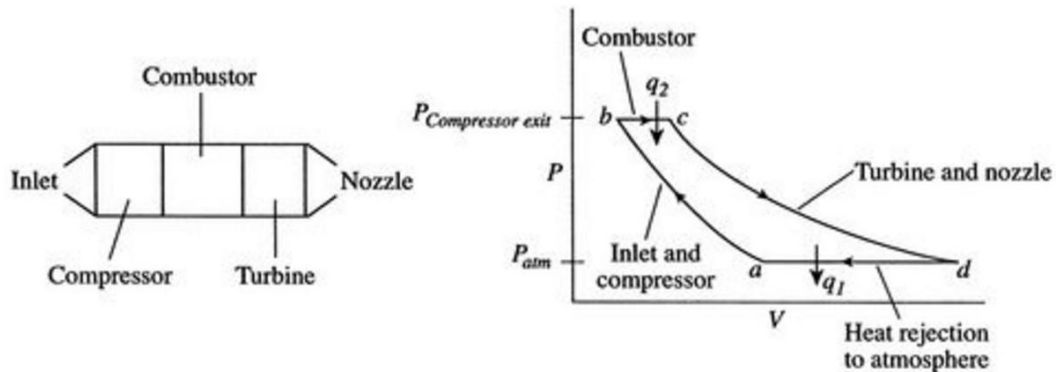


Figure 2-1: Schematic of gas turbine engine components and corresponding thermodynamic states (Massachusetts Institute of Technology, 2006)

The ideal Brayton cycle starts with an isentropic process (a-b) that involves compression of the inlet air. This process increases the air pressure and reduces its specific volume. It is followed by an isobaric constant pressure energy addition process (b-c). Normally this process is related to fuel combustion in the combustion chamber of the gas turbine. The heated gas then expands isentropically through the turbine and some energy is used to drive the shaft for power output purpose (c-d). Finally, the gas cools down at constant pressure in the atmosphere as an isobaric process (d-a). Gas turbine thermodynamic efficiency is related to the compression, combustion and gas expansion process (Olivier, 2015). In this project, a further study of the combustion process will be carried out.

2.2 Gas turbine combustion systems

The combustion process plays a key role in gas turbine engines because in most conditions it is the only way of energy addition in the gas turbine thermodynamic cycle. Unlike other components of a gas turbine, the combustion system is not so amenable to theoretical analysis. The design of a combustor can only be improved by using test results (Cohen et al., 1987). According to Lefebvre & Ballal (2010), the basic requirements of all combustors are listed below:

- High-combustion efficiency
- Reliable and smooth ignition

- Wide stability limits
- Low pressure loss
- An optimised outlet temperature distribution to maximise the life of the turbine blades and nozzle guide vanes
- Low emissions
- Optimised size and shape
- Easy maintenance
- Durability
- Multifuel capability

To achieve these requirements, it needs contributions from all three main components of the combustor: diffuser, combustor liner (flame tube) and fuel injector (Lefebvre, 1983). There are several types of combustors used in modern gas turbines, including tubular, tuboannular and annular type. Even though the choice of a particular combustor type is determined mostly by the overall engine design, the constructions of these combustors are very similar (Lefebvre & Ballal, 2010). The basic construction of a combustion system is shown in the figure below.

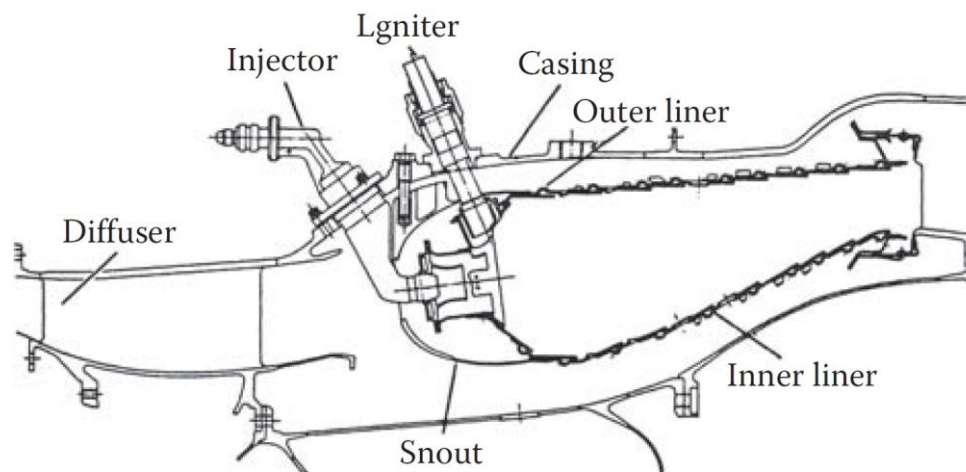


Figure 2-2: The construction of an annular combustor from CF6-50 (Lefebvre & Ballal, 2010)

2.2.1 Diffuser

The diffuser is located at the entrance of the combustor. A good design of a diffuser can minimise the pressure drop across the combustor (Lefebvre & Ballal, 2010). In the current project, the objective is to convert the fuel supply from kerosene to LPG with minimum modification and cost. Therefore, the first choice is to keep the diffuser unmodified. After successful tests with LPG, an improved diffuser design can be implemented if necessary.

2.2.2 Combustor liner

The combustor liner consists of three zones: the primary zone, the intermediate zone and the dilution zone. The figure below illustrates the details of a combustor.

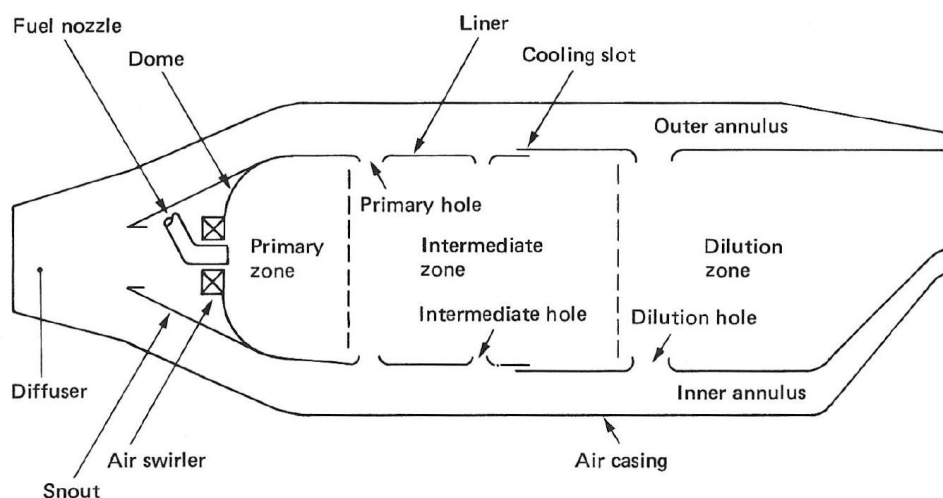


Figure 2-3: Main components of a conventional combustor (Lefebvre, 1983)

Compressed air is fed from left to right through the diffuser and some of the air passes through the combustor liner. Holes and cooling slots can be found on the wall of the combustor liner. These passages introduce the unheated air from outside the combustor liner into the combustion zone.

The major function of the primary zone is to create sufficient turbulence for complete combustion. Fuel and air mixes in the primary zone and starts to combust under the designated airflow pattern. The figure below illustrates typical airflow patterns in the primary zone.

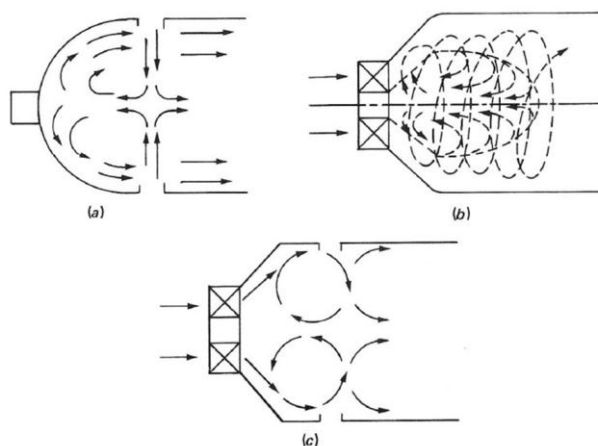


Figure 2-4: Primary zone air flow patterns. (a) Opposed jet. (b) Swirl-stabilised. (c) Combined swirl and opposed jet. (Lefebvre, 1983)

In Figure 2-4, the swirling air from the passage of the fuel injector (b,c) and the air from the primary-zone holes (a,c) create the flow recirculation in the primary zone. The recirculation not only provides the continuous ignition for the unburnt air-fuel mixture, but also extends the residence time of the combustion gas. The extended residence time will lead to complete combustion in the primary zone instead of combustion gas being carried away by the airflow.

The primary zone is followed by the intermediate zone. In early designs, the intermediate zone was mostly used to provide an extended combustion zone for unburned hydrocarbons, including CO from dissociation of CO₂ under high temperature. It also served for burning any imperfectly mixed fuel-rich gas mixtures. However, by around 1970, the traditional form of intermediate zone had largely disappeared (Lefebvre & Ballal, 2010). In modern combustor designs, the boundary between intermediate zone and dilution zone becomes unclear.

The dilution zone is located at the end of the combustor liner. It consumes a large amount of the total combustor airflow, usually between 20 % and 40 %. The major function of the dilution zone is to cool down the hot combustion gas so that the temperature meets the requirement for entering the turbine section (Lefebvre, 1983).

2.2.3 Fuel preparation and injection

The liquid fuel requires good atomization and evaporation for clean and complete combustion. The fuel is atomized into a great number of liquid drops with a dramatic increase in surface area. Therefore, the prepared fuel is able to produce sufficient vapour for ignition and combustion (Lefebvre, 1983). The figure below illustrates four common atomizers for liquid fuel.

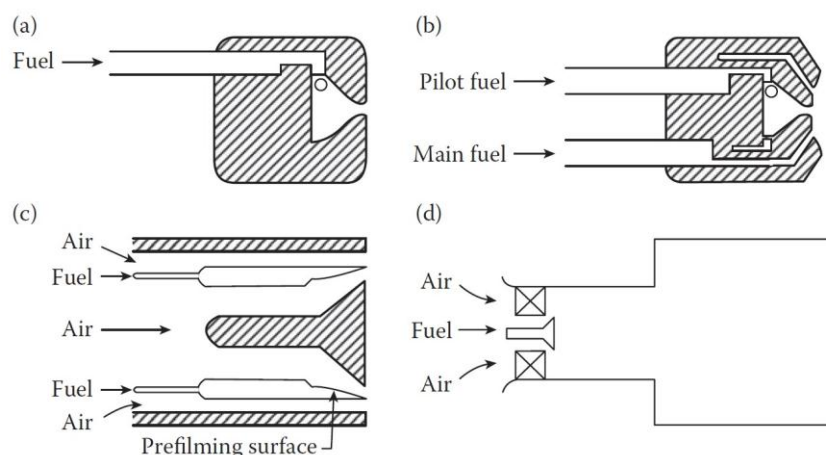


Figure 2-5: Atomizer designs. (a) Simplex pressure-swirl. (b) Dual-orifice (duplex). (c) Airblast. (d) Premix-prevaporize. (Lefebvre & Ballal, 2010)

Gas injection, especially for those fuels with high calorific value such as LPG, presents few problems from a combustion viewpoint (Lefebvre, 1983). However, by considering the whole system including flow control and data acquisition system, the gas injection may still encounter some problems during practical modification of the engine.

2.2.4 Flame and ignition stability

The gas turbine combustor is designed to operate within a wide range of air/fuel mixtures under all conditions. However, if the fuel mixture was too rich or too lean, the combustion flame would be extinguished. Flame stability can be obtained by adjusting the fuel flow rate until it reaches “lean blowout” and “rich extinction” points under constant air pressure and temperature. Normally, the flame stability range will decrease when the air mass flow rate increases. The combustion stability curve is shown in the Figure 2-6.

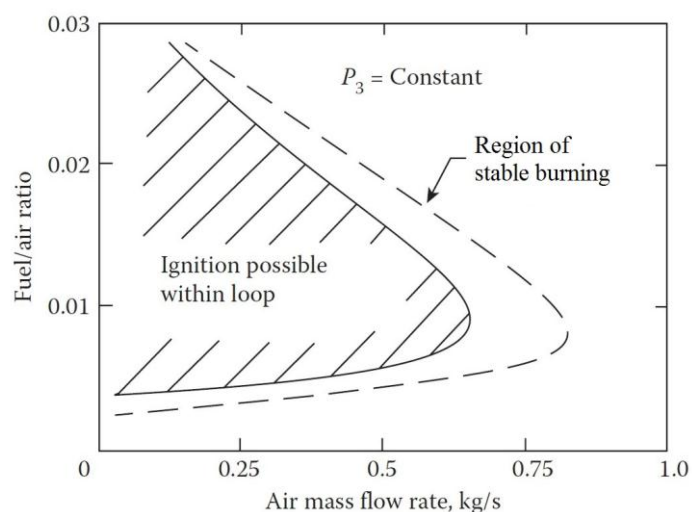


Figure 2-6: Typical combustion chamber stability curve and ignition curve (Lefebvre & Ballal, 2010)

Flame stability is also related to the combustor pressure and an increased pressure can improve the stability. The experimental data in Figure 2-7 was obtained by De Zubay (1950) and it shows clear evidence of this behaviour.

Increased pressure can expand the stability curve significantly. It improves the blowout velocity and the stability under fuel rich condition, but has little effect on the weak-extinction limit. This fact will benefit the combustion stability when a higher compression ratio is reached, normally found at higher engine speed.

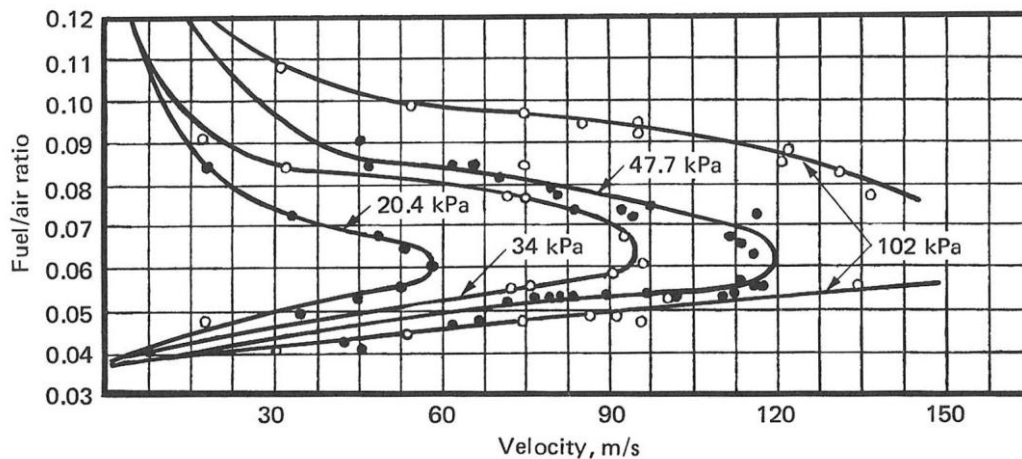


Figure 2-7: Effect of pressure on the stability characteristics of a 2.5 cm disk stabiliser (De Zubay, 1950)

Spark ignition is widely used in modern gas turbine engines. It can efficiently convert electric power into heat that is concentrated in a small volume (Lefebvre, 1983). Compared to the ignition by a hot surface, spark ignition does not require a warm-up time and it consumes less electric power. The ignition curve is determined by experiment and a typical combustor ignition curve is shown in Figure 2-6. The ignition curve is very similar to the flame stability curve but has a slightly smaller range. Theoretically, ignition will not be a problem when starting the engine with a proper procedure.

2.3 Gas turbine fuels

Fuel supply and control is one of the most important factors when operating gas turbines. The quality and quantity of the fuel supply play key roles in gas turbine combustion, and thus determine the power output and engine speed. A modern gas turbine is capable of operating with a wide range of different fuels, including gaseous, liquid, and even powdered solid fuels (Lefebvre, 1983).

In general, gas turbine fuels can be divided into two categories: gaseous and liquid. According to (Meher-Homji et al., 2010), the following fuels are regarded as common gaseous fuels for gas turbines:

- Natural gas / Compressed Natural Gas (CNG)
- Liquefied Petroleum Gas (LPG)
- Refinery gas
- Coal gas
- Biogas
- Coke oven gas

Liquid fuels include:

- No. 2 diesel
- Kerosene
- Naphtha
- Ethanol and methanol
- Crude oil and heavy residual-grade oils

The table below shows the typical lower heat value (LHV) of some gas turbine fuels. The unit Nm^3 stands for normal cubic meter and it refers to normal temperature and pressure conditions of 20 °C and 1 atm.

Table 2-1: Typical LHV of gaseous and liquid gas turbine fuels (Meher-Homji et al., 2010)

Gaseous fuel	Typical LHV [MJ/Nm ³]	Liquid fuel	Typical LHV [MJ/kg]
Natural gas	39 (Svenskt Gastekniskt Center AB, 2012)	No.2 diesel	42.7
LPG typical blend	104.8	Kerosene	43
Refinery gas	Varies	Naphtha	44.2
Biogas	23 (Svenskt Gastekniskt Center AB, 2012)	Ethanol	26.8
Coke oven gas	11.8	Crude oil	41.2

Kerosene and diesel are widely used in the gas turbine industry because they have relatively high energy contents and this property makes them economical to transport and store. For gas turbine application, the common unit for gaseous fuel is MJ/m³ instead of MJ/kg. This is because the unit in volume is more convenient compared to mass especially for storage, transportation and for use in combustion calculations. For some gaseous fuels, liquefaction under light pressure at ambient temperature makes them ideal fuel sources for both industrial and domestic applications. In fact, this is one of the most important reasons why LPG is being widely used in domestic markets (Williams & Lom, 1982). Seeking renewable energy sources is becoming a tendency, however, LPG is still widely used worldwide.

Some important technical properties of LPG will be discussed in the following section. Because the purpose of the test is to convert the gas turbine fuel system from liquid to gaseous, the properties of gaseous phase of LPG will be highlighted and only vital properties of liquid phase will be discussed.

2.3.1 Composition of LPG

Liquefied petroleum gas can derive from the condensate fraction of natural gas as well as from the light end fractions of crude oil (Williams & Lom, 1982). The specific production method of LPG depends on many factors including resource availability, regulations of the country, etc. However, regardless of the production methods, the composition of all types of LPG are similar. They consist of several hydrocarbons that contain three to four carbon atoms in each molecule. The main components of LPG are saturated hydrocarbons, which are known as propane and butane. Propane constitutes the most of LPG and its molecule contains three carbon atoms and eight hydrogen atoms. Another main component of LPG is butane and it is a saturated hydrocarbon with four carbon atoms. Two possible configurations of the butane molecule can be found in LPG: normal butane or n-butane has a straight C-chain and iso-butane has a branched C-chain. Such different configurations have no significant effect on their physical properties (Afrox, 2007). The figure below shows the molecule of propane and two configurations of butane.

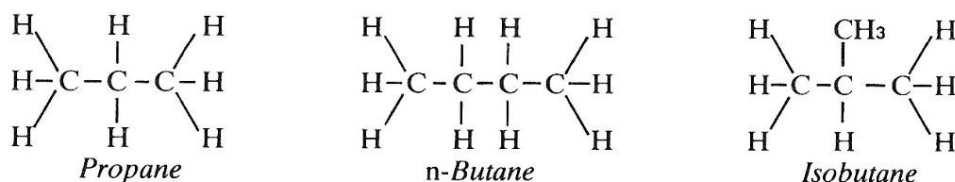


Figure 2-8: Molecules of propane and two configuration of butane (Williams & Lom, 1982)

Except for saturated hydrocarbons, LPG also contains small amounts of unsaturated C_3 and C_4 hydrocarbons. These unsaturated hydrocarbons mainly consist of propylene (C_3H_6) and butylene (C_4H_8). All these unsaturated hydrocarbons can be removed by purification if required. However, the molar concentrations of these chemicals are relatively small, and they will not change the physical, and combustion properties of LPG significantly, so their existence is acceptable.

The composition of LPG may vary for different countries. Typically, the composition of LPG from South African suppliers is 60 % propane with 40% n-butane. The purity requirement of domestic LPG (commercial name: Handigas) from Afrox is shown in the table on next page.

Table 2-2: Purity of Handigas from Afrox

Gas	Purity
Propane	> 60 %
Butane	< 40 %
Other hydrocarbons	< 2 %

2.3.2 Density, boiling point and vaporization

The table below shows some physical properties of commercial LPG, propane and butane at different conditions.

Table 2-3: Some physical properties of propane, butane and commercial LPG
(Afox, 2007)

		Propane		Butane		Handigas (Commercial mix)	
		Liquid	Vapour	Liquid	Vapour	Liquid	Vapour
Density at vapour pressure	[15 °C, kg/m ³]	507.6	15.9	574	5.9	536	-
Density at atm. pressure	[0 °C, kg/m ³]	-	2.03	-	2.67	-	-
	[15 °C, kg/m ³]	-	1.9	-	2.54	-	2.1
Boiling point at atm. pressure	[°C]	-42.045		-0.5		-42.045, -0.5	
Mass ratio of gas to air at atm. pressure	[15 °C]	1.52:1		2.01:1		1.716:1	
Vapour pressure (absolute)	[20 °C, kPa]	710		110		500	
Latent heat of vaporisation	[15 °C, kJ/kg]	20.43		21.27		20.77	

As shown in the table, the densities of all three gases are greater than that of air. This factor is vital when considering safety requirements, because LPG can flow along the ground and fill up the lowest levels of pipeline or electric wire ducts. It can remain there for a long period, and this could result in an explosion and a fire accident. Therefore floor level ventilation is essential for any LPG work that has a possibility of leakage. One unit (volume) of liquid LPG will vaporise to form approximate 280 units (by volume) of vapour at atmospheric pressure at a temperature of 15 °C. This property indicates that liquid leakage is much more

dangerous than gas leakage due to the significant volume of flammable gas mixture that could be formed by only a small volume of liquid.

The boiling points of propane and butane are significantly different at atmospheric pressure conditions. This physical property is independent and does not change when mixing propane and butane. When the valve of a LPG cylinder is opened, the in-cylinder pressure drops and the liquid phase LPG starts to vaporise. The vaporization requires heat to continue this process and the temperature of the cylinder and surrounding air will decrease. The latent heat of vaporisation is relatively high and cannot be disregarded. If LPG is drawn from a cylinder at a high rate, the in-cylinder temperature will drop to below -0.5°C , which is the boiling point of butane. Since the temperature is lower than the boiling point of butane, the butane remains in liquid phase in the cylinder while the propane continues to vaporise. To avoid this, it is possible to use a hot water bath to stabilise the cylinder temperature, or use pure propane instead of LPG. Compared to LPG, pure propane is suitable for any case that requires a high draw-off rate or where ambient temperature is low.

Another one of the most important physical properties of LPG is the vapour pressure. The figure below illustrates the vapour pressure of some typical commercial LPG mixtures.

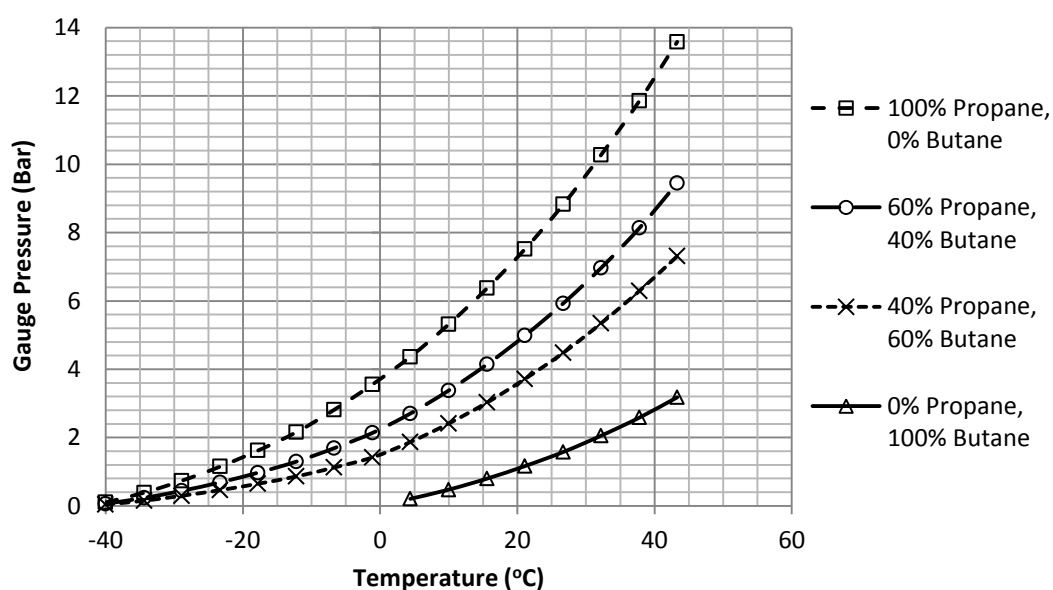


Figure 2-9: Vapour pressure of LPG with different mixture (Alternate Energy System, Inc., 2006)

At any specific temperature, propane has the highest vapour pressure while butane has the lowest, and mixtures of propane and butane have intermediate values. The pressure can be regulated by an appropriate regulator. However, using a regulator could restrict the maximum flow rate of the gas. If high flow rate and high

pressure are required, one can either increase the cylinder temperature or use pure propane instead of LPG.

2.3.3 Flammability limit

The flammability limit is an important factor to determine if the fuel mixture is combustible. This property is normally expressed as volume percentage at 25°C and atmospheric pressure. The flammability limit consists of two values: lower flammable limit (LFL) and upper flammable limit (UFL). Many references use the term flammability limits and explosive limits that consist of lower explosive limit (LEL) and upper explosive limit (UEL) interchangeably (Ensola AG, 2007).

Combustion and ignition are impossible when the fuel is too rich or too lean in its mixture. Any mixture with fuel concentration higher than UFL or lower than LFL cannot be ignited and therefore is not combustible. The flammability limit can be affected by pressure, temperature and concentration of the oxidizer (Williams & Lom, 1982). The table below shows the flammability limits under various pressure conditions.

**Table 2-4: Effect of pressure on flammability limits of LPG (vol. % in air at 100 °C)
(Williams & Lom, 1982)**

Pressure atm	Propane		Butane	
	LFL	UFL	LFL	UFL
1	2.0	9.0	1.8	7.5
5	2.0	10.0	1.8	8.5
6.4	2.0	11.4	-	-
10.0	2.0	15.0	-	-
18.0	-	-	1.8	16.5
19.3	1.9	23.4	-	-

In Table 2-4, a higher pressure has almost no effect on the LFL but expands the UFL obviously. This also explains the different stability characteristics under various pressures in Figure 2-7.

2.4 Compressible flow for gas injector

To design a gas injector with specific maximum flow rate, the concepts of compressible flow and isentropic flow are used. With such a design, the gas injector will automatically restrict the gas flow to prevent the engine from over speed.

When the gas flow speed reaches the speed of sound ($Ma = 1$), the properties of the gas are called critical properties. The critical properties are very important to determine the speed condition of the flow. Using superscript (*) for critical values

and k for the specific heat ratio, the relations between the critical properties and stagnation properties (P_0, T_0) are listed below:

$$\frac{T^*}{T_0} = \frac{2}{k+1} \quad (2-1)$$

$$\frac{P^*}{P_0} = \left(\frac{2}{k+1} \right)^{k/(k-1)} \quad (2-2)$$

where

$$\frac{T_0}{T} = \left(\frac{k+1}{2} \right) \text{Ma}^2 \quad (2-3)$$

$$\frac{P_0}{P} = \left[1 + \left(\frac{k-1}{2} \right) \text{Ma}^2 \right]^{k/(k-1)} \quad (2-4)$$

Assume gas flow through a converging nozzle with back pressure as shown in figure below. The whole flow process can be treated as isentropic and when the inlet flow speed is negligible, the inlet (reservoir) pressure and temperature are equal to stagnation pressure and temperature (P_0, T_0).

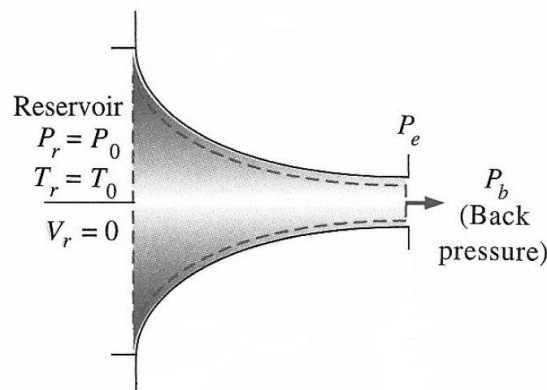


Figure 2-10: Gas flow through a converging nozzle with back pressure (Cengel & Cimbala, 2010)

The mass flow rate of gas flowing through an orifice plate or converging nozzle reaches its maximum only when the velocity of the gas is equal to the sonic speed at the throat, and then the flow is called “choked flow”. When the flow is choked $P_b \leq P^*$ and with constant reservoir condition, further decreasing the back pressure cannot improve the gas mass flow rate. P^* is called the critical pressure, it is also the pressure that is required to accelerate the gas to the speed of sound at the exit throat. (Cengel & Cimbala, 2010)

To understand the influence of back pressure on mass flow rate, consider 5 different conditions of back pressure along with their mass flow rates. By

increasing the back pressure from zero, the mass flow stays at maximum until $P_b = P^*$. During this process, the gas flow is always choked. Then with further increasing back pressure, the mass flow rate starts to drop until $P_b = P_0$ where there is no differential pressure to drive gas flow. It is very clear to see at what condition the maximum mass flow rate can be achieved. It is also useful to determine if the flow is choked by analysing the pressure difference across the throat.

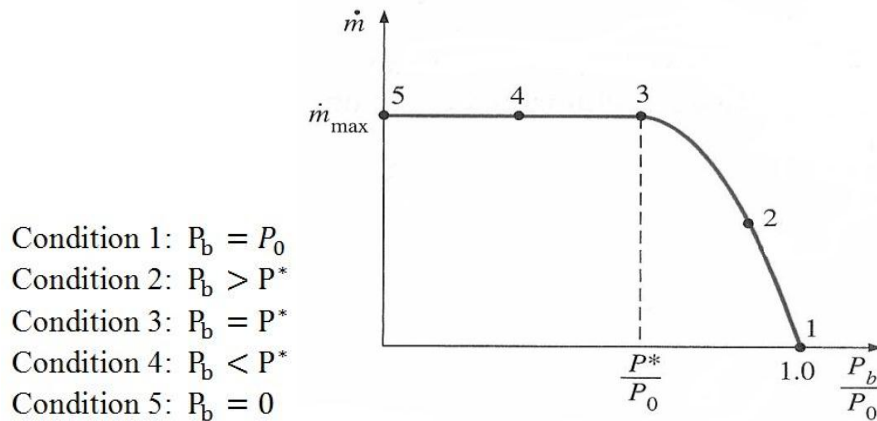


Figure 2-11: The effect of back pressure on the mass flow rate (Cengel & Cimbala, 2010)

To estimate the mass flow rate, assume the gas flow is steady and one-dimensional, according to the definition of mass flow rate:

$$\dot{m} = \rho AV = \left(\frac{P}{RT}\right) A (\text{Ma} \sqrt{kRT}) = P A \text{Ma} \sqrt{\frac{k}{RT}} \quad (2-5)$$

Substituting equation (2-3) and (2-4) into the above equation, it becomes:

$$\dot{m} = \frac{A \text{Ma} P_0 \sqrt{k/(RT_0)}}{[1 + (k-1) \text{Ma}^2/2]^{(k+1)/[2(k-1)]}} \quad (2-6)$$

Equation (2-6) for mass flow rate under a certain circumstance is a function of P_0, T_0, Ma and A , where A is the flow area. That means with fixed nozzle geometry and constant flow, the mass flow rate only depends on the stagnation properties of the fluid. Note that this equation is valid at any position along the converging nozzle.

As discussed above, the gas mass flow rate only reaches its maximum when the velocity of flow is sonic speed at throat. For a specified flow, the mass flow rate is constant at any section of the nozzle. It is easy to calculate the maximum mass

flow rate at the throat because $Ma = 1$, setting A^* for throat area. Therefore, equation (2-6) becomes:

$$\dot{m}_{\max} = A^* P_0 \sqrt{\frac{k}{RT_0}} \left(\frac{2}{k+1} \right)^{(k+1)/[2(k-1)]} \quad (2-7)$$

For the choked flow of ideal gas, the maximum mass flow rate depends on the throat area, stagnation pressure and stagnation temperature.

In the real situation of engine testing, the stagnation pressure is mainly determined by the LPG vapour pressure, which depends on in-cylinder temperature. However, the nozzle throat area can be designed precisely to restrict the maximum mass flow rate for LPG. The detailed design can be found in Appendix C.

During engine testing, the engine requires large amounts of LPG and it can be expected that the in-cylinder temperature will drop significantly. Such a temperature drop will decrease the vapour pressure, thus decreasing the gas mass flow rate and affect the combustion. Therefore, an engine speed drop should be expected during the continuous LPG test. For the initial test, it is acceptable and it is suggested to regulate the pressure for the further modification work.

3 Gas turbine components

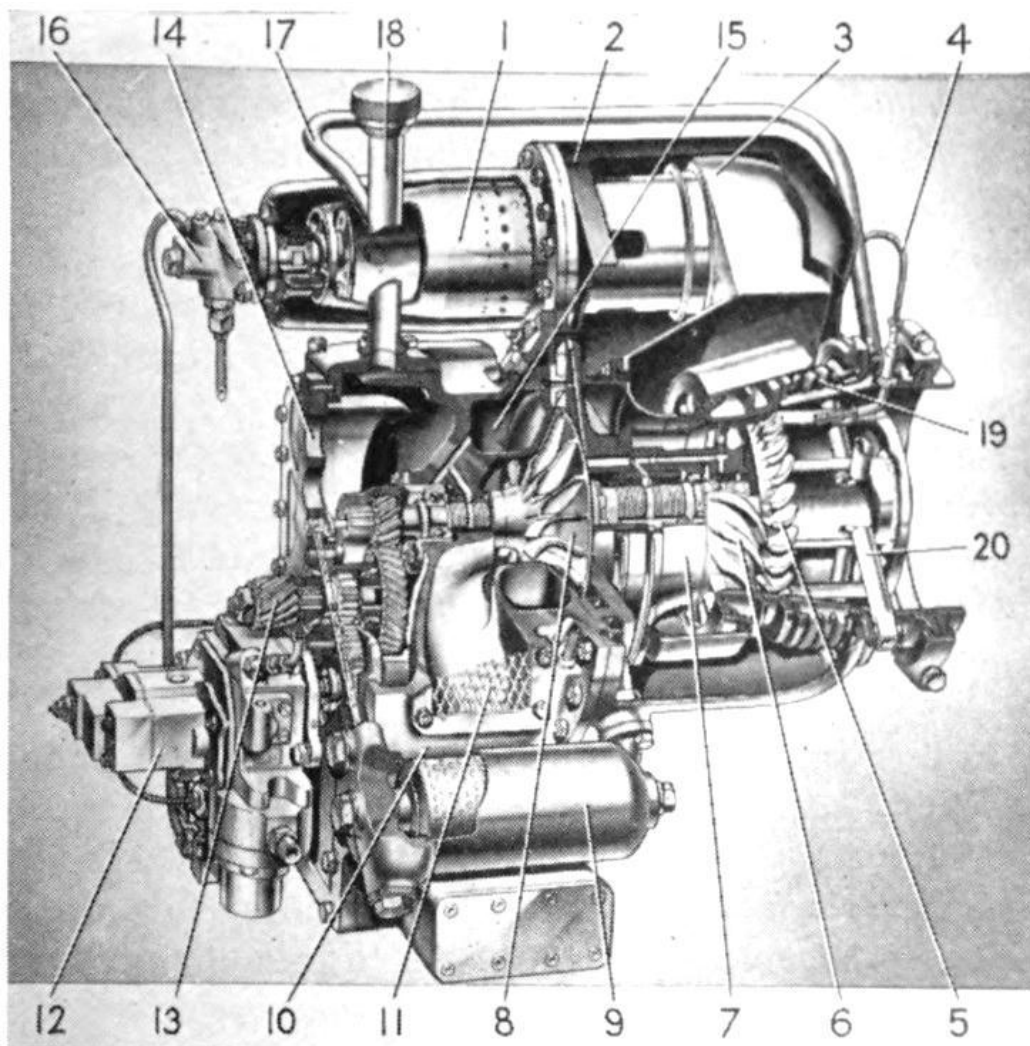
The gas turbine used in this project will be discussed in this chapter. Due to the age of the gas turbine engine, there was very little useful information available. Tests have been conducted to explore the mechanism and performance of each component and it is important to understand all the details so that further modification work can be carried out efficiently.

3.1 Rover gas turbine in general

The engine used in this project is a 1S/60 Rover gas turbine developed in the 1950's. The Rover Company became famous for producing the Rover gas turbine car, including JET1 with 100 brake horsepower (bhp) that, when first demonstrated to the public in March 1950 achieved a speed of 137 km/h (Hunt, 2011). After the first demonstration of the gas turbine car to the public, it developed a variant of a gas turbine engine that served for automotive use. These vehicles were lightweight and had slightly better acceleration performance compared to common production vehicles powered by piston engines. These advantages were due to the high power to weight ratio that is the natural benefit of gas turbine engines. The third model of the Rover gas turbine vehicle was named the Rover T3. It used a Rover 1S/60 single shaft gas turbine as power unit where was mounted on the rear chassis of the car (Judge, 1960).

Although the gas turbine vehicles showed the technological achievement of the Rover Company and the flexibility of gas turbines to the public, these models finally quit the market due to their extremely high fuel consumption. Some modified engines however found their way as auxiliary power unit for aircraft, or water pumps due to their light weight and small size. Between 1955 and 1965, the Rover Company manufactured more than 250 small gas turbines for educational establishments and these gas turbines were sent to 40 countries worldwide (Hunt, 2011).

The construction of the engine is relatively simple. It consists of five main components: a fuel control unit, a combustion chamber, a compressor housing (main air casing), an auxiliaries mounting plate and rotating parts (compressor, turbine and shaft). Each type of Rover 1S/60 gas turbine may vary slightly but the major construction is similar. Figure 3-1 shows the section view of a basic 1S/60 gas turbine.



- | | |
|------------------------------------|--------------------------------|
| 1 Reverse flow combustion chamber. | 11 Air intake. |
| 2 Compressed air receiver. | 12 Fuel control unit. |
| 3 Volute casing. | 13 Output pinion. |
| 4 Temperature control capillary. | 14 Auxiliaries mounting plate. |
| 5 Turbine. | 15 Low pressure air reservoir. |
| 6 Turbine nozzle. | 16 Spill-flow burner. |
| 7 Heat shield. | 17 Breather pipe. |
| 8 Impeller. | 18 Oil filter. |
| 9 Pressure oil filter. | 19 Expansion bellows. |
| 10 Compressor housing. | 20 Struts with cooling ducts. |

Figure 3-1: Section view of Rover 1S/60 gas turbine (Judge, 1960, p.15)

When the engine runs, the air is guided to the single-stage centrifugal compressor through two air intake ducts located on the sides of the engine. After the air leaves the impeller, it is decelerated and pressurised by passing through the radial diffuser vanes. The pressurised air fills up the main air casing that constitutes the middle part of the engine body. The air then enters the single can type reversed

flow combustor. The atomized liquid fuel from the fuel sprayer and the air form a flammable mixture which is ignited by an electric spark plug. The spark is only required during the start-up procedure. Once the gas turbine reaches a self-sustaining speed, the spark plug is disconnected from the power supply. The high temperature, high pressure combustion gas then expands and leaves the combustor through the volute casing, then enters the guide vanes (stator) of the turbine section and the rotating turbine drives the compressor to sustain a constant engine speed. After passing through the turbine section, the exhaust gas exhausts to atmosphere via the exhaust cone. The figure below illustrates details of the gas flow path.

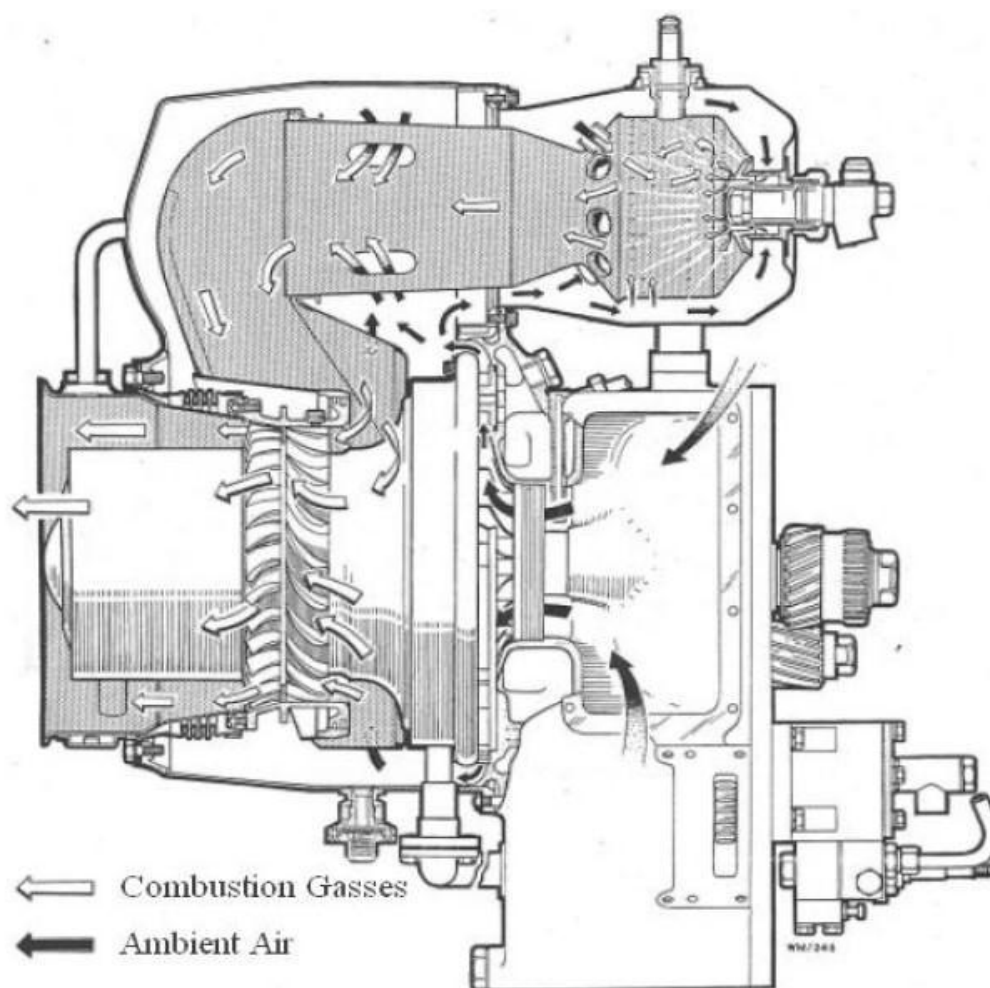


Figure 3-2: Gas flow diagram of Rover 1S/60 gas turbine (Rover Gas Turbine Ltd., 1966)

The commercial specification of the original Rover 1S/60 gas turbine is listed in Table 3-1. The unit comprises a single shaft that was designed to rotate at 46 000 RPM. It drives a series reduction gear with a final power output shaft rotating around 3 000 RPM, with an overall reduction gear ratio of 15.33. The main shaft also drives the fuel pump and oil pump through a reduction gear.

Table 3-1: Original Rover1S/60 specifications (Rover Gas Turbine Ltd., 1966)

Fuel type	Kerosene or Diesel
Compressor	Single stage, centrifugal
Turbine	Single stage axial, with guide vanes
Combustor	Reverse flow, single can type
Rotation direction	Clockwise, viewed in front
Pressure ratio of compressor	2.8:1
Maximum continuous exhaust gas temperature (EGT)	580 °C
Maximum power output	45 kW (60 bhp)

It is necessary to have a good understanding of each major part of the engine when testing and modifications are applied. The following section will discuss some primary components in general.

3.2 Air intakes

The air intake system is designed to deliver cool and clean air to the compressor. It is suggested to use inlet air filters for ground test units to prevent compressor damage from small particles. The air intakes on the Rover gas turbine engine are on the sides of the engine body. The air is guided into the engine by two ducts connecting to the engine body. The ducts then deliver the air to the compressor. All gas turbine engines draw in relatively large amounts of air when operating at maximum speed.

The air intake system used for current testing was designed by Prinsloo from University of Pretoria (Prinsloo, 2008). Figure 3-3 shows the detailed design of the air intake system with a reference table.

The design is based on *British Standard BS 848 Part 1: Fans for general purposes (1988)*. The system is installed with the air entrance facing towards the front of the engine to minimise the influence of hot unclean exhaust gas. The conical inlet duct consists of four static pressure taps for the calculation of inlet air mass flow rate. A thermocouple is also installed at the conical inlet to obtain an accurate reading of the inlet air temperature.

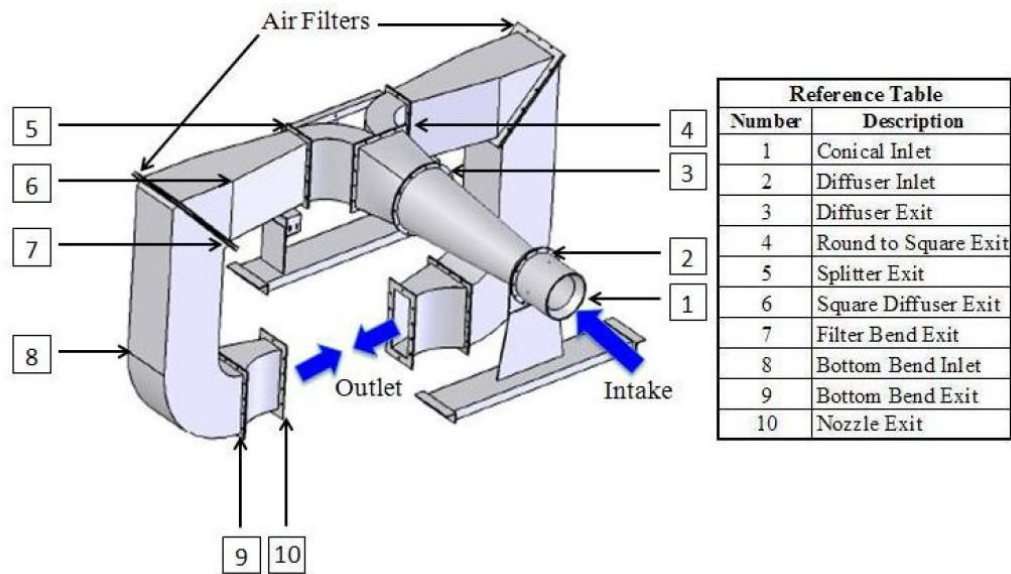


Figure 3-3: Air intake system, designed by Prinsloo (2008)

3.3 Compressor

The compressor section for the Rover 1S/60 gas turbine consists of a single stage centrifugal compressor and a diffuser. It compresses the air to transfer mechanical energy into kinetic and internal energy. The impeller is machined from an aluminium alloy forging and is fitted on the compressor shaft by hydraulic pressure (Rover Gas Turbine Limited, n.d.). The diffuser is used to reduce the speed and increase the pressure of the compressed air. The figure below shows the compressor (with shaft) and the diffuser of the engine.



Figure 3-4: The compressor and diffuser of the Rover 1S/60 gas turbine

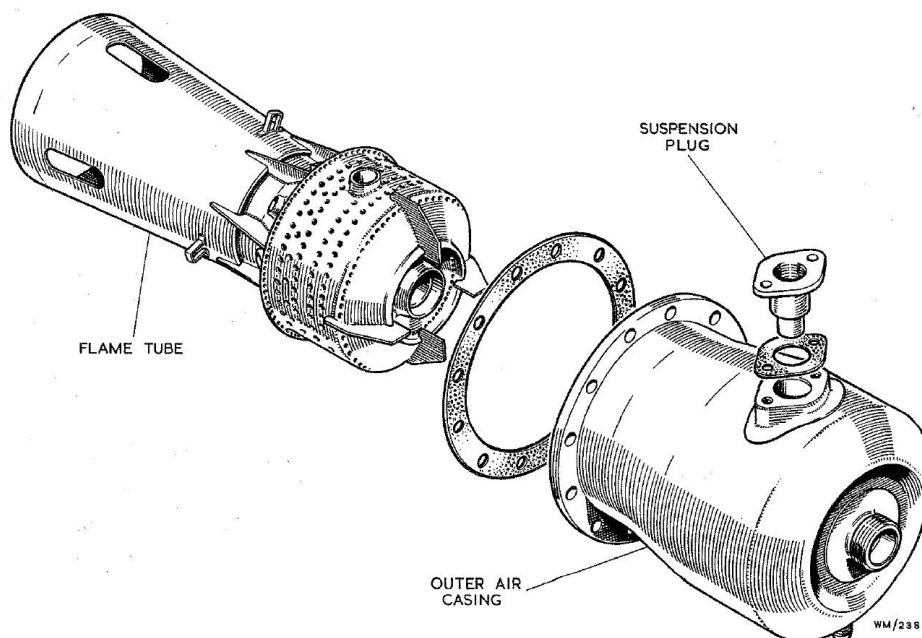
The holes on the diffuser are used for positioning purpose. The turbine disc is installed on the left side of the shaft and the dark colour of the shaft is caused by exposing it to an extremely high temperature environment. The geometries of the compressor impeller and diffuser are listed in the table below.

Table 3-2: Geometries of the compressor section (Quarta, 2012)

Impeller geometry	
Number of vanes	17
Diameter [mm]	165
Van thickness [mm]	1.75
Peripheral depth [mm]	8.45
Exit area [m ²]	0.00191

3.4 Combustion system

The combustion system is one of the most important parts of this project. It requires an in-depth understanding of the combustion process to carry out the conversion for the use of LPG. The type of combustor is a reversed flow single can type. It includes a combustion chamber and a flame tube located in the middle of the combustion chamber. The flame tube is positioned by four anti-swirl vanes and a suspension plug that is also used to insert the spark plug into the flame tube. Figure 3-5 shows the basic and detailed construction of the combustion chamber of the engine.



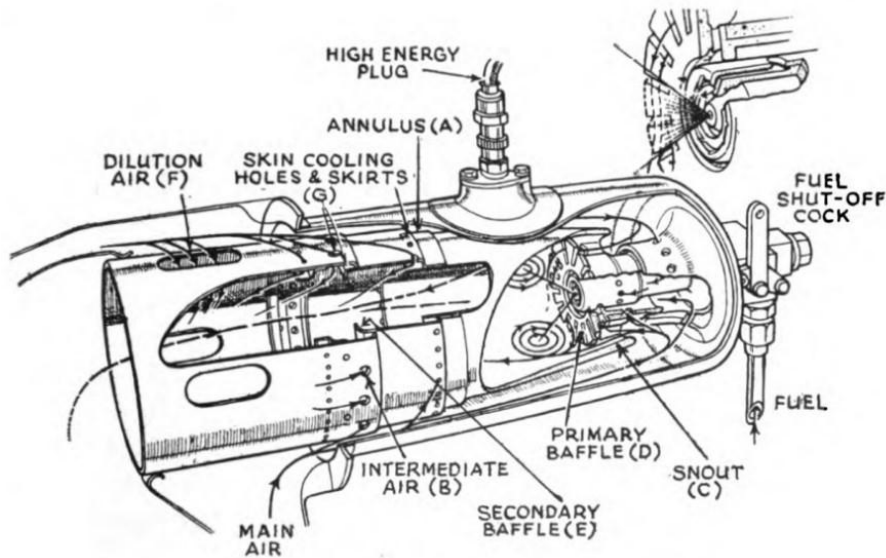


Figure 3-5: The combustion chamber construction of the Rover 1S/60 gas turbine (Rover Gas Turbine Limited, 1966) (Judge, 1960, p.213)

The compressed air is guided to fill the engine body casting and then flows into the combustion chamber. A 90° - 110° fine spray of liquid fuel is injected to the combustor to mix with air and the flammable mixture is ignited by a surface discharge spark plug. The angle of spray varies between different types of fuel sprayers depending on the manufacturer. The chemical reaction of combustion causes a temperature rise and an expansion of the gas, which will enter the turbine section. The combustor is designed to introduce the air for combustion in three stages. The figure below illustrates the detailed flame tube construction.

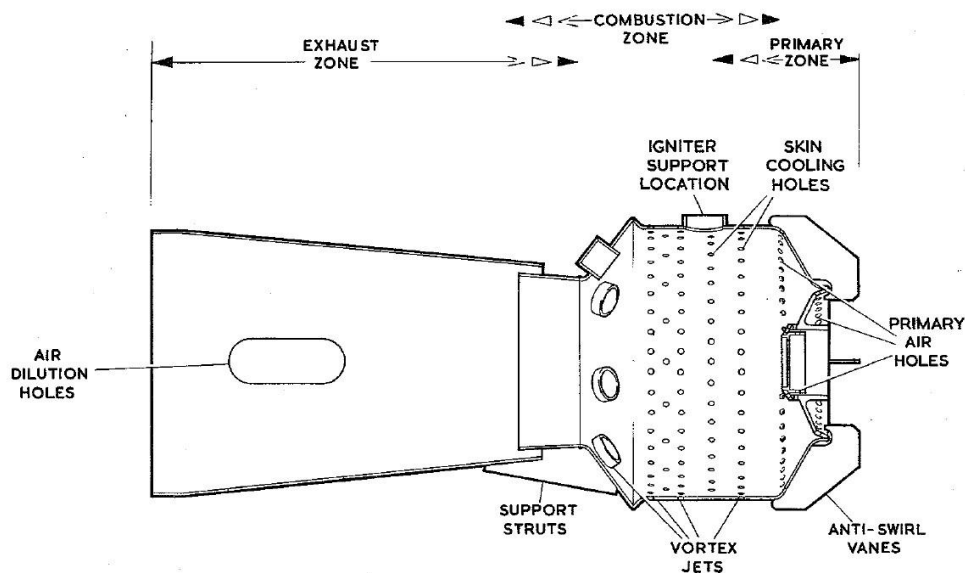


Figure 3-6: Flame tube of the Rover 1S/60 gas turbine

The air used for combustion only requires a small portion of the total air. Only about 15-20 % of the air is introduced around the fuel sprayer in the primary zone to provide sufficient air for a rapid combustion. Another 30 % of the total air is introduced through vortex holes to the intermediate zone (combustion zone) to create a designated vortex flow pattern for a complete combustion. The rest of the air is then mixed with the combustion gases in the dilution zone (exhaust zone) to cool it down so that the gas temperature is suitable for entering the turbine section.

3.5 Turbine

The engine uses a single stage axial turbine with guide vanes. The figure below shows the turbine disc and the guide vanes.



Figure 3-7: The turbine disc (left) and the guide vanes (right) of the Rover 1S/60 gas turbine

The expanded gas from combustion is guided by the stators and then the guided gas enters the turbine at a specific angle. The geometries of the turbine and guide vanes are listed in Table 3-3.

Table 3-3: Turbine section specification (Quarta, 2012)

Turbine geometry		
	Stator	Rotor
Number of blades	21	31
Pitch [m]	0.0246	0.173
Chord [m]	0.0410	0.236
Mean blade height [m]	0.124	0.155
Trailing edge thickness [m]	0.0008	0.0008
Tip clearance [m]	-	0.0005

The turbine inlet temperature is a key value to evaluate the turbine overall efficiency. However, the designed turbine inlet temperature cannot be found from any available information source. There is no accessible measurement port to obtain the turbine inlet temperature from the original construction of the engine. Generally, a higher turbine inlet temperature leads to a higher turbine efficiency. The turbine is exposed under high temperature conditions during the operation so that a special material is required. NIMONIC is used to forge the turbine disc and the blades and disc are machined integrally (Rover Gas Turbine Limited, n.d.). The NIMONIC is a registered trademark of Special Metals Corporation that refers to a family of nickel-based high-temperature low creep super alloys (Special Metals, 2015).

3.6 Fuel supply system

Due to the variety of Rover 1S/60 gas turbines, several different types of fuel systems were used. This particular engine uses a self-regulated mechanical fuel pump and an attached temperature control unit that can cut off the fuel when the engine is overheating. The fuel inlet port is located at the fuel pump body and the pressurised fuel outlet is located at the temperature control unit. These two components work together and cannot be separated.

The fuel pump produces the most significant resistance when the engine rotates freely without load. Therefore, the fuel pump was removed after all the tests with kerosene were finished to minimise the resistance for the LPG test. A piece of aluminium plate was then used as replacement to seal the engine.

The fuel pump is mounted on the auxiliary plate and is driven by the main gear through a plastic drive coupling with a gear ratio of 1:1. Figure 3-8 shows the section view of the fuel pump.

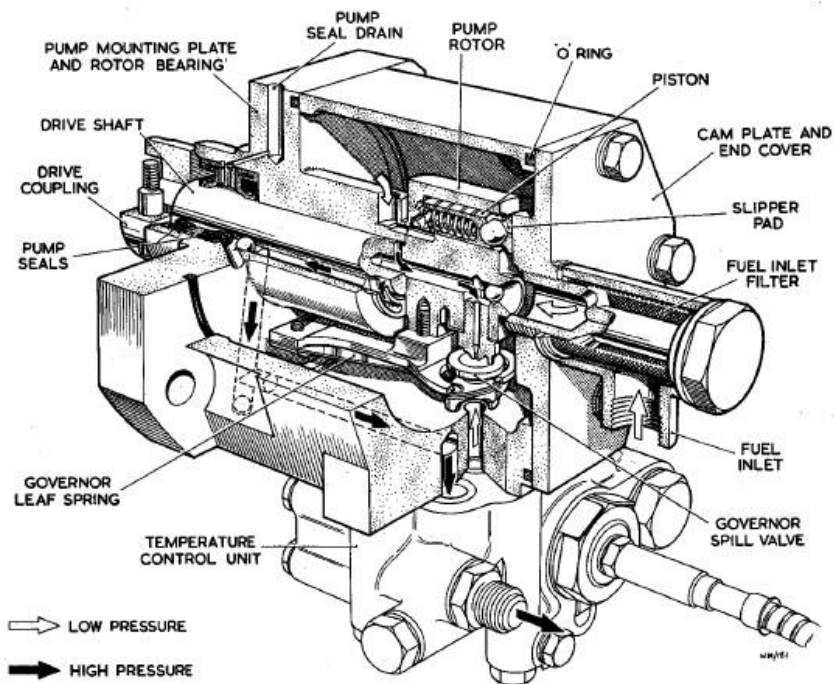


Figure 3-8: The construction of the fuel pump body (Rover Gas Turbine Limited, 1972)

The fuel is fed from the fuel tank by gravity. When the fuel pump is operating, the main body of the pump is filled with low pressure fuel. The fuel then enters three piston chambers as shown in Figure 3-8 and Figure 3-9. These pistons rotate together with drive shaft at a very high speed. Each piston has a half ball structure on top of it, covered with a slipper pad. These three slipper pads push against a slope surface by the spring inside the piston. When the pump shaft is rotating, the pistons are also rotating and pushing against the slope surface to create a reciprocal motion as pumping action. The continuous pumping action pumps the fuel in the piston chamber to the high-pressure fuel port A (H.P. - A) as shown in the figure below.

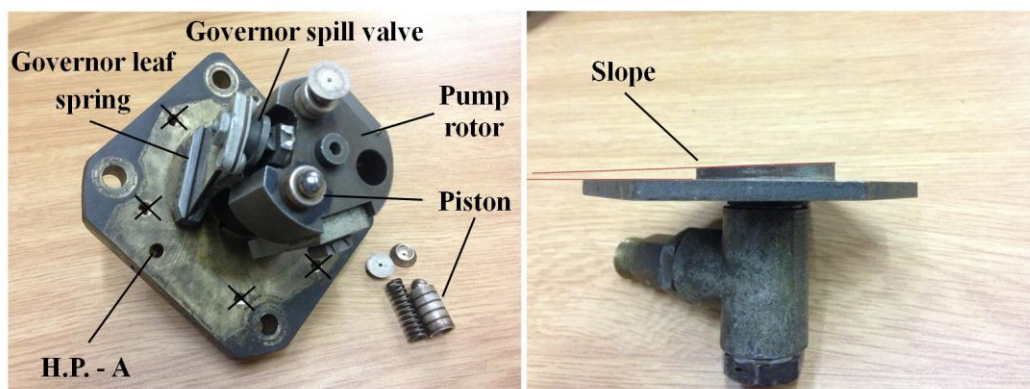


Figure 3-9: Inner view of the fuel pump

There are several built-in fuel channels on the pump casing and temperature control body. These channels can be easily confused with the holes for fastening screws. For convenience, the holes with black crosses on them are used for fastening screws as shown in Figure 3-10.

According to Figure 3-10, the high-pressure fuel will flow through “H.P. – A” to “H.P. – a1” located on the pump casing because these two ports are against each other when they are in one piece. Then it flows from “H.P. – a1” to “H.P. – a2” through a built-in fuel tunnel. When all the parts are constructed, “H.P. – a2” and “H.P. – a3” are also against each other and sealed with an O-ring. “H.P. – a3” is connected to the fuel exit port and the half ball spill valve. The half ball spill valve is fully closed when the engine is under normal operating condition. Therefore, the high-pressure fuel flows from “H.P. – A” and finally exits the fuel supply system through fuel exit port to the fuel sprayer. The above fuel flow path is used when the engine is running under normal condition.

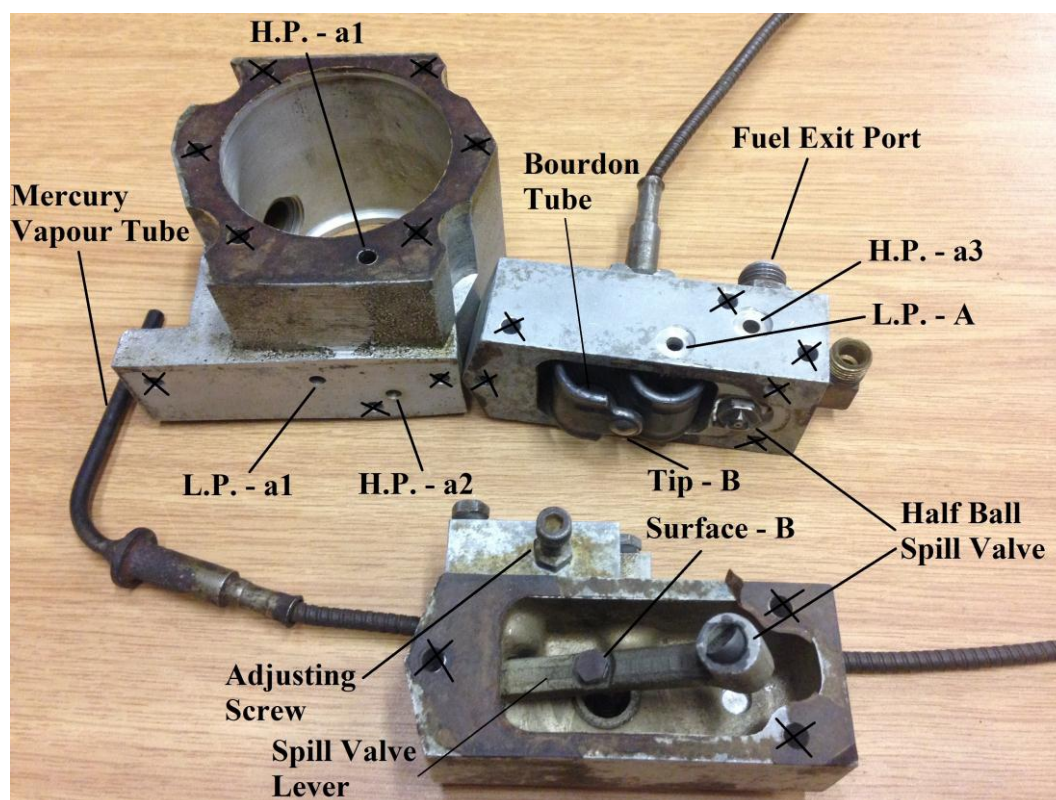


Figure 3-10: The fuel pump casing and temperature control unit

3.6.1 Engine speed regulation

When the engine is running without any load, the engine speed is solely related to the quantity of fuel used for combustion. In practice, the engine speed is regulated by the fuel pump. During the engine accelerating period, the pump rotator inside the fuel pump rotates together with the engine shaft. A governor leaf spring is

attached to the pump rotor as shown in Figure 3-9. When the engine reaches a specific speed, the centrifugal force generated by the counterweight on the tip of the governor leaf spring is strong enough to open the governor spill valve. This passage interrupts the pressurised fuel flow path that was supposed to flow from piston chamber to “H.P. - A”. It opens a bypass for the pressurised fuel to reduce the flow rate that flows to “H.P. - A”, and therefore reduces the fuel quantity that exits the fuel supply system. The spilled fuel returns to the pump body chamber that stores low-pressure fuel. When the governor spill valve is open, the total amount of fuel that exits the fuel supply system is just enough to sustain the idle speed.

When load is applied to the engine, it first reduces the shaft speed of the engine. With reduced shaft speed, the centrifugal force of the counterweight attached on the governor leaf spring is not strong enough to keep the governor spill valve open. Therefore, the high-pressure fuel bypass passage is closed and the pressurised fuel flow rate increases. The increased fuel leads to a more intense combustion, thus the power output also increases and the power then can be extracted from the driveshaft. This procedure will continue until the whole unit reaches a balance condition.

3.6.2 Temperature control unit

When the exhaust gas temperature is too high, the temperature control unit is used to protect the engine from overheat. To achieve this function, a mercury vapour tube is mounted on the exhaust cone and it is exposed to the high temperature exhaust gas. When the engine is under load, the exhaust gas temperature will rise rapidly. As soon as the exhaust gas reaches the maximum allowable temperature, the mercury vapour expands along the capillary tube to the “S” shape bourdon tube as shown in Figure 3-10. The bourdon tube expands and the “Tip - B” pushes the “Surface - B” of the pivot spill valve lever. At the tip of the spill valve lever, a half-ball valve is positioned in the hollow and the spill valve will be open when the lever is pushed by the expanding bourdon tube.

The open half ball spill valve interrupts the high-pressure fuel that originally flows from “H.P. - a3” to the fuel exit port. Part of the high-pressure fuel now flows through the spill valve to the chamber of the temperature control unit. It then flows through the low-pressure passage “L.P. - A”, “L.P. - a1” and back to the pump body chamber. Therefore, an overheated mercury vapour tube will result in a reduced fuel flow that exits the fuel supply system to prevent the engine from overheating.

3.7 Starter motor system

A starter motor is mounted on the side of the engine and it is powered by a 12 V battery. To be able to operate the starter motor, an electromagnetic relay is used to conduct high current from the battery to the starter. The relay can be controlled by

a separate switch as originally designed or computer control system for testing purpose. In the current project, it is connected to the PLC and controlled by ETA. Figure 3-11 shows the original relay system used for the starter motor.

For convenience, the components inside the relay are labelled as “Part 1”, “Part 2” and “Part 3”. “Part 1” is used for the original starter system as a timer between the relay and the starter switch. It can be used to control the total duration for connecting the relay to energise the starter motor and it will disconnect the relay after reaching a pre-set time. Since the starter motor will be controlled manually through the PLC, this timer device is not required anymore. To keep the original component integrity, “Part 1” will be kept in its position but disconnected from other devices.

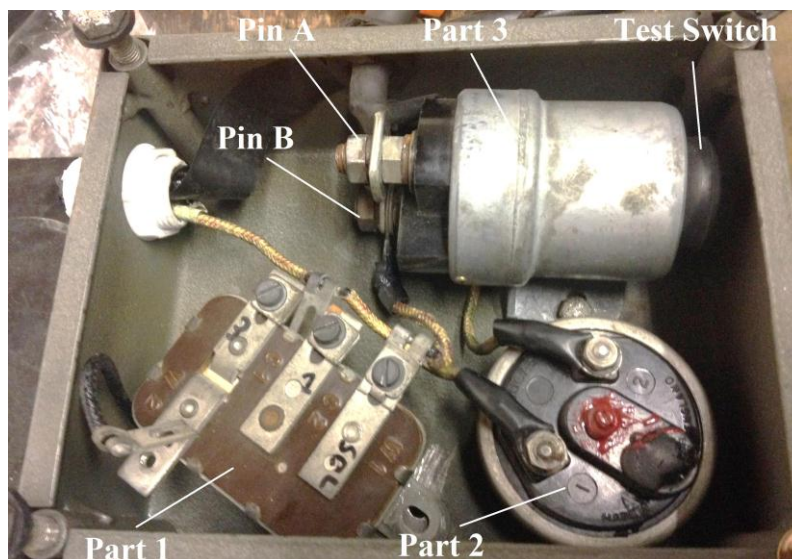


Figure 3-11: Original relay system for the starter motor

“Part 2” is also used for the original configuration. At the back of “Part 2”, a pressure measurement port is available. However, no explanation for this part can be found in any available document. After several tests on “Part 2”, it is believed that it was used as a pressure triggered switch and it measured the compressor delivery pressure. The two connectors on “Part 2” are connected under atmospheric pressure and they will be disconnected after reaching a specific pressure. This would keep the starter motor energizing until the engine reached a certain speed to produce sufficient pressure to disconnect the relay. “Part 2” will also be kept at its place for the original integrity.

“Part 3” is the relay and it is being used in the current project. “Pin A” and “Pin B” are disconnected when no external power is connected to the relay. During the starting procedure, an external power source is connected to the relay and it will connect “Pin A” and “Pin B”. Therefore, a high current circuit from the battery to the starter motor is closed and the starter will be energised.

When the starter motor is operating, it consumes a lot of power. At the point of energizing the starter, the electric current can reach about 600 A. The current then decreases to approximate 300 A while the starter motor is running at steady speed. The starter should be monitored regularly because it has a tendency to overheat.

3.8 Igniter unit

The original high energy ignition unit is made by “British Thomson-Houston” in, England. The igniter unit is powered by 24 V DC, unlike most igniters that require 12 V power supply. Except for the specification plate on the igniter, there is no information available for this particular unit. The figure below shows the inside of the igniter unit.

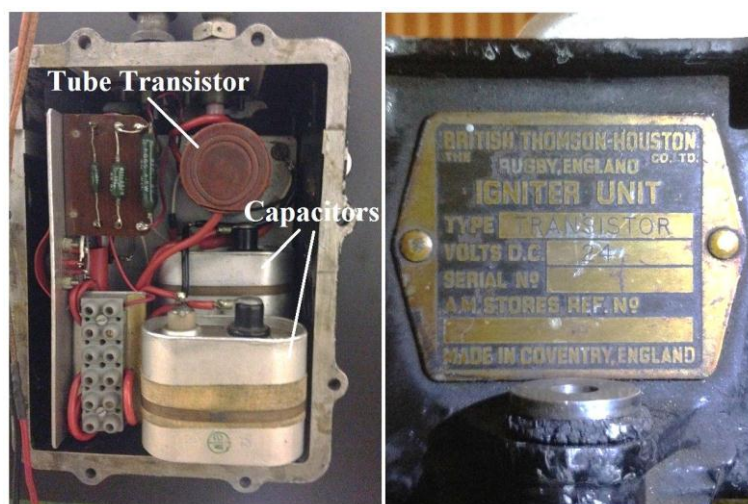


Figure 3-12: The original igniter unit

The igniter unit consists of a spark plug with flexible electric cable. It is a surface discharge spark plug and it releases more energy than those used in piston engines. The construction of the spark plug is shown in the figure below.

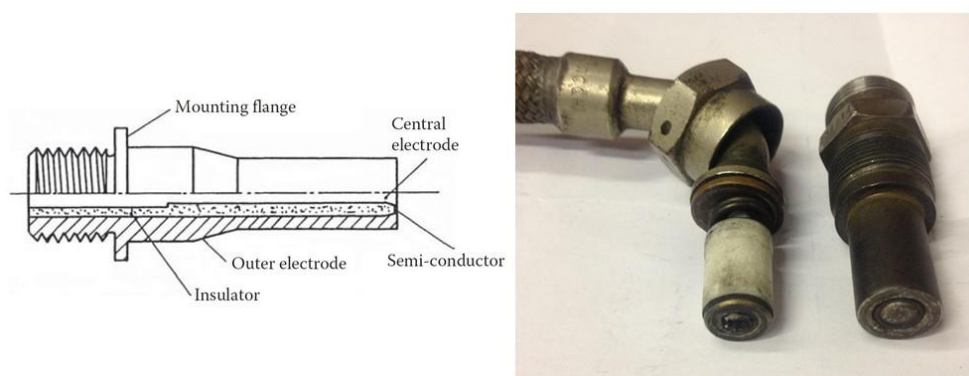


Figure 3-13: The construction of the spark plug (Lefebvre & Ballal, 2010)

Since the igniter unit is designed to use 24 V DC power, the 12 V lead-acid battery cannot be used as the first choice. An additional 24 V DC power supply is then provided in the test cell control room. However, it is still necessary to understand the operating behaviour of the igniter unit. Several tests were carried out to test the igniter with adjustable DC power supply. The figure below shows the discharge moment of the spark plug operating on 24 V DC.



Figure 3-14: Igniter unit test on 24V

The igniter unit was connected to a 24 V DC power supply for test purposes. When the power was on, the spark plug produced proper and stable sparks about every 0.7 second. After several tests, it was proved that the original igniter unit was in a stable working condition and usable for the current project. Another test then used 12 V DC as power supply. The spark plug could also produce the same stable and proper spark but it took much longer (about 1.5 seconds) to generate one spark. It indicates that the igniter unit is functional when using a 12 V battery but with a longer discharge time. Considering that for safety reasons the fuel should be ignited as soon as possible to prevent fuel building-up, a shorter discharge time is preferred.

4 Test facility design and installation

To carry out the testing of the Rover 1S/60 gas turbine, it requires a well-established test cell with ventilation, data acquisition and a remote control system. All the work related to the experimental test setup will be discussed in this chapter.

4.1 Test cell overview

It was decided to test the Rover gas turbine in Room 172, and it shared the same control room (Room 170) with a piston engine test cell. The test cell came with the air ventilation, cooling water supply and fire fighting system, which was ideal for small gas turbine testing. The major components for the test setup were a Rover 1S/60 gas turbine, a Schenck W130 eddy-current dynamometer and an Allen Bradley programmable logic controller. All relevant sensors and wirings were organised and connected to the control room through an underground tunnel. A new exhaust gas duct was installed since the gas turbine produced gas with high temperature, volume and speed.



Figure 4-1: Test cell layout

4.2 Engine and dynamometer

The Rover gas turbine and a Schenck dynamometer are two major pieces of equipment for this project. They are installed in the test cell and connected by a driveshaft. It is required to remotely monitor all relevant data and control the operating condition of the engine in the control room for safety reasons. The installation of the engine and the dynamometer also needs to meet the requirements for further modification of the engine.

4.2.1 Test bench

The engine is rated at 45 kW for the maximum continuous power output. The installation of the gas turbine requires a rigid test bench and shock absorbers. Therefore, the engine and the dynamometer are both installed on a steel test bench. The test bench is positioned perpendicular to the control room to prevent high-speed fragments hitting to the control room when experiencing components failure. The direction of the exhaust gas is also directed at the opposite end of the control room for safety concerns.

The test bench is installed with eight shock absorbers underneath to eliminate potential vibration. The test bench also comes with three crossbeams that support the engine and the dynamometer. The dynamometer is bolted on two crossbeams with high tensile bolts, allowing it to be moved in two directions (along with the test bench and perpendicular to it). The engine is installed on two screw jacks so that the height of the engine is adjustable to match the dynamometer. The output shaft of the Rover gas turbine is not in the centreline, therefore the engine has to be shifted to one side of the test bench to allow the output shaft to align with the dynamometer. Since the test bench is not wide enough, extra spacers and shifting holes are needed to extend the shifting range.

4.2.2 Driveshaft, dynamometer flange and shaft guard

The engine and dynamometer are connected by a customised driveshaft as shown in Figure 4-2 (top left). It consists of a constant velocity (CV) joint, two rubber vibration dampers, two flanges connection and a spacer. The whole driveshaft has been checked for weight balance to ensure stability when it spinning at high speed. The CV joint was fully lubricated before connecting to the engine output shaft.

A custom flange was designed and manufactured to connect the driveshaft and the dynamometer (Figure 4-2, top right). It was designed to be able to transfer more torque than the maximum torque produced by the Rover gas turbine. All bolts used for fastening are high tensile bolts.



Figure 4-2: Customised driveshaft (top left), dynamometer flange (top right) and shaft guard (bottom)

During the engine test, the driveshaft and flanges are rotating at high speed. A shaft guard is required to avoid any possible damage from spinning out particles. The design requirements of the shaft guard are listed below:

- Provide maximum protection from high-speed particles or shattered components of the driveshaft.
- The lock of the shaft guard needs to be strong while easy to use.
- It should not touch any part of the engine during the opening or closing of the shaft guard.
- Leave enough space for repair work and further modification.

The shaft guard was constructed from 8 mm thick steel for the main body to ensure strength and it is bolted on the crossbeam of the test bench by a fixed length support.

4.2.3 Dynamometer setup

The Schenck W130 dynamometer is installed on the test bench between the control room and the engine. The control unit is mounted in a cabinet located in the control room. The dynamometer control unit connects to the PLC, so that it can be controlled either by the control panel on the cabinet or the ETA through the computer. The major part of the control panel is illustrated in Figure 4-3. The setting shown in the figure below is for engine testing instead of default setting.

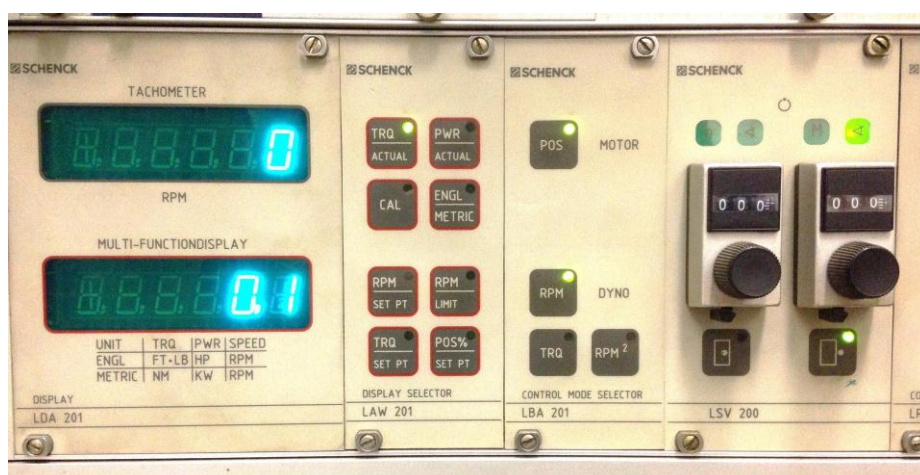


Figure 4-3: Major part of Schenck LSG2000 dynamometer control unit (shown in the setting for engine testing)

The dynamometer requires continuous water supply as coolant to dissipate the heat generated by the excitation coil. The water from the roof water tank of the department is used as coolant. The dynamometer has two water inlets at the bottom and two outlets at the top. It is designed in such a way to ensure the excitation coil of the dynamometer is always filled with the cooling water to prevent overheating.

As shown in Figure 4-4, two water level sensors are used to detect the water flow in the outlet water pipe. The sensors are located on top of the water pipes so that they could detect if the water level is higher than the excitation coil. A current loop will be closed from one sensor to another when both of the sensors have contact with the water. If the current loop is closed, it indicates the dynamometer body is filled with cooling water. When the current loop is open, it then shows the water level does not meet the safety requirement and it will trigger the warning light and buzzer on the control panel. Two thermostatic switches are used to monitor the temperature of the outlet water. According to the Schenck manual, the operation will be interrupted as soon as the outlet temperature exceeds 60 °C (SCHENCK Pegasus GmgbH, 1997). However, these two thermostatic switches can only be used as safety switches and they cannot indicate the real-time temperature. Therefore, two additional thermocouples are added to monitor the precise outlet temperature.

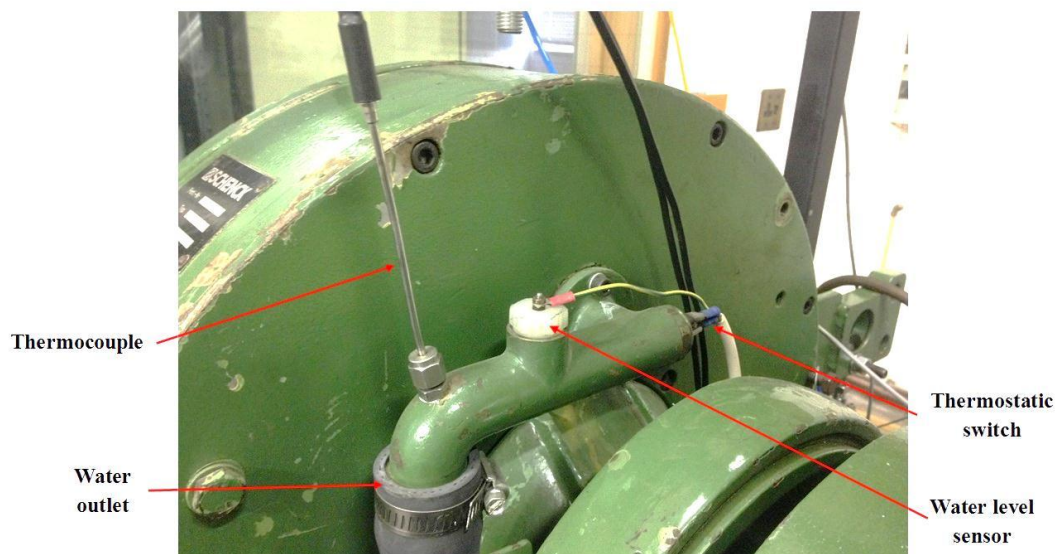


Figure 4-4: Water outlet of the dynamometer

4.3 Liquid fuel system

Kerosene is selected for engine testing. The Rover gas turbine consumes a relatively large amount of fuel during operation. As mentioned before, the engine is equipped with a self-regulated fuel pump and there is no throttle device for this particular engine. Therefore, a fuel supply system and a remote control throttle device are needed for testing purpose.

4.3.1 Fuel supply system

The fuel supply system consists of a fuel tank, fuel transfer pipes, control valves and a fuel filter. The engine requires “fuel supply with a minimum free flow at the fuel pump inlet of 114 litres/hour and a pressure head between 0.04 kg/cm^2 (3.9 kPa) and 0.9 kg/cm^2 (88.3 kPa)” (Rover Gas Turbine Limited, 1966). To supply fuel to the fuel pump, a gravity feed stainless fuel tank and $\frac{1}{2}$ inch fuel pipe are used to minimise the system complexity and yet provide sufficient fuel flow. Based on the fuel pressure requirements, the differential height between the fuel pump and tank is from 0.49 m to 11.11 m when operating on kerosene with a density of 810 kg/m^3 . The fuel tank is then mounted on the wall as high as possible to provide required fuel pressure by gravity feed. The fuel tank comes with a fuel level indicator that is attached on the side of the tank as shown in Figure 4-5.

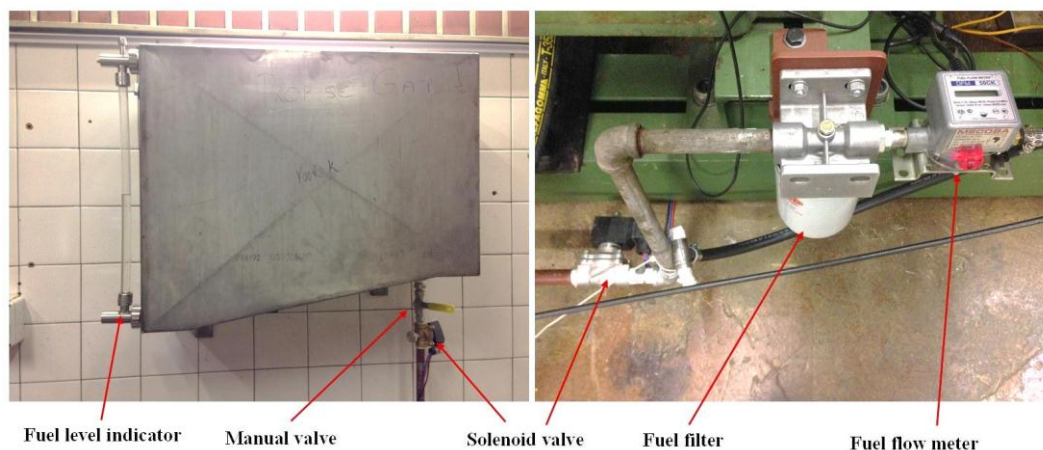


Figure 4-5: Fuel tank with level indicator and valves, fuel filter and flow meter

The slope at the bottom of the fuel tank is used to prevent contaminants from flowing into the fuel supply pipe. Two normally closed two-way solenoid valve and one manual ball valve are used in the fuel supply system. The solenoid valves are chosen for remote control purpose and the manual ball valve is used as a backup shut off valve. One of the solenoid valves is connected to the manual valve located just under the fuel tank and another one is mounted as close as possible to the fuel pump of the engine to ensure the engine can be shut down immediately. Both of the solenoid valves are powered by a 24 V DC power supply that is mounted in the control cabinet. All solenoid valves can be control through ETA or an emergency switch as shown in Figure 4-7.

The fuel pump and sprayer can be damaged by small particles. Even with a coarse build-in fuel filter, there is still a chance for contaminants to go through and damage the fuel system. An external fuel filter is used to provide maximum protection and it is installed as closely as possible to the fuel pump. The main body of the filter is positioned below the fuel supply pipe, so that the fuel will fill up with the filter and then exit to the engine. Such an installation can use the full filtration capacity to provide clean fuel to the engine. It requires extra caution when changing the filter because the main body of the filter is filled with fuel.

The fuel flow rate is measured by a FUEL-VIEW DFM-50C-K fuel flowmeter installed just after the fuel filter as shown in Figure 4-5. The details of the fuel flow meter can be found on the manufacturer's website.

4.3.2 Liquid fuel control system

The Rover gas turbine used in the current project does not have a throttle control device or anything that can control the fuel flow rate. Instead, it uses a self-regulated fuel pump for the operation. It is impossible to adjust the engine running

speed by only using original components. For experimental purpose and further modification, a controllable throttle is preferred and an extra control system should be designed. The basic requirements of the fuel control system are listed below:

- Reliable and easy to maintain
- Can be controlled remotely
- Fuel flow can be adjusted precisely
- Able to cut off the fuel immediately

According to these requirements and the construction of the engine, the fuel control system can be divided into two parts: fuel sprayer control and flow restriction control. According to the fuel sprayer test in Appendix B, the fuel sprayer only has two conditions: fully closed and fully open. The status of the sprayer is controlled by a barrel cam lever, which acts as a shut-off valve. During the tests, the fuel sprayer is preferred to be operated as fast as possible to minimise the delay. Therefore, it requires a mechanism that can change the position of the barrel cam lever with minimum time lag. To achieve these requirements, a boat throttle with push-pull cable was used for the sprayer control. The boat throttle device is able to control a solid flexible cable in two ways: push and pull. It is ideal for the coarse but direct control required for the sprayer control. The construction of the sprayer control system is shown in the figure below.

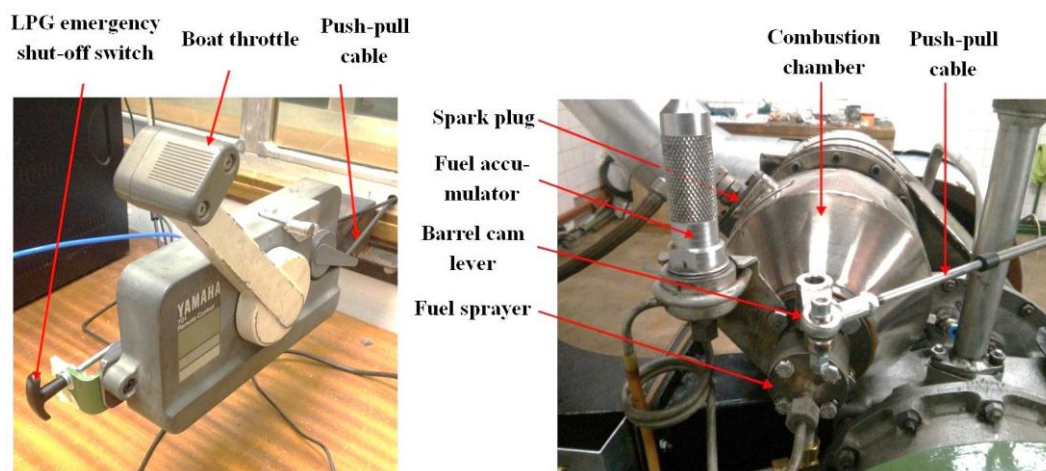


Figure 4-6: Boat throttle (left), fuel sprayer control (right, (Luiten, 2015))

To control the fuel flow rate, a mechanical needle valve is selected to restrict the fuel flow. A two-way normally closed solenoid valve is then connected to the needle valve as an emergency shut-off valve. To control the needle valve from the control room, a geared motor is connected to the valve with a PVC connector. The geared motors can be controlled in the control room by using switches. The construction of the needle valve control system can be found in Figure 4-7.

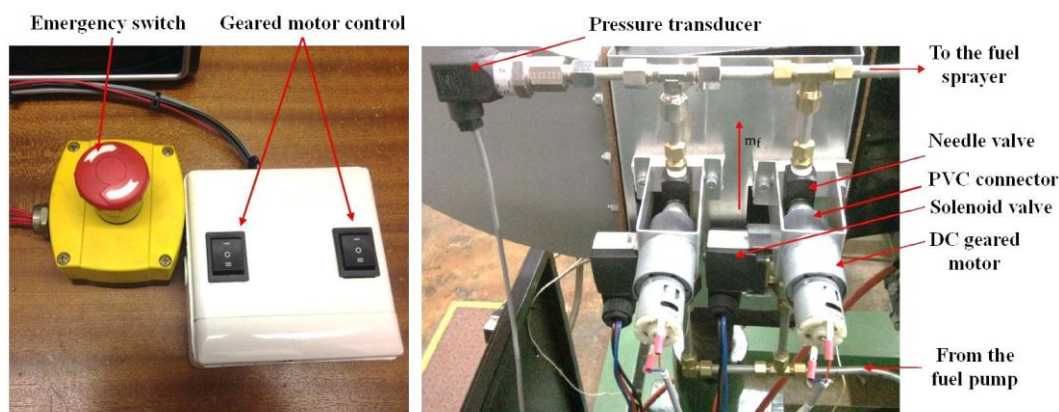


Figure 4-7: Emergency switch and motor control (left), Needle valve control (right, (Luiten, 2015))

To be able to adjust the needle valve precisely, the maximum speed of the geared motor was selected at only 10 RPM. It is impossible to switch the valve to fully open or fully closed immediately by only using the low speed motor. Therefore, a dual flow system was designed. Each of the fuel lines has a remote controllable needle valve and a solenoid valve, each of them can be controlled separately. The system also consists of a pressure transducer to monitor the fuel pressure. The emergency switch controls all the solenoid valves including two in the fuel supply system.

4.4 Exhaust gas system

The engine discharges the exhaust gas directly into the air without a silencer or catalytic converter. Due to the large amount and high speed of the exhaust gas, it requires a relatively large diameter exhaust duct. The exhaust gas temperature for continuous operation is 580 °C and the speed is calculated at 25 m/s. The design of the exhaust duct must consider the heat insulation and jet blast prevention to ensure safety. The exhaust duct is constructed with three layers: the steel inner layer to act as high temperature gas duct and provide body strength, a heat insulation material filled middle layer and an aluminium sheet outer layer. Even though the duct consists of heat insulation materials, the surface can still be extremely hot after the engine test. A gap is left between the exhaust cone of the engine and the exhaust gas duct so that cool air can be sucked into the exhaust gas stream to reduce its temperature. Figure 4-8 shows the exhaust gas system of the engine.



Figure 4-8: The exhaust gas system of the engine

4.5 Gaseous fuel system

The ultimate goal of this project is to operate the engine with LPG. A gaseous fuel system is designed and fitted to the current gas turbine system. The original liquid fuel pump and other components is removed. Safety is one of the most important factors when operating the engine with LPG. All details will be discussed in this sub-chapter.

4.5.1 Outdoor LPG supply system

The engine consumes relatively large amount of fuel even at idle and it was measured at 34 litres/h when running on kerosene. Therefore, the supply system must provide large volumes of LPG during the tests. However, drawing a large amount of LPG from the cylinder in a short period will dramatically decrease the temperature so that the in-cylinder pressure will drop below the requirement. To provide sufficient LPG to the engine, two 45 kg cylinders have been installed to minimise the LPG pressure drop during the engine tests. The LPG directly feeds to the engine from the cylinders without regulator to maintain a maximum gas pressure and flow rate. According to the university safety regulation, the LPG cylinders cannot be stored in the test cell or the control room. Therefore, the cylinders were stored in a cage located outside of the building. An approximate 10 m long LPG pipe was built to supply the gas to the engine. The supply pipeline consists of a manual emergency shut-off valve located next to a fire hydrant on the outside wall of the building. Figure 4-9 shows the LPG supply line and the shut-off valve.



Figure 4-9: LPG supply and outside emergency shut-off valve

4.5.2 LPG control system

The LPG is supplied from the outdoor cylinders to the indoor control system through a certified LPG flexible hose. The flexible hose is connected to an emergency shut-off valve, which was originally used as a quick action valve for liquid LPG filling. The lever of the valve is connected to a single-direction cable, so that the valve can be closed remotely in the control room by pulling the shut-off handle (shown in Figure 4-6). Figure 4-10 illustrates the installation of the quick action shut-off valve, the needle valve control device and the data acquisition system.

The needle valve control device uses the same design as the one for liquid fuel control and the details have been discussed in Chapter 4.3.2. It can also be controlled in the control room by using the same switch box. Between the needle valve control device and the gas injector, the LPG line consists of a thermocouple, a static pressure transducer, a customised venturi tube and a differential pressure transducer as shown in Figure 4-10. All the sensors will be discussed in the following chapter. The gas injector is bolted on the combustion chamber and it is connected to a manual ball valve. The manual valve is connected to the push-pull cable and controlled by the boat throttle device in the control room. It uses the same principle as liquid fuel sprayer control system and details have been discussed in Chapter 4.3.2.

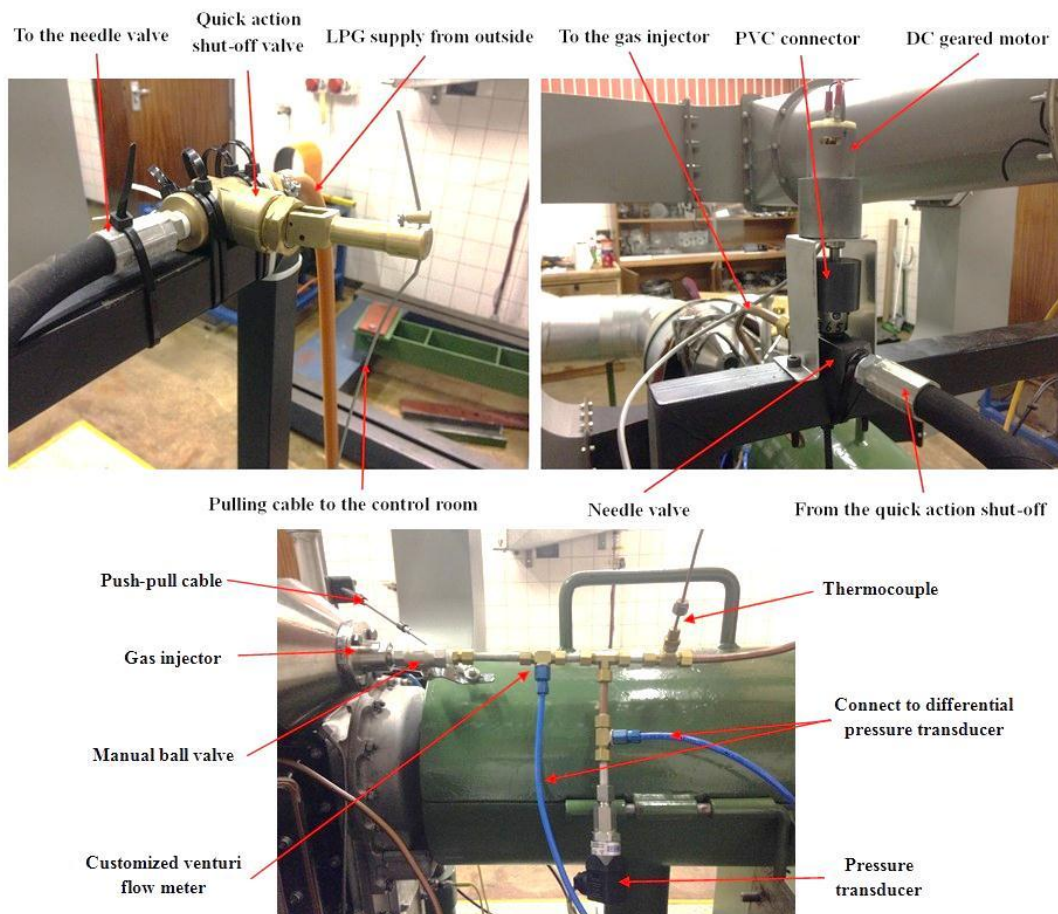


Figure 4-10: Quick action shut-off valve (left), needle valve control device (right) and data acquisition system (bottom)

4.5.3 Gas fuel injection

To switch fuels from kerosene to LPG or propane, a new fuel injector must be designed for the gas turbine. The purpose of the fuel injector is introducing the fuel into the combustor to mix with the air and becoming flammable mixture. No atomization or evaporation is required when using gaseous fuel. There are several concepts to inject the gaseous fuel into the combustor, including plain orifices and slots, swirlers, and venturi nozzles (Lefebvre & Ballal, 2010). For initial testing purposes, the plain orifice concept was chosen because of its simplicity. However, the gas injector still has to meet several criteria for engine operation.

The flow rate of the gas fuel should be under control at all times during the engine testing. The control function is achieved by using a needle valve system as discussed in the previous chapter. In any circumstance, the engine must not run at over speed for any reasons. However, it is possible that the control valve is accidentally switched to the fully open position by mechanical failure or human operation error. This can cause engine over speed and the components can be

damaged permanently. Except for the emergency shut-off valve, there should be another method to avoid such an incident happening.

By applying the concept of compressible flow as discussed in Chapter 2.4, it is possible to design a fuel injector with a specific maximum fuel flow rate. With such a design, the gas injector can prevent the engine from over speeding while it can still provide sufficient fuel to maintain normal operation. However, the maximum required fuel flow rate of the engine may change under different running conditions. The required fuel flow rate will be obviously different between the conditions of idle running and maximum power output. For safety and research purposes, it is strongly suggested to conduct all initial tests at idle conditions or at lower speed. Because the gas injector is an independent component of the engine, it is easy to change the injector alone if further tests are needed.

The diameter of the orifice is initially designed at 2 mm and it can maximally provide the fuel flow to sustain the engine running up to 40 000 RPM when having an overall air/fuel ratio of 100. The injector has been tested by using compressed air and the results are discussed in Appendix C. The orifice can easily be expanded if necessary and it is best to keep the orifice diameter as small as possible for the initial test since the LPG powered engine behaviour is completely unknown. The injector is designed to be able to use separate fuel injection caps for research purpose as shown in Figure 4-11. The details of the fuel injector design and the injector testing will be discussed in Appendix C.

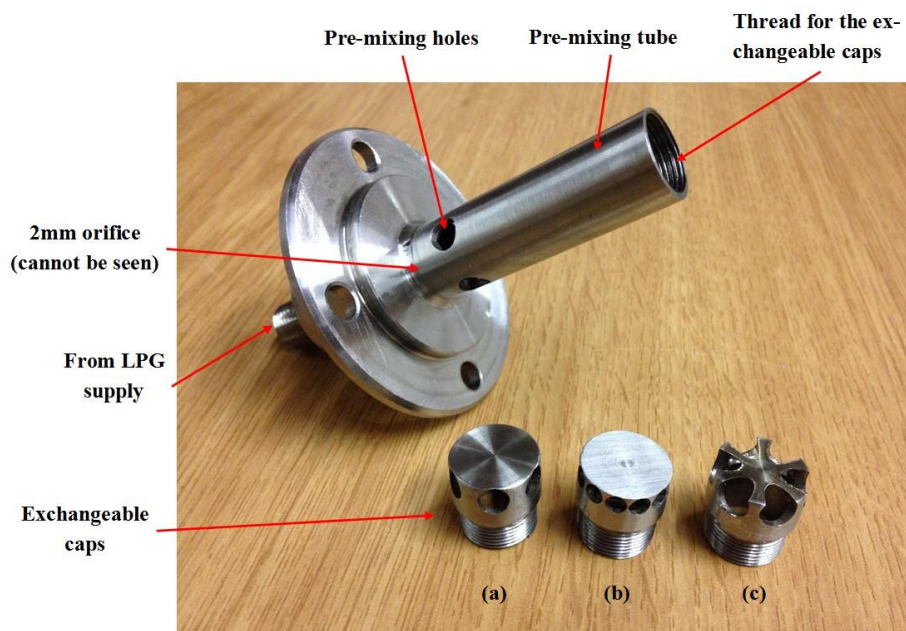


Figure 4-11: Fuel injector and exchangeable caps

4.6 Sensors for measurement

The test setup is designed to use a computer to monitor all necessary data. The data is acquired by electronic sensors used to measure temperature, pressure, fuel flow rate and engine speed. The complete data acquisition system includes sensors, PLC, relays and controller. All details will be discussed in the following contents.

4.6.1 Basic measuring sensors layout

During the engine testing, basic values are monitored and recorded at multiple positions of the Rover gas turbine. Figure 4-12 shows a schematic drawing of the layout of the measuring sensors for the kerosene powered engine.

In Figure 4-12, the torque of the engine and the air mass flow however are not measured directly from the equipment but from the calculation of basic values. The torque is calculated from the engine speed and the dynamometer load while the air mass flow rate is calculated from the differential pressure, based on the concept from British Standard (BS 848, 1997). After converting the fuel supply from kerosene to LPG, the measuring instrument layout has changed slightly but the basic sensors are kept the same. Details will be discussed separately in the following sub-chapter.

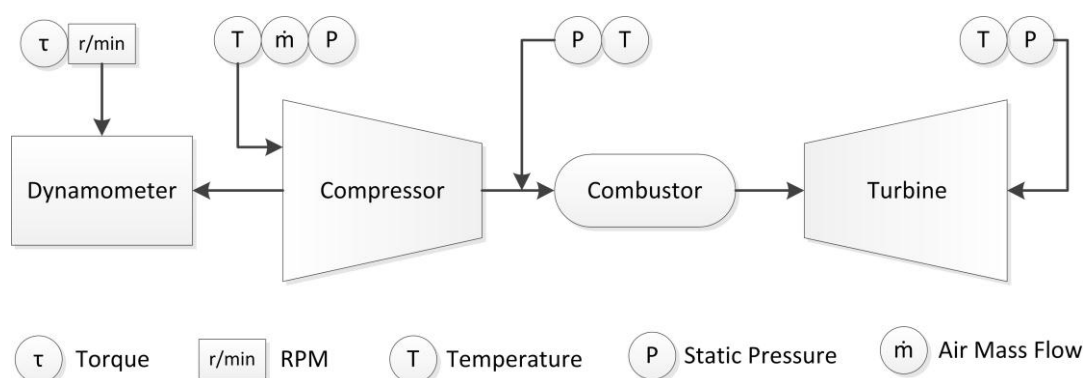


Figure 4-12: Basic measuring instrument of the engine

4.6.2 Engine speed

It is better to clarify some definitions of the Rover gas turbine before this discussion. The speed of 46 000 RPM is to describe the main shaft speed that is the same as the compressor and the turbine speed. However, after a series of reduction gears with a ratio of 15.33:1, the power output shaft speed is then reduced to approximate 3 000 RPM. The main shaft speed is only used to monitor the engine running condition and for data processing.

The output shaft of the Rover gas turbine is directly connected to the dynamometer and it is simple to measure the speed of the dynamometer. The rotational speed is measured by a variable reluctance (VR) speed sensor located

near the measuring toothed gear of Schenck dynamometer as shown in the figure below.

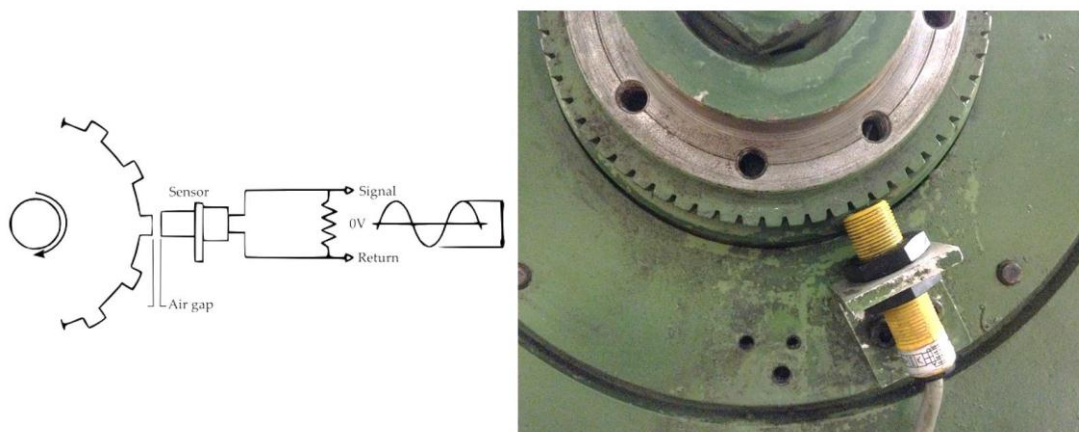


Figure 4-13: Speed measurement by using a VR speed sensor (SCHENCK Pegasus GmgbH, 1997)

The tip surface of the sensor is installed just next to the toothed gear which rotates along with the dynamometer. The VR speed sensor detects the variable magnetic flux generated by rotating toothed gear. The magnetic flux reaches its peak when the top land of the gear passes next to the sensor and it has a minimum flux when the bottom land is align with the sensor. By processing the time-varying voltage signal, it is possible to convert the signal to the speed value.

4.6.3 Torque measurement

The installation of the dynamometer includes a component named “load cell”, which connects the base and rotational outer case of the dynamometer. Without a load cell installed, the rotational outer case could rotate freely on top of the base. When the engine and dynamometer are operating, the engine drives the flywheel inside the outer case of the dynamometer. By applying load from the control terminal, the electric current through the coil increases the magnetic force and therefore increases the resistance of the flywheel. When the whole system reaches a stable state, the torque produced by the engine equals the resistant torque produced by the coil attached onto the dynamometer outer case. The reading of the force generated by the outer case can be obtained from the tension-compression strain load cell. By multiplying the length of the torque measurement arm, it gives the torque produced by the engine. The torque measurement arm is the distance from the load cell pivot point to the centre of the dynamometer. Figure 4-14 shows the construction of the dynamometer with load cell.

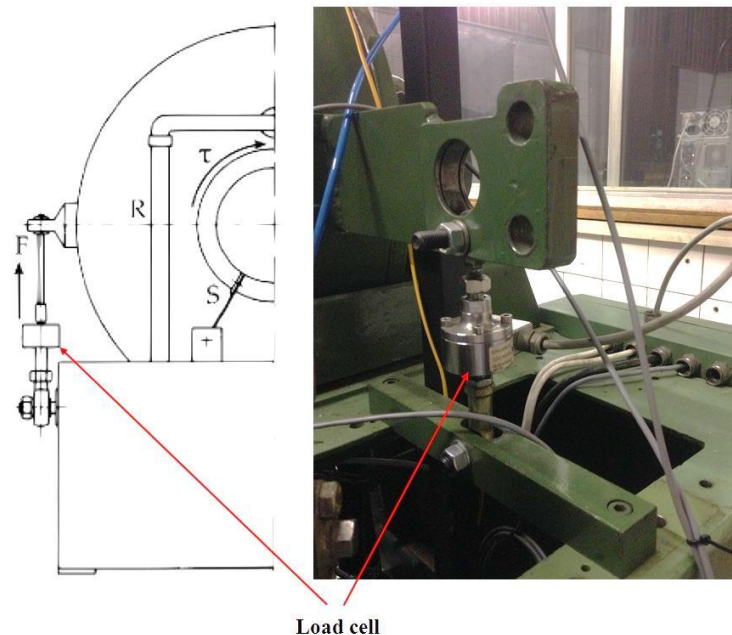


Figure 4-14: Torque measurement and the load cell (SCHENCK Pegasus GmgbH, 1997)

4.6.4 Temperature

The temperature reading throughout the Rover gas turbine is essential for monitoring the engine condition and further performance evaluation. The dynamometer also needs to monitor the outlet water temperature to prevent it from overheating.

The inlet air temperature is measured by a K-type thermocouple positioned underneath the conical inlet duct. The temperature of the pressurised air after the compressor is also measured by a K-type thermocouple inserted into the outer casing of the engine. As shown in Figure 4-8, four thermocouples with heat resistant shields are used to measure the exhaust gas temperature. Another K-type thermocouple is used to monitor the temperature of the oil sump. All thermocouples used for temperature measurement on the engine are K-type due to their range, accuracy and price. All K-type thermocouples are coated with yellow PVC covers except for those used for the exhaust gas, where they use metal heat resistant shields. The sensor elements of the K-type are NiCr-Ni and their normal ranges are from $-200\text{ }^{\circ}\text{C}$ to $1350\text{ }^{\circ}\text{C}$ with sensitivity of $41\text{ }\mu\text{V}/^{\circ}\text{C}$. Generally, the accuracy of K-type thermocouples falls between $0.8\text{ }^{\circ}\text{C}$ to $2.6\text{ }^{\circ}\text{C}$, which is acceptable to be used for engine testing (WIKA, 2015). All thermocouples used in the test setup were calibrated.

The thermocouples used for the dynamometer outlet water are two J-type dual output thermocouples with black PVC coating as shown in Figure 4-4. Because of the relatively low temperature of the outlet water, J-type thermocouple was selected due to their higher sensitivity of $50 \mu\text{V}/^\circ\text{C}$, even though they have a lower temperature ranges.

After converting the fuel supply from kerosene to LPG, the temperature of the gaseous fuel also needed to be monitored. Due to the limited space of the PLC, no more thermocouple could be added to the control system. Therefore, one J-type thermocouple was removed from the dynamometer and installed on the LPG supply pipe to monitor the gas temperature.

4.6.5 Static pressure

WIKA A-10 type pressure transducers were selected and used to measure all static pressure values. The A-10 type pressure transducer has an accuracy of $\pm 0.5\%$, which is ideal for the pressure measurement requirement. The range of each pressure transducer is selected individually based on the performance estimation to maintain a maximum accuracy. All the pressure measurement points are listed below:

- Oil pressure, measured at oil return line
- Liquid fuel pressure, measured at needle valve control system as shown in Figure 4-7 (removed after the LPG conversion)
- Exhaust gas pressure, measured at the exhaust gas cone
- Bearing air seal pressure, measured at the original built-in port
- Air delivery pressure, measured at the original built-in port
- Gaseous fuel pressure, measured at the fuel supply pipe (installed after conversion)

The results of the pressure measurement will be discussed in Chapter 5.

4.6.6 Air mass flow rate

The air mass flow rate cannot be measured directly from equipment in the current test setup. It is calculated by using differential pressure measured between the throat of the conical inlet and atmospheric pressure. The measurement port is illustrated in Figure 3-4. The details can be found in Chapter 5.3.3.

4.6.7 Liquid fuel flow rate

A rotary piston fuel flow meter (model: DFM-50C-K) was used to monitor the liquid fuel flow rate as shown in Figure 4-5. The instantaneous fuel flow rate can be either displayed on the screen of the flow meter or transferred to the PLC

through a cable. However, due to the limited number of channels of the PLC and an unknown error for the signal communication, the fuel flow rate could not be recorded and displayed in ETA. Even so, the fuel flow rate can still provide the flow rate value on its screen.

4.6.8 Gaseous fuel flow rate

Similar to the measurement of the air mass flow rate, the gaseous fuel flow rate could not be measured directly with current available equipment. To monitor the flow rate, a customised venturi flow meter has been designed. A FOXBORO differential pressure transmitter was used to measure the pressure difference between the venturi throat and the upstream location. The customised venturi tube was inserted into a 5/16 inch T-piece compression fitting so that the venturi throat pressure can be measured accurately. The details of the construction, testing results and calibration will be discussed in Appendix D.6.

4.7 Control cabinet

All electronic control units and the dynamometer were connected and controlled by the control modules mounted in the control cabinet. The control unit of the dynamometer has been discussed and is shown in Figure 4-3. The rest of the electronic units are then connected to the Allen Bradley MicroLogix 1200 PLC, including solenoid valves, sensors, relays, starter motor, etc. The Allen Bradley PLC is shown in the figure below.

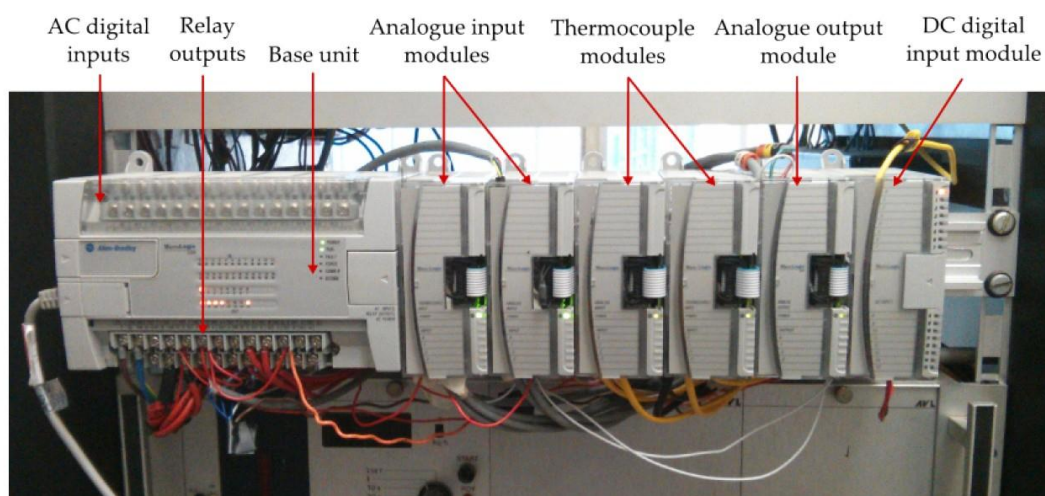


Figure 4-15: Main controller and separate modules of the PLC (Luiten, 2015)

The PLC consists of one main controller and six separate modules. The main controller is used to supply power to the separate modules and it also has a 24 V DC output unit, which is used to power all measuring equipment. The analog input modules can detect the signal of 4-20 mA for all pressure transducers and 0-10 V for the dynamometer speed and torque. The thermocouple modules can

maximally process the signal from eight different thermocouples. The analog output module was used to control the dynamometer and the throttle in the previous project. Now it is only used for communication between the dynamometer and ETA.

The relays were installed on a separate rail and they were positioned inside the control cabinet due to the space restriction. The relays were used to control the starter motor, the spark plug and all the solenoid valves. Due to the limited power output from the 24 V DC output unit of the PLC, two additional power supplies were used. The 24 V DC supplies not only supply the power to the relays, but also power all the solenoid valves. The solenoid valves require relatively high electric current during operation. The stability of the power supply is another major concern to conduct the test safely. Therefore, it is best to use a separate power supply for the solenoid valves during the test.

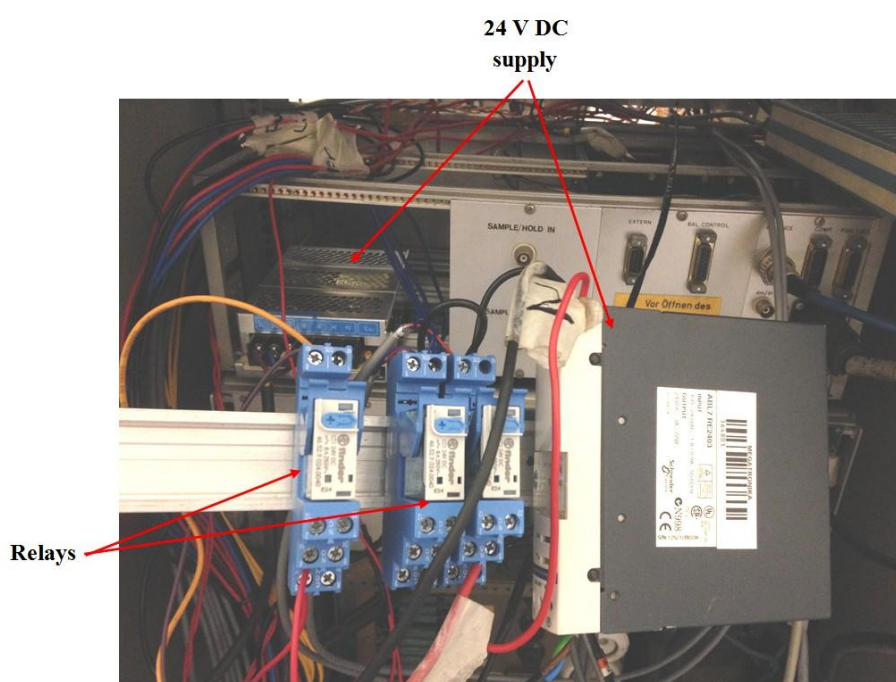


Figure 4-16: Relays and 24 V DC supply

5 Testing and results

5.1 Testing layout overview

The Rover gas turbine was tested on the test bench when fully equipped with the data acquisition instruments. For engine testing purposes, the first step was to obtain initial test result while running on kerosene. The second step was to set and test the new engine running procedure for kerosene. Finally, the engine was modified and tested with the new LPG supply system.

During initial tests, the basic engine behaviour, power output and other relevant data were recorded. However, due to the lack of previous experimental details, there was little information to serve as practical reference. The only available experimental record comes from Prinsloo (2008), but he paid more attention to the recuperator performance study. Besides, the engine used in the current project is different from the one used by Prinsloo (2008). Therefore, the initial engine testing results and behaviour of this particular test setup were critical for further tests.

Since the Rover 1S/60 gas turbine was designed to operate only on liquid fuel, some modifications had to be made to the original engine to operate with gaseous fuel. The engine operating condition is sensitive to the fuel flow rate and the flow rate controls the engine speed directly. Therefore, an accurate and reliable fuel flow control device is crucial to operate the engine on the gaseous fuel. It also needs a theoretical analysis for finding the exact amount of fuel required during the engine starting procedure.

Finally, the engine testing with gaseous fuel was conducted. In this part, one of the most important tasks is to start the engine smoothly and set up a repeatable starting procedure. During the engine starting procedure, the firing up timing and the exact amount of fuel injected are vital. The general engine performance and behaviour would be recorded and analysed.

The original test results measured by the data acquisition system are used for all the plots. Some of the plots do not use markers to indicate each measured value. By doing this, the plot is clearer and it illustrates the trend of the measured results. All the original test results can be found in the accompanying CD.

5.2 Engine starting and performance verification without load

The engine was fully equipped with the data acquisition system and all values were displayed on a monitor in the control room. As mentioned before, the original engine is self-regulated which indicates that once the engine is fired up, it would run up to its operating speed of 46 000 RPM. Nevertheless, there is still a chance that the engine might over speed due to incorrect adjustment of the fuel

pump or faulty, setting of other components. Such characteristics indicate that the initial test on kerosene should only focus on two tasks: the precise firing up time and preventing engine over speed/overheat.

5.2.1 Engine firing up

The proper ignition and complete combustion require a fine atomization of the kerosene from the fuel sprayer. The cone angle of atomization of this particular fuel sprayer is 110° . The lever of the shut-off valve on the fuel sprayer is either in the open or closed position. The sprayer requires a pressure of at least 0.1 MPa (gauge pressure) to produce a fine atomization and any higher pressure will not change the angle of the atomization. However, if the sprayer is opened with a pressure under 0.1 MPa, it cannot produce an acceptable atomization. Instead, only large fuel drops will be injected to the combustor. This results in losing large quantities of fuel and it prevents building up of the fuel pressure, thus, it becomes a vicious cycle that cannot be recovered automatically. When a large amount of un-atomized fuel enters the combustor in a short period, the combustor will be “flooded”. The excessive fuel will cause incomplete combustion and the flame tube will not be long enough to contain the flame. The high temperature flame may damage the turbine stator and rotor, especially when the engine speed is low so that the cooling air is insufficient. Therefore, the liquid fuel must be perfectly atomized, which means the fuel pressure must be higher than 0.2 MPa to inject the fuel.

To study the engine and fuel pump behaviour during the starting procedure, several tests were carried out. The pressure to open the fuel shut-off valve is set to 0.4 MPa to maintain a fine atomization. Opening the fuel valve at a high pressure (higher than 1.0 MPa) will introduce a large volume of atomized fuel into the combustor and it will cause violent combustion or even an explosion inside the combustor. This should be avoided as far as possible to minimise the damage to the engine.

Figure 5-1 shows the relationship between the engine speed and the fuel pressure during several different tests. In the figure below, the top of each curve indicates the moment of opening the shut-off valve. Before the engine speed reached 7 000 RPM, the fuel pump was able to build up the required pressure of 0.4 MPa to open the shut-off valve in all five tests. When the engine passed 7 000 RPM, the engine speed and the fuel pressure had a one-to-one correspondence relation. The engine speed and fuel pressure had a good linear relationship after opening the shut-off valve.

The most important fact from the figure is that fuel pressure before the shut-off valve opened did not match each other for the different tests. After considering all the possible circumstances, it is believed that this huge difference in pressure level is caused by the air trapped in the fuel pump. When the fuel pump was completely filled with kerosene, it built up the pressure straight away resulting in a rapidly

increasing pressure. If there were some air trapped in the fuel pump, the efficiency of the pump would be affected significantly. The pistons inside the pump would continuously compress the air instead of the fuel. The air in the piston could be compressed many times without being ejected due to the compressibility of air. The fuel pump could only work efficiently after pumping out all the air.

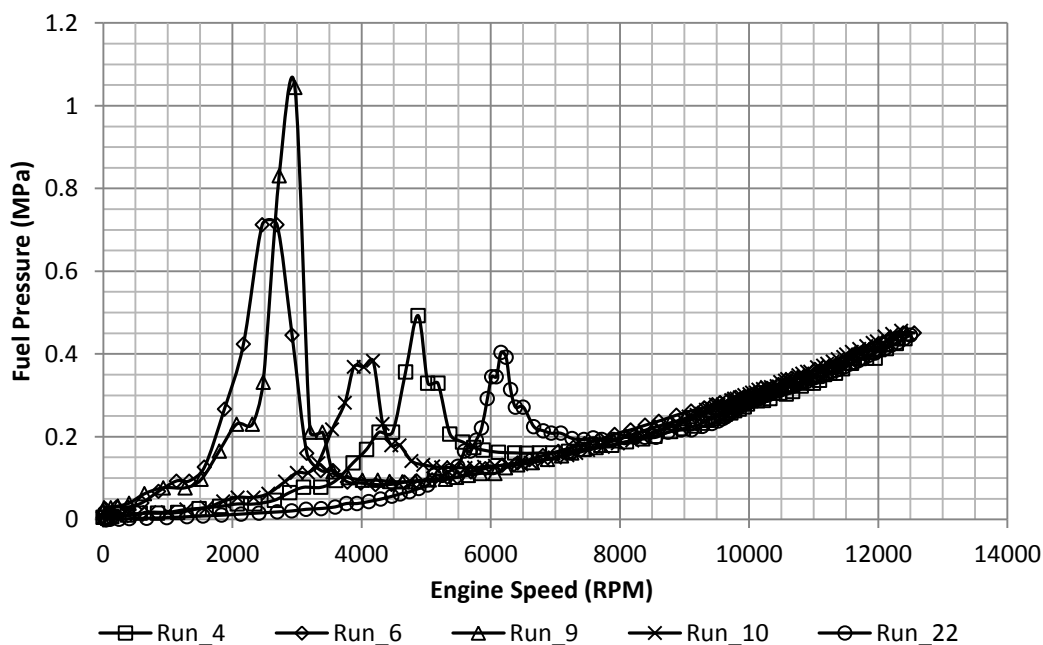


Figure 5-1: Relationship between the engine speed and the fuel pressure

According to the Rover maintenance manual, the fuel pump needs bleeding by unscrewing the bleeding bolt located on top corner of the pump main body. This procedure should be done every time before cranking the engine to ensure the pump is filled with the kerosene. Failure to do so could result in lack of lubrication and the pump would be unable to build up the pressure as discussed above. However, this procedure cannot eliminate all the air in the pump. In “Run_22”, the engine had not been running for several days. During the start procedure, the pressure-building rate was relatively slow so that the shut-off valve could only be opened when the engine speed reached 6 000 RPM to produce sufficient pressure. This is not a major problem during the starting of the engine and such a low pressure-building rate is to be expected every time in cold start condition.

When it comes to “Run_6” and “Run_9”, there was a rapid increase in fuel pressure when the engine speed was low. The pressure changed so fast that human reaction could not keep up to ensure opening the shut-off valve exactly at 0.4 MPa in the practical test. In fact, the pressure rose from 0.2 MPa to nearly 1.1 MPa in less than 0.5 seconds in “Run_9”.

Referring to test results, the starting oil temperatures of “Run_6” and “Run_9” were 67.5 °C and 54.4 °C. It indicated that these tests with a high pressure increasing rate were positioned at the second, third or even further position in a series of engine tests when the engine was still warm. Because of the previous tests, the air in the fuel pump was completely pumped out. This rapid rise in fuel pressure could be dangerous because the sprayer injected an excessive amount of atomized fuel in a short period at low engine speed and this may result in violent combustion.

The extremely high fuel pressure during the warm engine starting can be relieved by loosening the fuel accumulator, where it is attached onto the fuel sprayer. It can discharge the excessive pressurised fuel from the fuel line through a plastic tube. However, this technique cannot prevent the circumstance completely. It is best to keep at least 30 minutes between two individual tests to avoid excessively high fuel pressures.

To have a better view of the fuel pressure during the starting procedure, the figure below shows the relationship between the fuel pressure and the time.

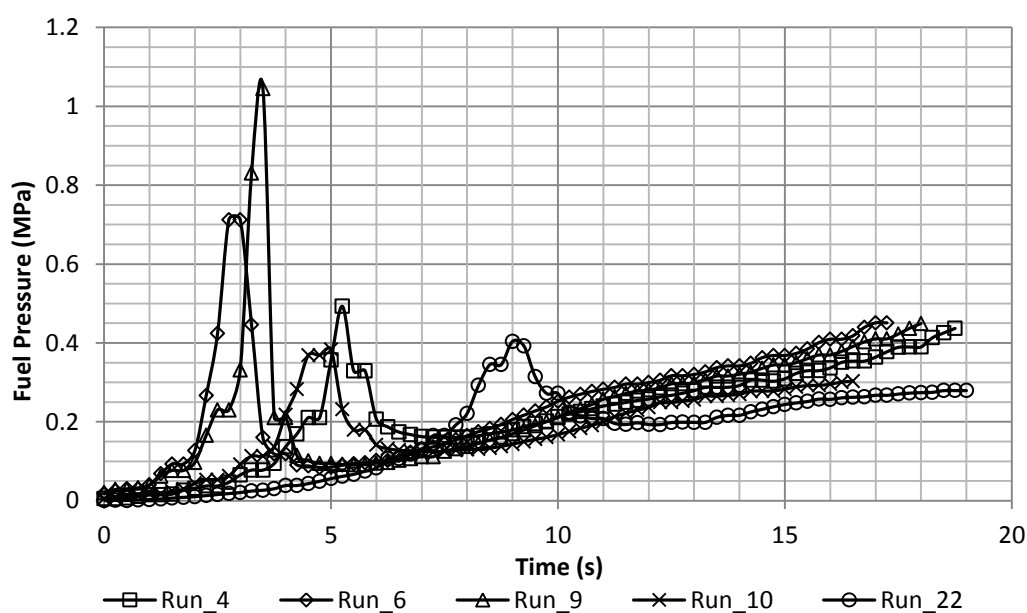


Figure 5-2: Fuel pressure change along with time

By considering the time, “Run_22” clearly took more time to reach the required fuel pressure for opening the shut-off valve than “Run_6” and “Run_9”. After opening the valve, the increasing rates of fuel pressure from each test were similar even though the valve opening times were different. A slow increase in the fuel pressure should be expected during the cold engine starting and it could take up to approximate 10 seconds to reach the required pressure. The fuel pressure also required extra attention when starting a warm engine due to its very rapid rate of increase.

5.2.2 Performance verification without load

After understanding the precise engine firing-up sequence, engine performance verification without load could be carried out. The engine is almost 50 years old since it was built in the 1960s. Due to the lack of repair work documentation, the engine condition was unknown. It could be expected that the engine performance would not meet the original certified standard.

The test was designed to allow the engine run up to its full speed and maintain the idling condition for several minutes without applying load. During the idling condition, it was important to monitor the EGT, oil pressure/temperature and other relevant readings to ensure the engine was in a good working condition. According to the Rover manual, once the engine reaches its maximum speed, it is important to check the instrument readings below:

- Oil pressure should be approximately 18 lb./in² (124 kPa) and must not be less than 7 lb./in² (48 kPa).
- The bearing seal air pressure should be approximately 5 in/Hg to 8 in/Hg (16 932 Pa to 27 091 Pa).
- The engine speed should be 47 000 ± 500 RPM. (Rover Gas Turbine Limited, 1966)

After the EGT stabilises, check the above readings again and the following instrument readings:

- The EGT should not exceed 400 °C.
- The oil temperature must not exceed 110 °C.
- The compressor delivery air pressure should be approximately 26 lb./in² (179 kPa) to 31 lb./in² (214 kPa).
- The engine speed should be 47 000 ± 300 RPM. (Rover Gas Turbine Limited, 1966)

The checking list was obtained from the Rover maintenance manual. The relevant test results will be discussed in the following sections.

Figure 5-3 illustrates the oil pressure and the bearing seal air pressure as listed in the check list above. One can clearly find that the test results did not match the requirements in the Rover manual. The oil pressure was not stable during the test of “Run_22”. From the 90th second after the start, the oil pressure started to decrease steadily due to the decreased viscosity caused by the increasing oil temperature. Besides, the oil pressure was approximately 100 kPa higher than the required value in the Rover manual. After careful thought and some discussions, it was believed that the higher oil pressure would not damage any components or

affect the engine performance. The oil pressure was kept within the limit as discussed previously after the EGT stabilised.

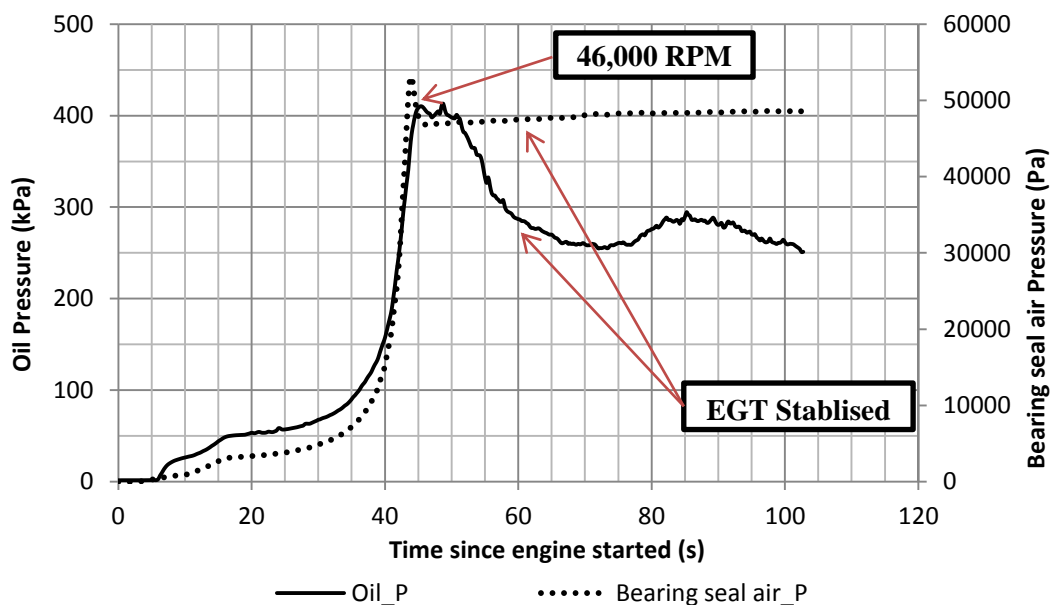


Figure 5-3: Oil pressure and bearing air seal pressure along with time (Run_22)

The figure below shows the engine speed along with time. Clearly, the engine speed increased slowly before 15 000 RPM. It is then followed by a rapid increase up to 46 260 RPM and the speed was kept stable from the 45th second. Compared to the requirements of $47\,000 \pm 500$ RPM and $47\,000 \pm 300$ RPM, the engine speed was slightly off the lower limit. After considering all relevant factors, it was believed a slightly off-limit engine speed would not cause any damage.

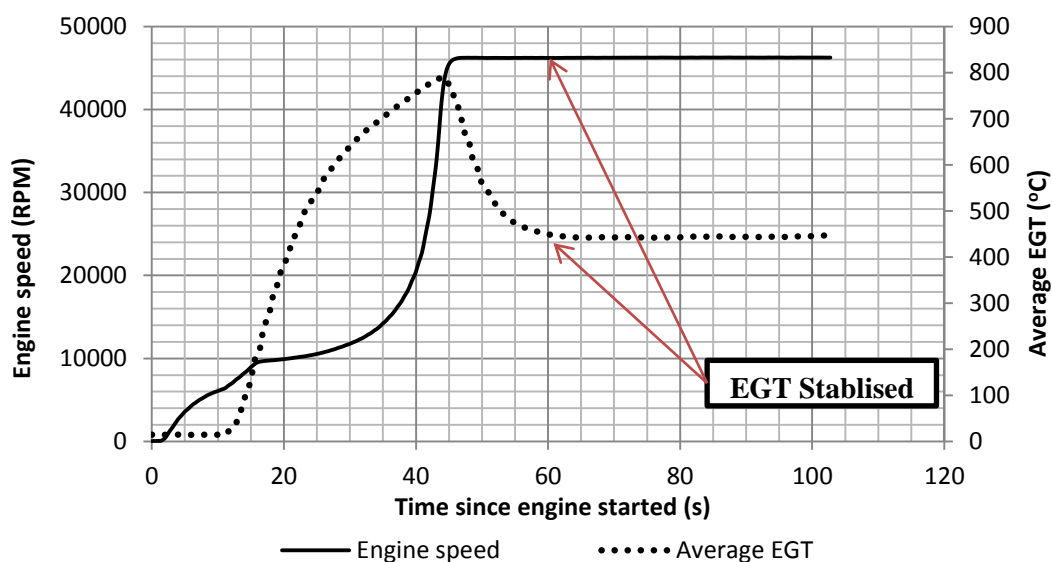


Figure 5-4: The engine speed and the average EGT along with time (Run_22)

There were still three readings to be checked after the stabilization of EGT. The average EGT was used for the checking list and it became stable at the 60th second as shown in Figure 5-4. The EGT recorded from the test is approximately 40 °C higher than the maximum allowable value of 400 °C. Although the EGT was higher than the requirement, there was no significant impact on other components and the engine condition. This is because the maximum continuous running EGT is 560 °C, which is much higher than the temperature readings in the current test. The EGT still needed to be monitored at all times during the test.

The oil temperature and compressor delivery air pressure are shown in the figure below.

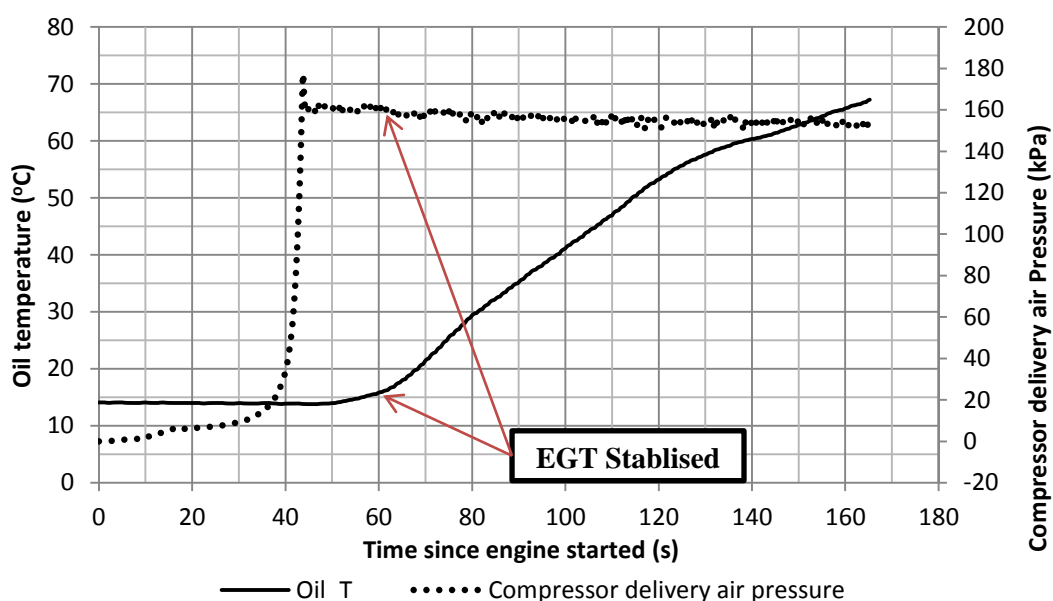


Figure 5-5: Oil temperature and compressor delivery air pressure along with time (Run_22)

The average EGT stabilised after 60 seconds. The oil temperature steadily increased from the 60th second onwards and it was kept below 110 °C during the whole test. However, the oil temperature would exceed 110 °C if the test continued for approximately 5 minutes due to the lack of oil cooler. It was necessary to monitor the oil temperature and terminate the test before it reached the maximum allowable temperature of 110 °C. Generally, the oil requires approximate 30 minutes between two tests for cooling down.

The compressor delivery air pressure was directly related to the compression ratio. It describes the air pressure before reaching the combustor. During the test, there was an obvious pressure drop at the 44th second and it may be caused by the possible movement of the shaft, however, the exact explanation is still unclear. After the EGT stabilised, the pressure had a slight tendency to decrease during the test. The results showed the compressor delivery air pressure varied between 150

kPa and 160 kPa while the standard requirement was 179 kPa to 214 kPa. The low pressure would decrease the engine performance but would not have other negative effects to the engine.

As mentioned previously, the Rover gas turbine is almost fifty years old and it is easy to understand that the instrument readings of the engine are off the standard limits due to its extremely long lifetime. By analysing the test results above, it was found even the data acquired did not match the standards from the manual but those values kept its own standards. Therefore, it is important to set up a new operating standard for the current condition of the engine.

5.3 General engine test for setting new operation standard

The engine is tested to acquire all relevant data after the performance verification. By combining the following results and those from the previous sub-chapter, a new operating standard can be set for this particular Rover 1S/60 gas turbine.

5.3.1 Fuel pressure and engine speed

It starts with one of the most important parameters for gas turbine operation: fuel pressure. The detailed behaviour of the fuel pressure before firing-up has been discussed previously. The following content will focus on its behaviour during a complete engine test.

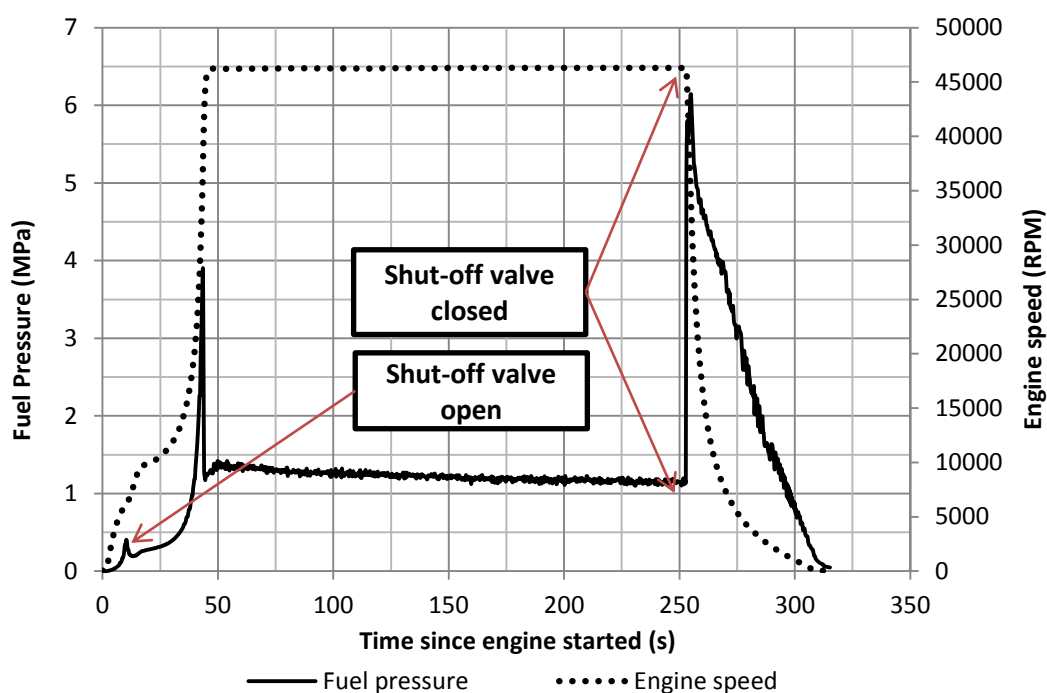


Figure 5-6: Fuel pressure and engine speed along with time

The detailed fuel pressure behaviour during the engine-cranking period has been discussed in Chapter 5.2.1 and normally a starting procedure can take up to 25 seconds. The fuel pressure had a steady increasing rate before it reached 0.5 MPa. After opening the shut-off valve, the pressure and the engine speed shared steeply increasing profile until the engine speed reached 46 000 RPM as shown in Figure 5-6. Before the fuel pressure stabilised, there was a significant pressure drop. This sudden pressure drop was caused by the opening of the governor spill valve as discussed in Chapter 3.6.

During idling, the fuel pressure stabilised at 1.25 ± 0.1 MPa. In longer term engine operation, there was a slow but steady decrease in the fuel pressure, which was 985 Pa per second. It was most probably caused by the oil temperature increasing, which would heat up the fuel pump thus affecting the governor leaf spring inside the pump. The decrease in the fuel pressure was so small that it could not affect other instrument readings or working condition of the engine.

The fuel shut-off valve was closed at the 253rd second after engine start up. The closed valve cut off the fuel supply to the combustor, therefore the engine speed started to decrease immediately. This action also closed the exit of the pressurised fuel but the pump was still working during the engine shut down procedure. This caused an immediate, dramatic increase in fuel pressure. The pressure rose from 1.13 MPa to 5.08 MPa in less than 0.25 second and even reached more than 6.0 MPa. The actual pressure could be even higher than 6.0 MPa because the pressure value had already passed the limit of the pressure transducer, which had a maximum of 5.0 MPa. However, the transducer would not be damaged according to its specification sheet. The pressure then started to decrease due to the backflow of the high-pressurised fuel. It is suggested to avoid high pressure as much as possible to minimise the stress on the fuel sprayer and the pump.

In general, the fuel pressure is stable during the idling condition. Extremely high fuel pressure can be expected during the starting and shutting down procedures. The operating procedures should be followed precisely to conduct the engine test safely.

To set up a new operating procedure for engine starting, a study of the fuel pressure and the engine speed during the starting procedure should be carried out. Figure 5-7 illustrates these two parameters along with time during a complete starting procedure. As seen in the figure below, there was a sudden fuel pressure drop at the 10th second. Such a pressure drop was caused by the opening of the shut-off valve as discussed in Chapter 5.2.1.

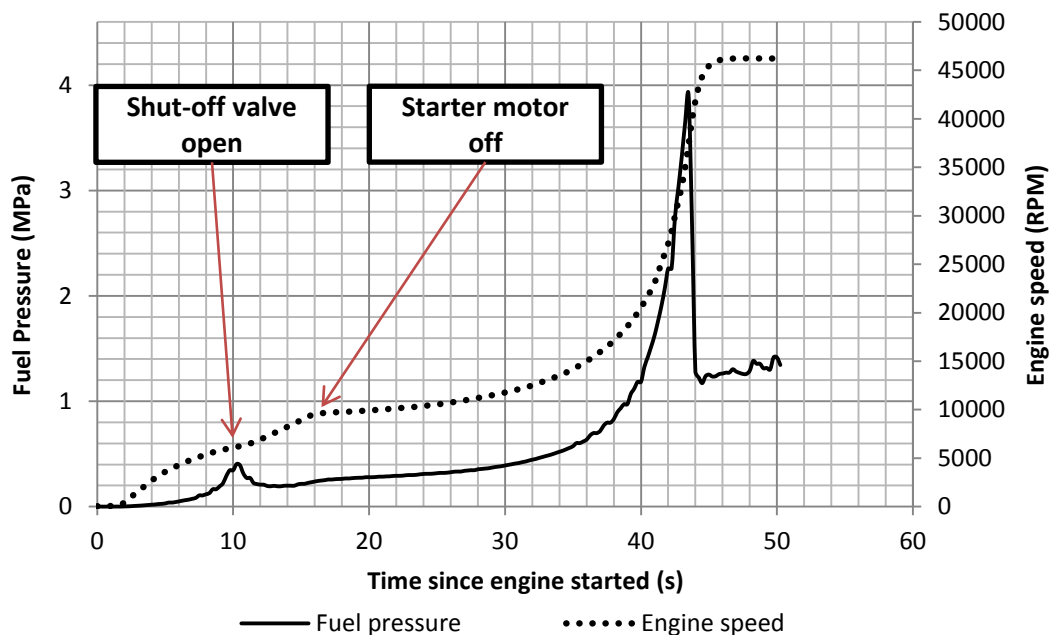


Figure 5-7: Fuel pressure and engine speed during the starting procedure

According to the results from several dry run tests, the starter was able to crank the engine up to 7 000 RPM when the battery was fully charged. During the first 10 seconds, the engine speed was increased at a constant rate because the engine was solely driven by the starter. The fuel valve opened at 10 seconds and it started the combustion to help the engine speed up. Therefore, the rate of acceleration improved slightly until the 16th second where it had an engine speed of 9 000 RPM. Such an improvement was caused by the combustion and the starter working cooperatively to increase the engine speed, until at the 16th second which is the exact time to switch off the starter motor.

After switching off the starter motor, the engine speed had a very low acceleration of only 222 RPM per second until the 34th second. The increase of the engine speed was then solely based on combustion and the combustion was not efficient at low RPM range due to the limited airflow. Therefore, the acceleration of the engine speed is low before the speed reached 12 500 RPM.

It can be expected that the acceleration of the engine would be much higher if the starter motor was still on. It is ideal to maintain a high increase rate of the speed to allow the engine reaching its idling speed as quickly as possible. This also helps to prevent carbon formation inside the combustor. To achieve such a high increase rate, it requires the starter motor to be switched off as late as possible to maximise the energy provided by the starter. However, this operation could cause the starter to overheat and it might damage the motor coil. Therefore, it is suggested to switch off the starter motor at 12 000 RPM.

The engine speed reached its maximum between the 34th to the 43rd second. The acceleration was caused by the increased performance of the fuel pump in this speed range beyond 15 000 RPM.

As mentioned at the beginning of this sub-chapter, there was a significant fuel pressure drop just before engine speed reached its maximum as shown in Figure 5-8. The fuel pump consists of a pressure relief valve, which is officially named the “governor spill valve”. The governor spill valve is closed when engine speed is low. At a certain speed, the valve will open due to the centrifugal force generated by the rotating pump drive shaft. When the valve is open, part of the high-pressurised fuel will flow through the valve then back to the low-pressure zone and this causes the sudden fuel pressure drop. The figure below shows the relationship between the fuel pressure and the engine speed during the starting procedure.

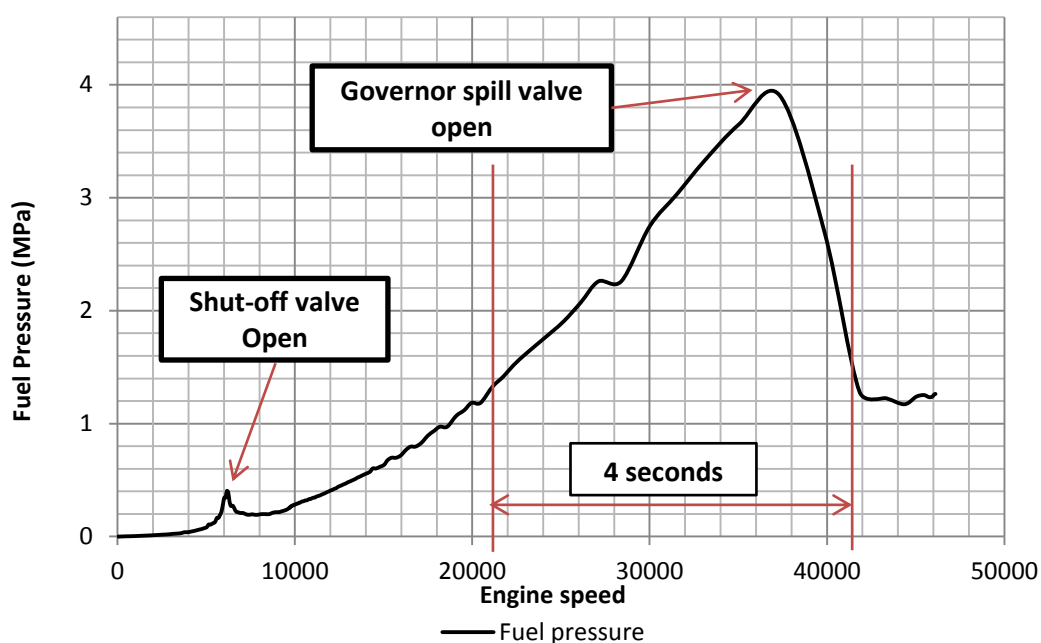


Figure 5-8: Relationship between the fuel pressure and the engine speed during the starting procedure

According to the test results, the critical speed for the governor spill valve to open was $37\,300 \pm 1\,500$ RPM. The exact speed was difficult to find by only analysing the available test results because the engine speed rose too fast. The duration for the fuel pressure rise from 1.3 MPa to 3.9 MPa (maximum during starting) and pressure drop back to 1.3 MPa only took 4 seconds. During this period, the engine speed rose from 21 138 RPM to 41 836 RPM, which had an acceleration of more than 517 RPM per 0.1 second. It was still possible to find the exact critical opening speed by increasing the frequency of measuring points or building a specialized fuel pump test rig, but it was not necessary since the pump

was functioning properly and in a good working condition. However, if any unstable fuel pressure or engine speed fault is experienced, it requires fine adjustment to the governor of the pump. The adjustment shifts the position of counterweight so that the governor spill valve can open or close at a different speed.

5.3.2 Exhaust gas temperature

The exhaust gas temperature is one of the most important factors to monitor the engine condition. There are four thermocouples located at the exhaust cone to measure the exhaust gas temperature. Monitoring all four individual values during the test is nearly impossible. Therefore, the average of these values can be calculated and used as indication of the EGT. The figure below shows the average EGT along with time during the starting procedure.

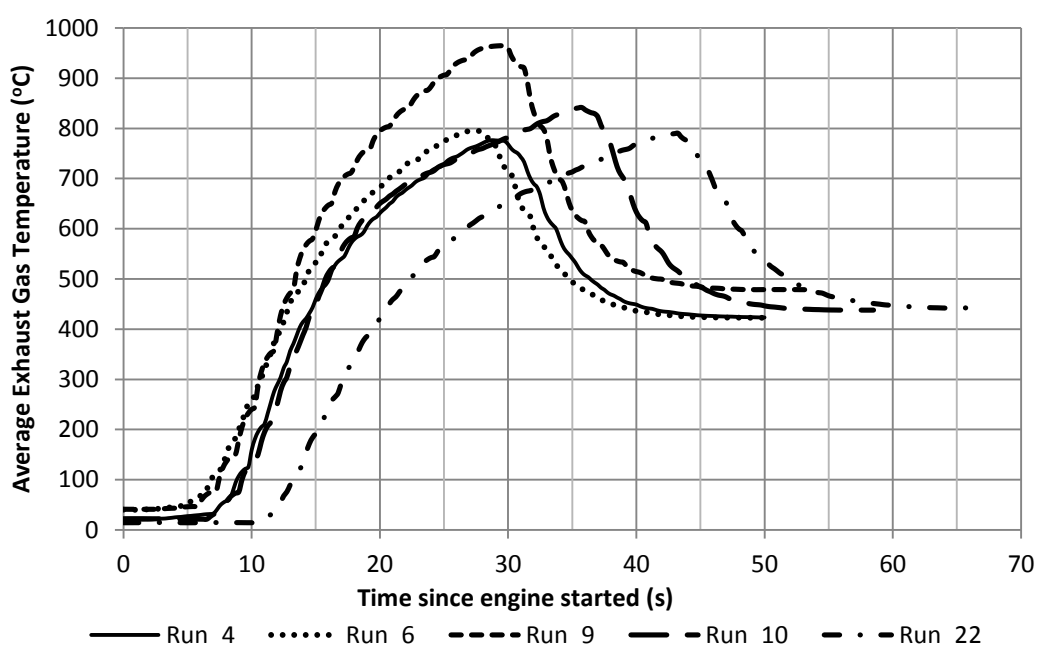


Figure 5-9: Average EGT along with time

Apart from the starting times, all average EGT profiles had a similar tendency along with the engine running time. The different points for temperature rise were caused by the fuel pressure build up rate as discussed in Chapter 5.2.1. The average EGT rose up to approximately 800 °C, or even 970 °C in “Run_9”, and then dropped to a range between 420 °C to 500 °C. According to the Rover manual, the maximum continuous running EGT was 560 °C and all values obtained from the tests were below the limit.

The reason for the excessively high temperature before it became stable was the flame that extended all the way from the flame tube to the exhaust cone. During the starting procedure, the compressor could not build up sufficient air pressure

and airflow to create a strong flow recirculation in the flame tube to trap the flame inside as discussed previously in Chapter 2.2.2. Meanwhile, a fuel rich combustion was taking place and some of the unburnt fuel could be delivered after the turbine section. The unburnt fuel could create a yellow diffusion flame that could be seen outside the engine. The figure below showed the visible flame during the fuel rich starting procedure.



Figure 5-10: Visible flame during the fuel rich starting procedure

Due to the asymmetric design of the engine, the flame is more likely to appear at the top right corner of the exhaust cone when viewed from the control room. This causes the thermocouple located at the top right corner to have a much higher reading than any of the others. Figure 5-11 shows the temperature readings from each thermocouple in the engine test of “Run_22”.

The position of each thermocouple is listed below:

- T_Exh_1: Bottom right corner, viewed from control room
- T_Exh_2: Bottom left corner, viewed from control room
- T_Exh_3: Top left corner, viewed from control room
- T_Exh_4: Top right corner, viewed from control room

Due to the limited slot provided by PLC, only three thermocouples were used to measure the EGT.

The thermocouple marked “T_Exh_4” is located at the point where the flame usually appears and the reading was obviously higher than the others. The

position clearly has a significant influence on the temperature reading. The flame during the starting procedure often can be observed and it will disappear as the engine speed increases. However, if the flame continues even after the engine reaches its maximum speed of 46 000 RPM, the engine should be immediately stopped and inspected.

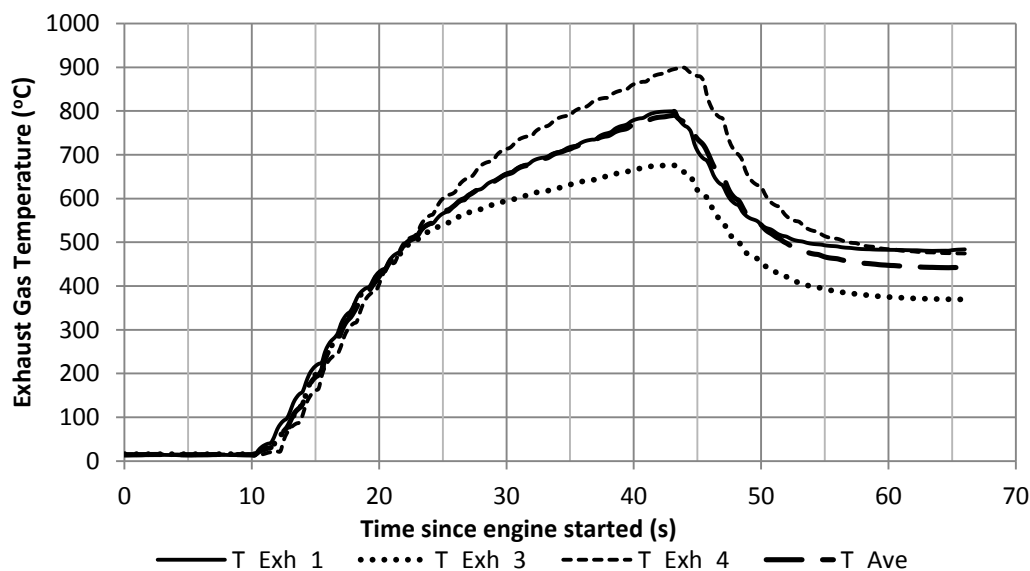


Figure 5-11: Typical temperature reading from different measuring points of the exhaust gas (Run_22)

When conducting the test, the average EGT needs to be monitored at all times. The average EGT may reach approximately 440 ± 40 °C depending on the ambient temperature, oil temperature and fuel atomization. When the engine is operating at 46 000 RPM without applying load and the flame is extinguished, the reading of “T_Ave” should not exceed 500 °C at all times. During the test without load, any sudden increasing in EGT is unacceptable and the engine should be stopped immediately.

5.3.3 Air mass flow rate and overall pressure ratio

The air mass flow rate is calculated by measuring the differential pressure of the conical air inlet duct designed by Prinsloo (2008). The construction of the conical inlet has already been discussed in Chapter 3.2. The equation used to calculate the mass flow rate is listed below:

$$\dot{m} = \alpha \varepsilon \frac{\pi d^2}{4} \sqrt{2 \rho_a \Delta P} \quad (5-1)$$

The variables in Equation 5-1 are explained in Table 5-1:

Table 5-1: Variables for the air mass flow rate calculation (Prinsloo, 2008)

Variably	Value
d, diameter of conical throat	0.11 m
ρ_a , ambient air density	Calculated
$a\epsilon$, compound coefficient	0.96

The diameter of the conical throat and the compound coefficient are fixed in these tests, but the ambient air density still needs to be calculated. The density is calculated by using the ideal gas law and the equation is listed below:

$$\rho_a = \frac{M_a P_a}{RT_a} \quad (5-2)$$

where

$$M_a = 0.02897 \text{ (kg/mol)},$$

$$R = 8.314 \text{ (J * K}^{-1} * \text{mol}^{-1}\text{)}$$

The ambient pressure P_a is measured by a barometer and the ambient temperature T_a is measured by a thermocouple located underneath the conical air inlet. The differential pressure is measured by a WIKA differential pressure transducer. Since the pressure value measured is very small ($< 2\,500$ Pa) and turbulence may appear around the measuring port due to the high volume ventilation in the test cell, the data has a severe fluctuation. A more practical reading can be obtained by using the concept of “Low Pass Filter (LPF)”, which is a build-in optional function of ETA. The LPF can be described as below:

$$\begin{aligned} \text{Input} = & [(1 - \alpha) * \text{Previous Input Value}] \\ & + (\alpha * \text{Current Input Value}) \end{aligned} \quad (5-3)$$

where α can be set to a different value and it is sets to the default of 0.3 for this project. Figure 5-12 shows two different reading with and without LPF.

“Run_17” and “Run_24” are two individual dry run tests without firing up the engine. The purpose of these tests are verifying the use of the LPF. The differential pressure data obtained from “Run_17” used the LPF and “Run_24” did not use it. As one can find, the value from “Run_24” was almost unreadable. It had a severe fluctuation and could not be processed to deliver the proper information. On the contrary, those values from Run_17 that used the LPF were more smooth and the pressure change could be described clearly. Therefore, all values for the differential air pressure used in this project are processed by using the LPF method.

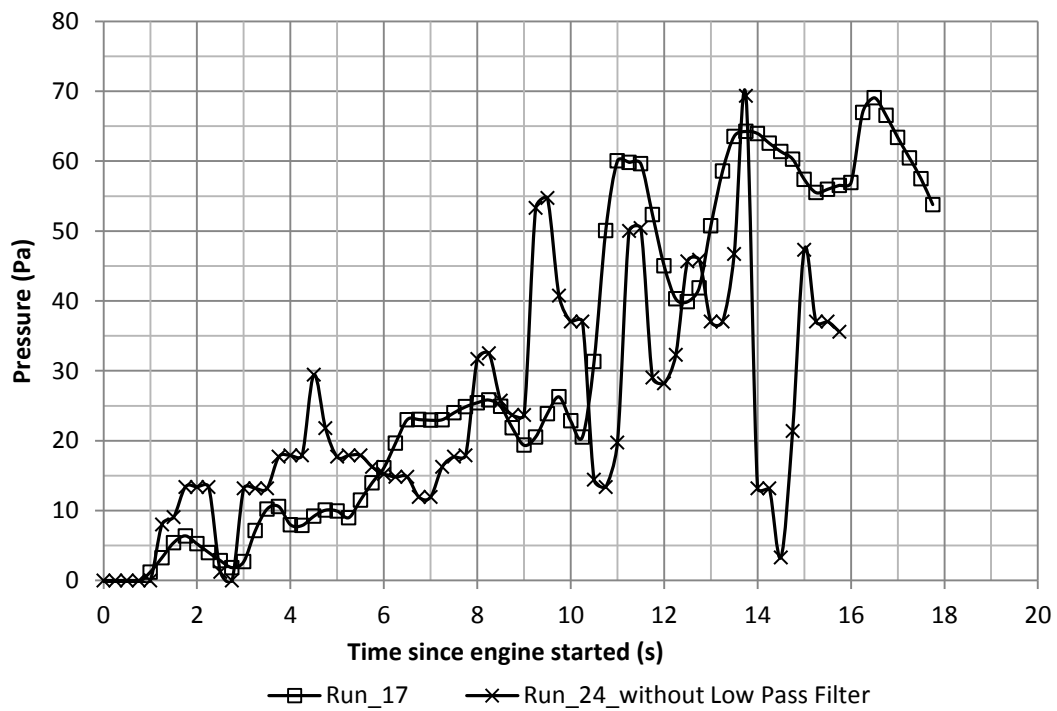


Figure 5-12: Differential air pressure along with time, with and without LPF

By selecting three individual tests (“Run_9”, “Run_10”, “Run_22”), a figure of air mass flow rate along with time is presented as below.

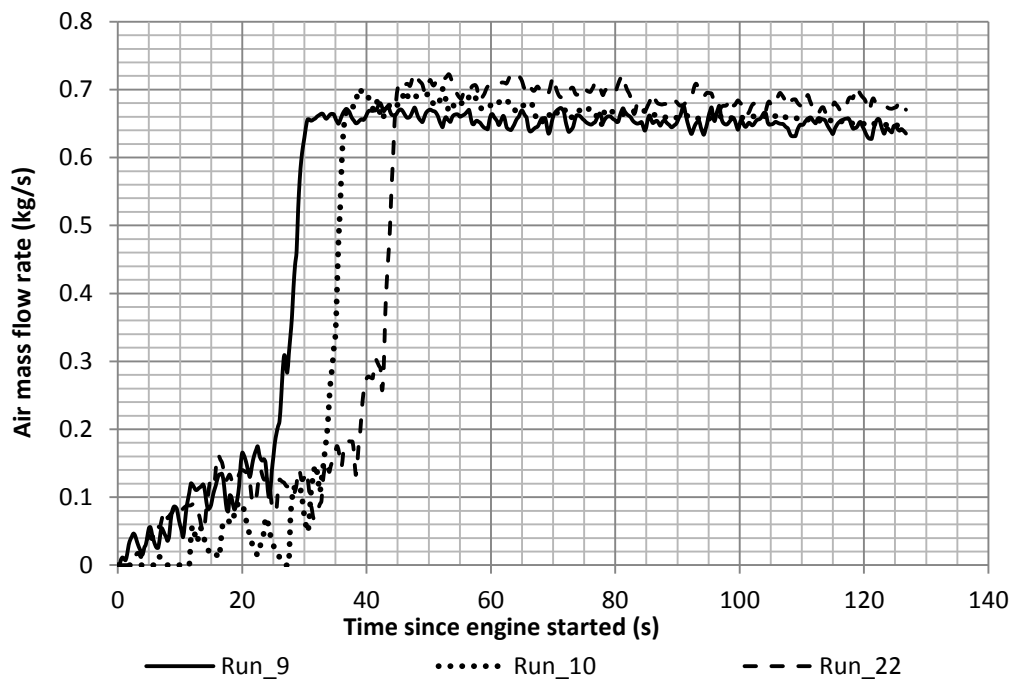


Figure 5-13: Air mass flow rate along with time from three different tests

Figure 5-13 illustrates the air mass flow rate during three different tests. Clearly, the air mass flow rate of three different tests all have severe fluctuations before they reach the points of 0.2 kg/s. After reaching 0.2 kg/s, the air mass flow rate rose so fast that it increased from 0.2 kg/s to 0.68 kg/s in just 6 seconds. On the contrary, it took almost 38 seconds for it to increase from 0 kg/s to 0.15 kg/s. After the rapid increase, the air mass flow rate reached its maximum and was kept stable during the whole tests. However, the air mass flow rate decreased slightly with time during idling. This was caused by the continuous running of the engine heating up the air, thus its density decreased.

The fluctuation during the starting procedure was mainly caused by the excessive sensitivity of the data capturing equipment. When the air mass flow rate equalled 0.15 kg/s, which was the maximum value during engine cranking, the differential pressure was only 117 Pa. Such a low pressure could be easily affected by any air movement around the air inlet including the airflow generated by the ventilation. Therefore, the original air mass flow rate during the starting procedure may not be used directly to analyse the engine performance. The instrument used is WIKA A2G-50 differential pressure transmitter with an accuracy of $\pm 1.5\%$ and it is calibrated by a Betz micromanometer every three months as suggested by the manufacturer.

The figure below shows the original air mass flow rate calculated by using the differential pressure transducer and the trendlines of these results.

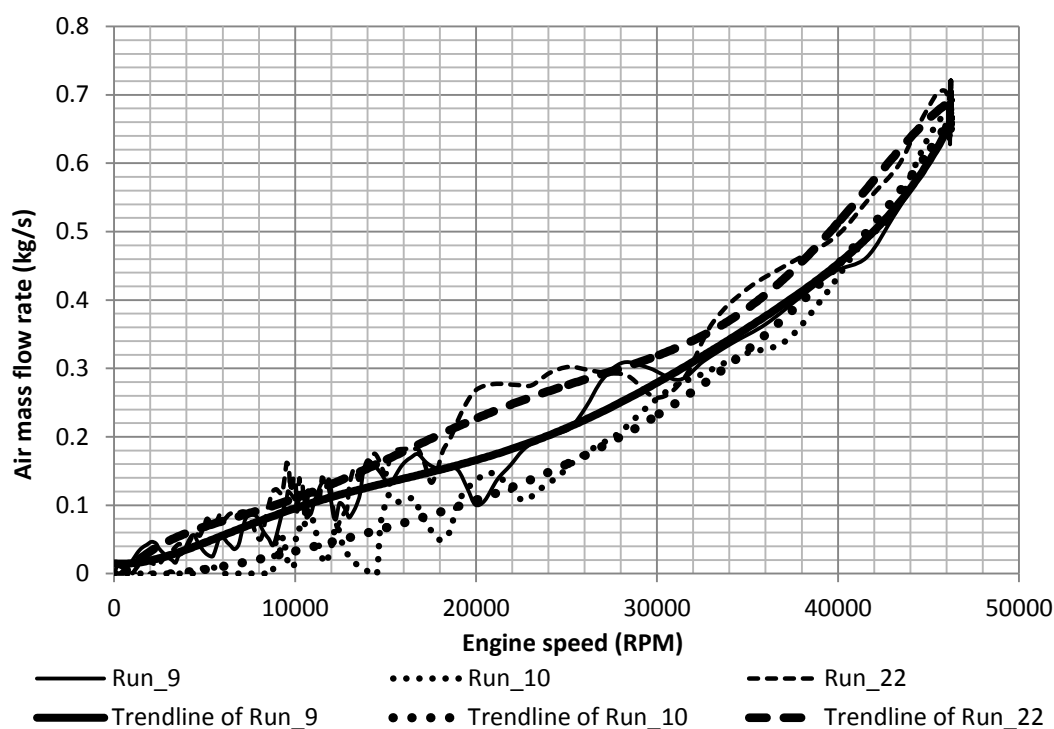


Figure 5-14: Air mass flow rate along with the engine speed

The air mass flow rate had a direct relation to compressor speed, which could be described as engine speed. The figure above shows the mass flow rate along with engine speed from three individual tests. As discussed before, due to the extremely low differential pressure, the data without processing cannot describe the behaviour of the mass flow rate accurately. In these tests, there were lots of fluctuations before the engine reached 20 000 RPM. Therefore, polynomial method trendlines were added to the figure to show the tendency of the air mass flow rate.

All these trendlines had a similar increasing tendency and they all gradually increased with the engine speed until reaching the maximum value. Except for trendlines, all original data shared the same tendency after the engine speed reached 30 000 RPM. After this point, the reading obtained from the differential pressure transducer was high enough to other airflow impact from the environment.

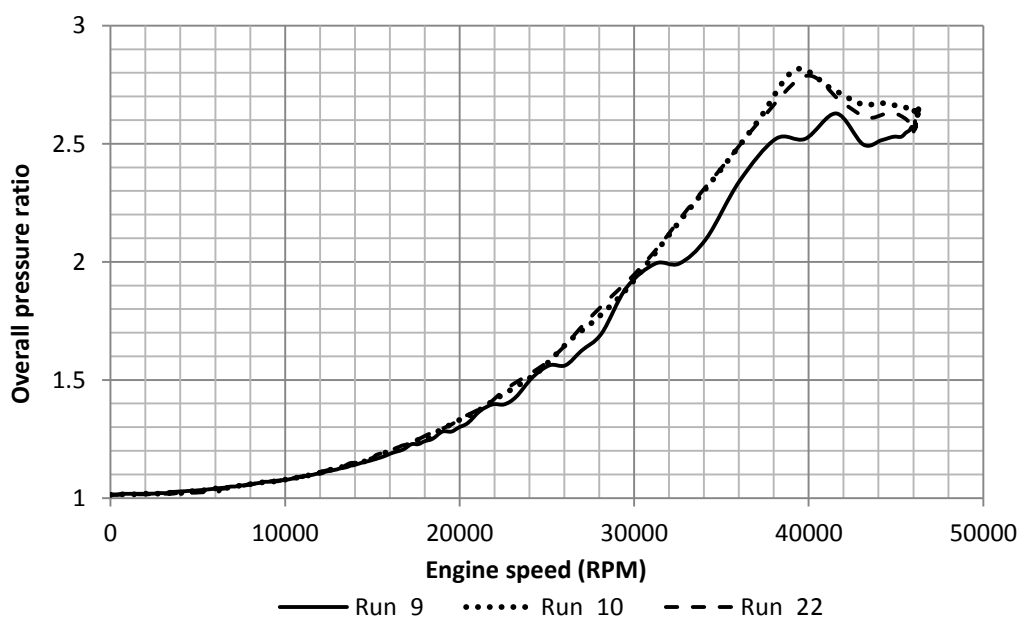


Figure 5-15: Overall pressure ration along with the engine speed

The overall pressure ratio showed good correspondence with the engine speed from “Run_10” and “Run_22”. However, in “Run_9” there was some fluctuations between the engine speeds of 24 000 RPM and 46 000 RPM. The overall pressure ratio still showed a same tendency as those from another two tests. The explanation for these fluctuations is unclear. The overall pressure ratio increased smoothly with engine speed until the speed reached 40 000 RPM. It reached a maximum of 2.82 and then the ratio decreased to a steady state value of 2.6. The peaks shown in Figure 5-15 are most probably caused by the movement of the shaft, however, the exact explanation is still unclear.

The behaviour of the overall pressure ratio during the whole test is shown in the figure below.

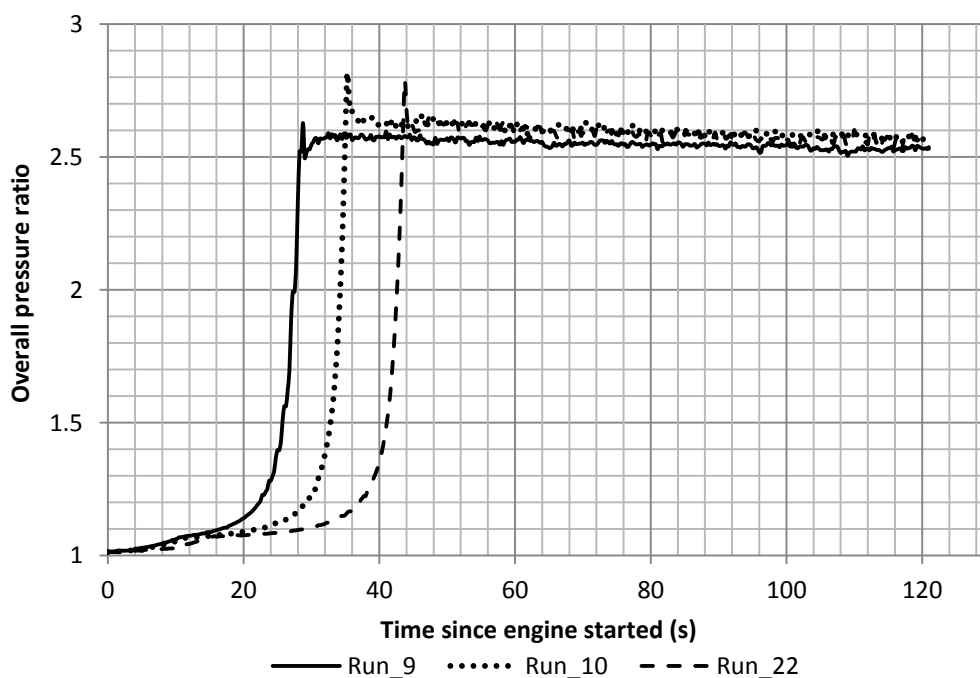


Figure 5-16: Overall pressure ratio during the whole engine tests

During the engine cranking period, the overall pressure ratio increased slowly. It then increased rapidly to its maximum and then dropped to the nominal value of 2.6. From the 40th to 120th seconds there was a slight drop in pressure ratio. This was caused by the ambient air temperature increasing slowly but steadily during the whole engine testing and it decreased the density of the inlet air.

The compressor map can describe the relationship between air mass flow rate and the overall pressure ratio. Unfortunately, the compressor map is not available in the Rover manual. Due to the limitation of the equipment and time, it is also impossible to draw a compressor map from the experiments. However, the relationship between the air mass flow rate and the overall pressure is still available from the tests and the results are shown in Figure 5-18.

The data at a low air mass flow range had a lot of fluctuations due to the high sensitivity of the pressure measurement equipment as discussed previously. The trendlines of the original results use a thicker line style. They use a polynomial method with an order of 6 for the best results. All three trendlines showed a similar tendency which was a steady increase followed by a slightly decrease. The curves did not match each other perfectly because the engine firing up timing had a slight difference.

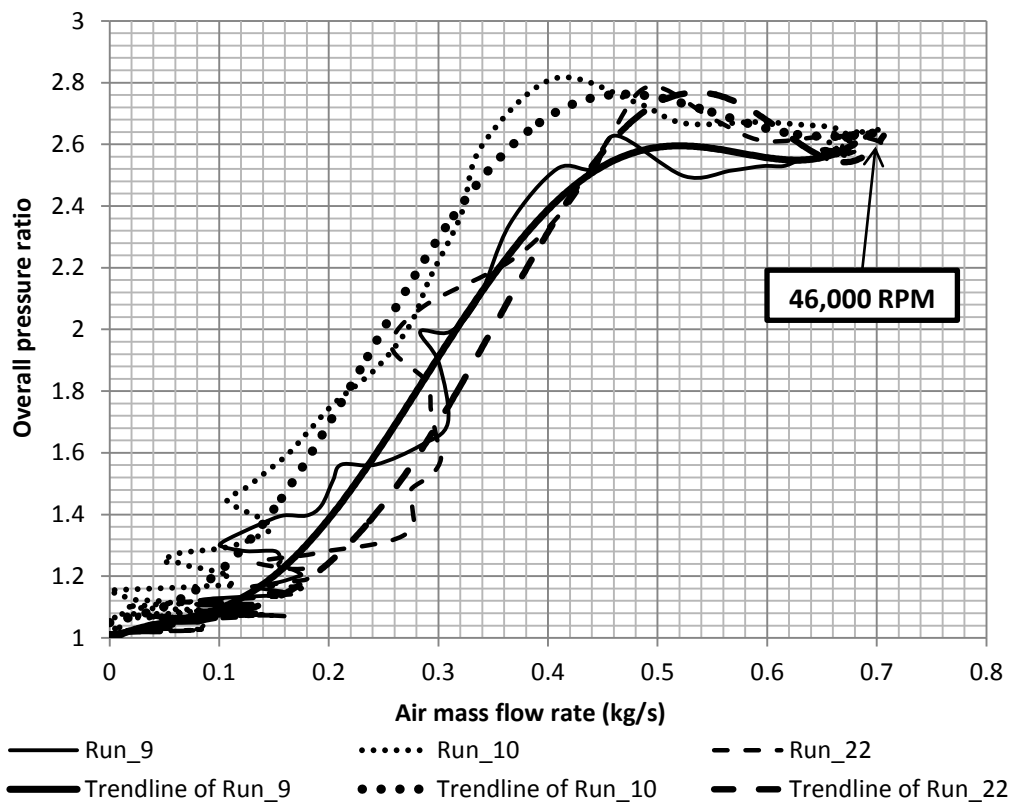


Figure 5-17: Relationship between the air mass flow rate and overall pressure ratio

The efficiency of the compressor is another important factor for the performance evaluation. When the engine starts from still to the maximum speed, the efficiency of the compressor is changing all the time. However, it is not important to analyse the compressor efficiency at each different speed because the engine is designed to operate only within a small speed range. According to the Rover engine test manual, the idling speed is $47\,000 \pm 300$ RPM and the speed under load is $46\,000 \pm 500$ RPM (Rover Gas Turbine Ltd., 1966). Therefore, the normal operating speed has a very small range and it is not advised to operate the engine out of this range due to the possible decrease of the compressor efficiency.

5.3.4 Air inlet and main air casing temperature

The air inlet temperature is related to many other factors including engine performance and it indicates the environment for the engine test. The air is sucked into the compressor and it flows through the diffuser into the main air casing. The main air casing contains compressed air and the air will be delivered to the combustor. The figure below shows the temperature profiles along with time.

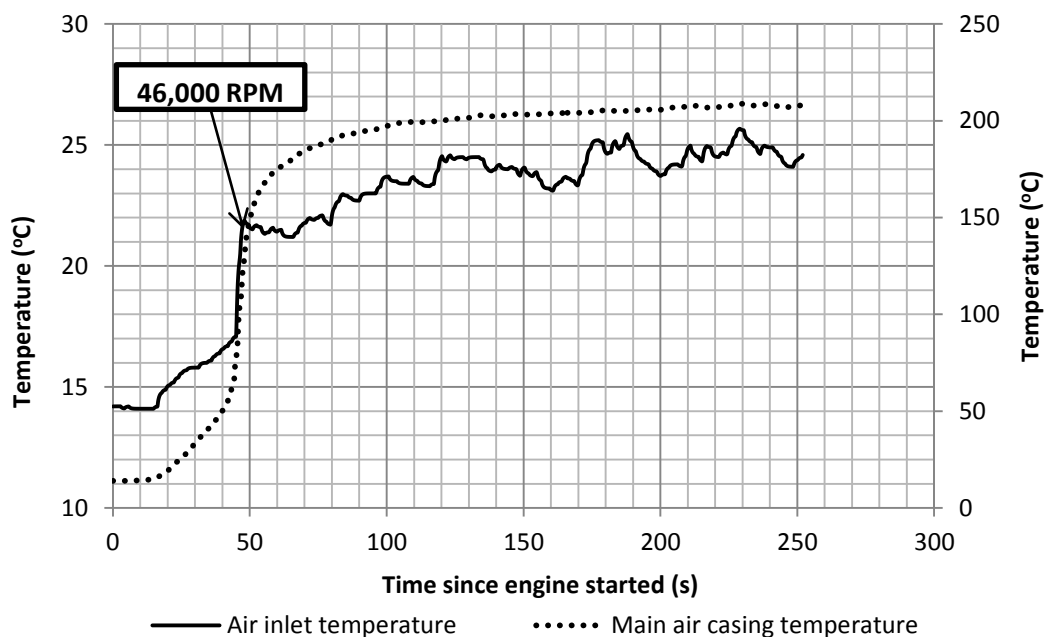


Figure 5-18: Air inlet and main air casing temperature during a complete engine test

The starting temperature at air inlet was 14 °C, which was the same as ambient air temperature. This indicated that the engine was started in a cold condition. The air inlet temperature rose rapidly to 22 °C when the engine reached the maximum speed of 46 000 RPM. Such a steep increase was caused by the running engine heating up the surrounding air and the warm air being circulated to the air inlet duct. During the engine test, the air inlet temperature had a steady increase with fluctuations. When the engine was running, it heated up the surrounding air and produced high temperature exhaust gas. The ventilation could not eliminate all the hot air and it may create turbulence around the engine. This would bring some hot air to the position where air inlet duct is located. The fluctuation of the temperature was caused by the mixing of hot air and fresh cool air from outside of the test cell. As long as the air inlet temperature was below 40 °C, the engine was still operational and tests could be carried out.

The temperature of the main air casing was measured by a single thermocouple located on the side of the engine body. It was supposed to monitor the temperature increase by the effect of compressor heating. However, it was found that the temperature reading could reach more than 200 °C during the engine test. The excessively high temperature reading was caused by the extremely hot exhaust gas flowing through the volute cone located inside the main air casing. The main air casing temperature rose to 180 °C in a short period of time after the engine started. After reaching 180 °C, the temperature then increased slowly with time. It rose from 180 °C to 208 °C in almost 3 minutes, which is an extremely slow increase rate. During this stable period, the heat absorbed from the exhaust gas

was only slightly more than the heat dissipation. It is advised to maintain the air casing temperature below 220 °C during all test conditions.

5.3.5 Oil pressure and temperature

The oil pressure and temperature along with time has already been illustrated in Figure 5-3 and Figure 5-5. The detailed behaviour has also been discussed previously. The oil pressure and temperature require constant monitoring during the whole engine test period because a lubrication system failure may damage the engine permanently. The oil pressure must not be less than 48 kPa and the temperature must not exceed 110 °C at any condition.

5.3.6 Needle valve control system test

A needle valve control system was designed to control the engine speed as shown in Figure 4-7 (right). The system consists of two needle valves and two solenoid valves, the details can be found in Chapter 4.3.2. It was designed to use needle valve to restrict the fuel flow rate thus control the engine speed. However, several attempts were made but the engine speed could not be controlled by the needle valves. The fuel pressure was extremely high and the restriction could not decrease the fuel flow rate to reduce the engine speed. In practice, the engine operated at its full speed all the time until the needle valve is fully closed. Therefore, the engine speed cannot be controlled by this system when the liquid fuel is provided from the original fuel pump.

5.3.7 New operation standards

After conducting several general engine tests, it was found that many readings measured during tests were out of the original ranges, which were set by the Rover Company. By considering the age of this particular engine, it is considered acceptable to have off-limit readings.

During the tests, all values measured from the engine had a stable and reasonable tendency. These facts indicated the engine could be operated safely under a new standard. Future experiments on the Rover gas turbine should follow the new standard and the old requirements can only be used as reference for the original factory design.

Therefore, a new operation standard will be set to suit the current condition of the engine. These standards for cold starting are listed below.

When the engine accelerates to its maximum speed, immediately check the following readings:

1. The oil pressure should be about 250 kPa and must not be less than 48 kPa.
2. The bearing seal air pressure should be between 46 000 Pa to 49 000 Pa.

3. The engine speed should be $46\,100 \pm 500$ RPM.

When the average exhaust gas temperature stabilises, check the following readings:

1. The average exhaust gas temperature may not exceed $480\text{ }^{\circ}\text{C}$. The temperature reading of each individual thermocouple may not exceed $500\text{ }^{\circ}\text{C}$.
2. The oil pressure must not be less than 48 kPa.
3. The oil temperature must not exceed $110\text{ }^{\circ}\text{C}$.
4. The engine speed should be $46\,100 \pm 300$ RPM.
5. The fuel pressure should be approximately 1.2 MPa and may not exceed 1.4 MPa without load.
6. The bearing seal air pressure should not exceed 51 000 Pa.
7. The compressor delivery air pressure should be approximately 150 kPa and may not be less than 140 kPa.
8. The differential air pressure measured at the conical inlet should be approximately 2 400 Pa.
9. The inlet air temperature may not exceed $50\text{ }^{\circ}\text{C}$.
10. The dynamometer cooling water temperature must not exceed $60\text{ }^{\circ}\text{C}$.

5.4 Engine test under load

In the previous tests, the Rover gas turbine had very good stability and repeatability on continuous running without applying load. A new standard for the normal engine operation has been set up to meet the current engine condition.

The next step is to conduct the test and record the engine performance under partial and full load. It is highly recommended to start the load test by only applying partial load to the engine because the engine behaviour under load is completely unknown. The engine was started and freely accelerated to the maximum speed. It required at least 20 seconds before all readings stabilised. The partial load test then could be carried out by applying load in small increments.

Due to the absence of throttle control on the Rover gas turbine, the engine speed could only be controlled by the dynamometer by using the “Speed Mode”. The “Speed Mode” required the manual input for a specific driveshaft speed and the dynamometer then adjusted the load to match its speed to the input value. However, it should be noted that the dynamometer would not response immediately after setting a new driveshaft speed value. According to several separate tests, the dynamometer would only apply load 8 seconds after setting a new speed value. When the dynamometer has already applied load, it will adjust

its load condition immediately if there is any change in the speed value. The details of these test will be discussed in Appendix D.5.3.

5.4.1 Engine power check

According to the Rover test manual, the engine can continuously produce approximate 45 kW while the EGT is 560 °C. The performance verification tests were carried out to verify the maximum output power of the engine.

After starting the engine, it would run up to its maximum speed freely and the load test would begin after the EGT stabilised and then started to apply load on the dynamometer in small increments, until the average EGT reached 560 °C. During the test, the average EGT could be pushed up to 600 °C, which is the temperature for the stress testing and the engine would not be damaged. The test results are illustrated in the figure below.

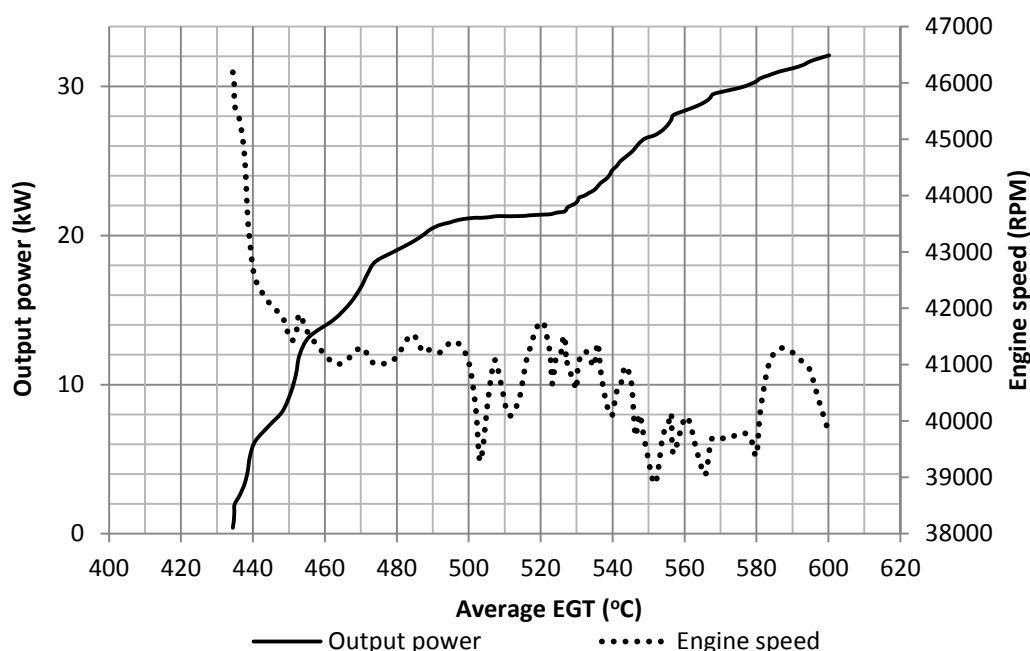


Figure 5-19: The output power and engine speed under different EGT

At the moment of applying load, the average EGT was 434 °C. By increasing the load, the dynamometer started to extract power from the engine. When the average EGT reached 560 °C, the engine output power was 28.4 kW while the engine speed was 40 079 RPM. However, the Rover manual indicated that the output power should be approximate 45 kW and the engine speed should be $46\,000 \pm 500$ RPM. The results were all below the requirements when the engine reached the designated EGT. The continuous output power (28.4 kW) was decreased by 36.9 % compared to the factory rated power (45 kW). The engine speed was also lower than the designated speed and this may be caused by an inaccurate setting on the fuel pump governor. As discussed previously, the engine

could no longer produce the factory rated power and the fuel pump governor requires maintenance. Therefore, it is not advised to stress the engine with the average EGT exceeding 560 °C when conducting continuous running test.

5.4.2 Fuel pressure and engine speed under 10 kW load

For further study, the engine is tested with an output of 10 kW so that the engine is not under a high stress condition. The fuel pressure is generated by the fuel pump and the pump is driven by the engine shaft through a series of reduction gears. Therefore, any change in the engine speed may influence the fuel pressure. The figure below illustrates the fuel pressure and engine speed along with the time under 10 kW power output.

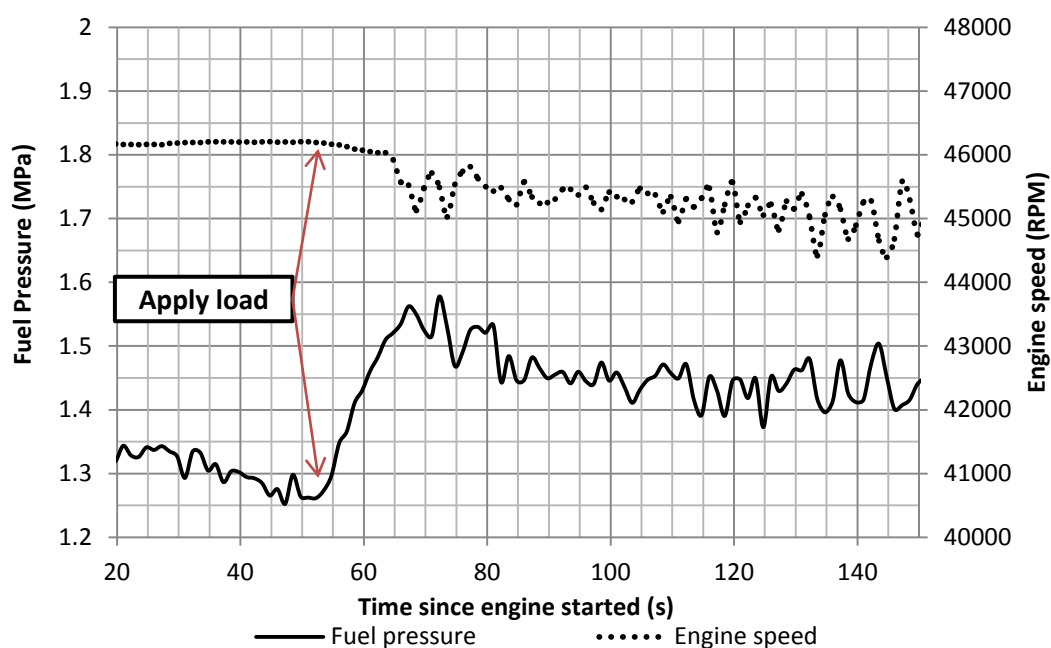


Figure 5-20: Fuel pressure and the engine speed during 10kW load test

The load was applied at the 52nd second. Thereafter the engine speed started to decrease and the fuel pressure started to increase. The load on the dynamometer directly caused the decrease in engine speed since it created a “clamping” force on the driveshaft. As mentioned previously, the decreased engine speed would reduce the centrifugal force generated by the fuel pump rotor and it resulted in a partially open governor spill valve. This would allow an increase in fuel pressure and the fuel flow rate. The fuel pressure and the engine speed was stable during the rest of the test. The fluctuations of the fuel pressure and the engine speed were caused by the constant adjustment of the fuel governor spill valve. Any small change in the engine speed could adjust the spill valve and then affected the fuel pressure. The fuel pressure was related to the combustion intensity, thus affecting the engine speed. The whole process could be described as a stable equilibrium system.

5.4.3 Fuel pressure and engine speed under various load

The relationship between the fuel pressure and the engine speed is clear under the 10 kW power output. Figure 5-21 illustrates the relationship of these two parameters with different power output. For research purpose, the output power in this test is higher than the advisable value, but the tests were only conducted over a very short period while the engine could still corporate with the stress.

As shown in the figure, the value of fuel pressure was almost constant between 10 kW to 20 kW outputs. When the output was more than 20 kW, the fuel pressure rose dramatically up to 3.5 MPa where it produced 38 kW. The engine speed was relatively stable between 10 kW to 20 kW outputs, which was similar to the fuel pressure. The speed only decreased from 41 700 RPM to approximate 40 000 RPM while output increased from 20 kW to 38 kW. According to the Rover manual, the engine speed should be $46\,000 \pm 500$ RPM when stress test is being carried out (Rover Gas Turbine Limited, 1966). In practice, the value of the engine speed was much lower than 46 000 RPM when the engine was under load.

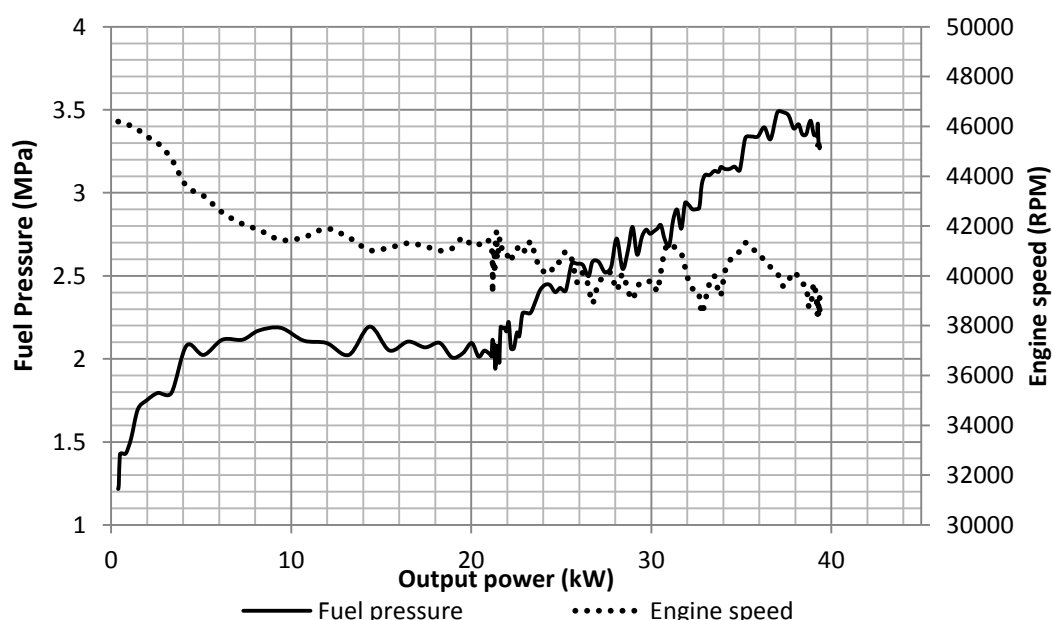


Figure 5-21: Fuel pressure and the engine speed under different power output

The decreased engine speed indicated that the engine was not at its optimum running condition when under load. As discussed in Chapter 5.4.1, the reduced speed is probably caused by inaccurate setting of the fuel pump governor.

5.4.4 Engine power and torque curves

After conducting several tests under load, the engine power and torque curves can be drawn as shown in Figure 5-22. The speed had severe fluctuations along with

the power and the torque during the tests. Several different tests have been conducted but the fluctuations could not be avoided completely. The thin lines in Figure 5-22 illustrates the original data and the thicker lines indicate the trends.

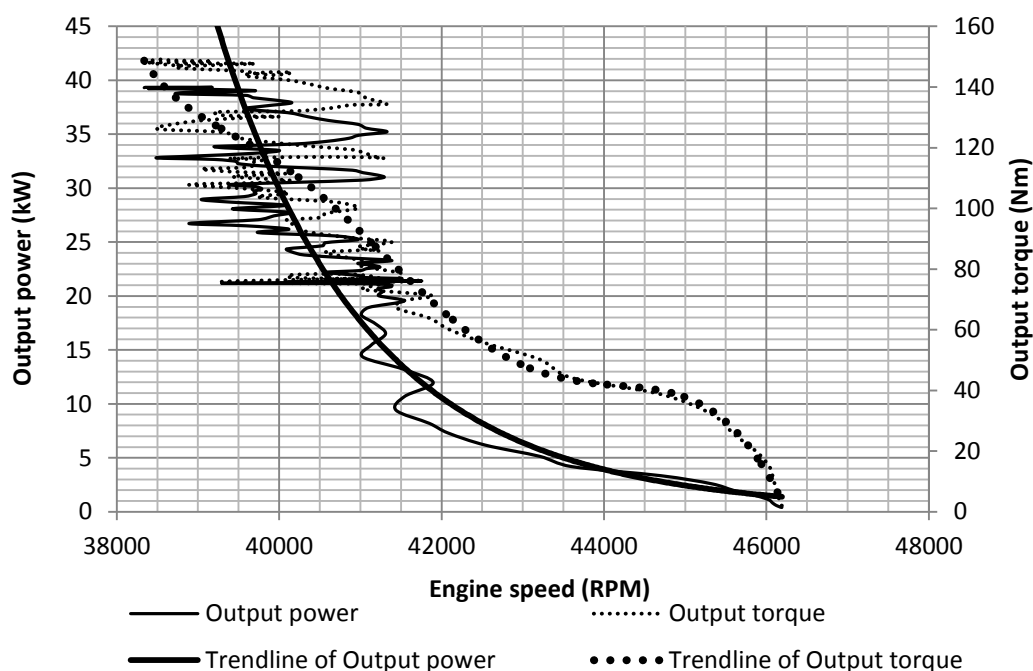


Figure 5-22: Engine power and torque curves

5.5 Engine test using LPG

After installation of the LPG supply equipment and the gas injector nozzle, the engine could be tested using LPG as the fuel source. Because this was the first test on the modified LPG gas turbine and the starting procedure had not been set, it was decided to minimise the complexity of the LPG supply system. Therefore, a 5 kg LPG cylinder was put in the control room and it was connected to the quick-action shut-off valve as shown in Figure 4-9 through a certified flexible LPG hose. The LPG flow rate then could be controlled manually and directly. Several short tests were conducted and the results will be discussed in the following section.

The first ignition attempt failed, when using the gas injector without modified caps. When injecting the LPG into the combustor, it could not be ignited by the spark plug. After conducting several tests on the gas injector, it was believed that the problem was caused by the gas injection angle. The details will be discussed in the Appendix C. After modifying the injection system, the gas could be ignited successfully by using the gas injector with type (a) cap as shown in Figure 4-10. The engine then started and it could run up to the maximum speed, determined by the gas injection orifice size, as shown in the figure below. The starting procedure will be discussed in Appendix A.

5.5.1 Average EGT and engine speed

During the test, the maximum speed of the engine was only 21 100 RPM because the gas flow was restricted by the gas injector for safety reason as designed. Unlike the original fixed speed design with the fuel pump, the engine speed could be control directly by the LPG cylinder valve, which controlled the gas flow rate. The average EGT reached its maximum temperature of 622 °C during the starting procedure and then dropped to a stable value of 515 °C for the rest of the test. The temperature was well below 560 °C (continuous running temperature) when the engine reached its maximum allowable speed. However, it should be noted that the average EGT of the idle running on kerosene is only approximately 430 °C, which is much lower compared to the current test. Such an increased EGT was caused by the lack of cooling air due to the lower engine speed. Since the average EGT was within the safety limit, the engine would not be stressed or overheated during the test, even when having reduced intake airflow.

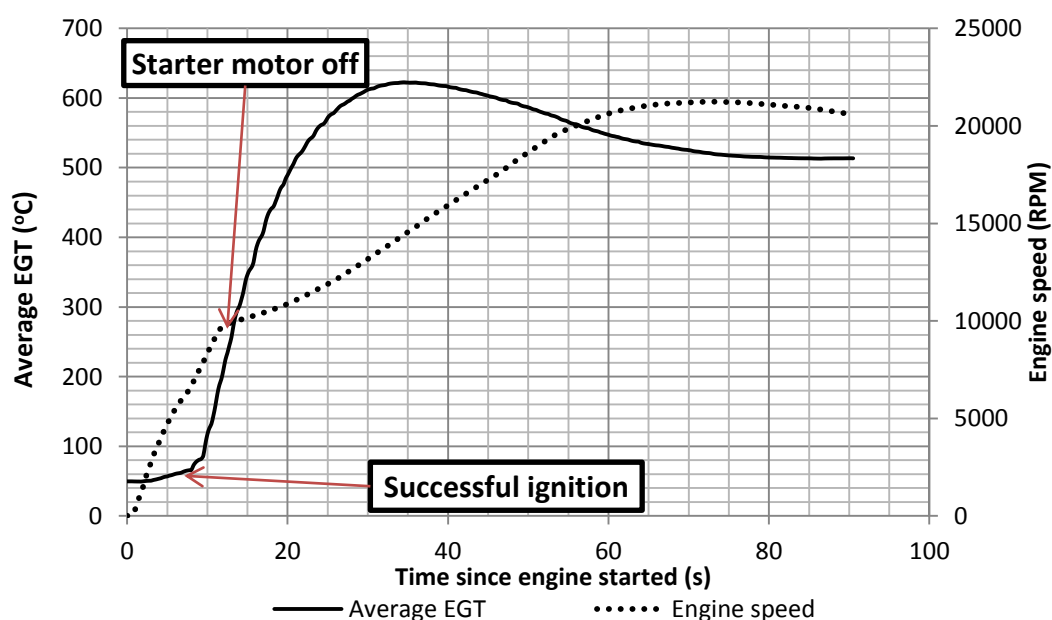


Figure 5-23: The average EGT and engine speed during LPG test

5.5.2 Air mass flow rate and overall air/fuel ratio

The air mass flow rate can be calculated by the differential pressure measured at the conical inlet throat and the LPG mass flow rate can be calculated by using the customised venturi flow meter. The overall air fuel ratio then can be drawn in Figure 5-24 and the figure also illustrates the air mass flow rate along with the time. The air mass flow rate has a peak of 0.25 kg/s, which is less than half of the value (0.6 kg/s) for normal operation. The most important consequence of having reduced intake airflow is the engine may not have sufficient air for cooling and it

will increase the EGT. However, according to Figure 5-23, the average EGT was well within the limit even though the air mass flow rate was low.

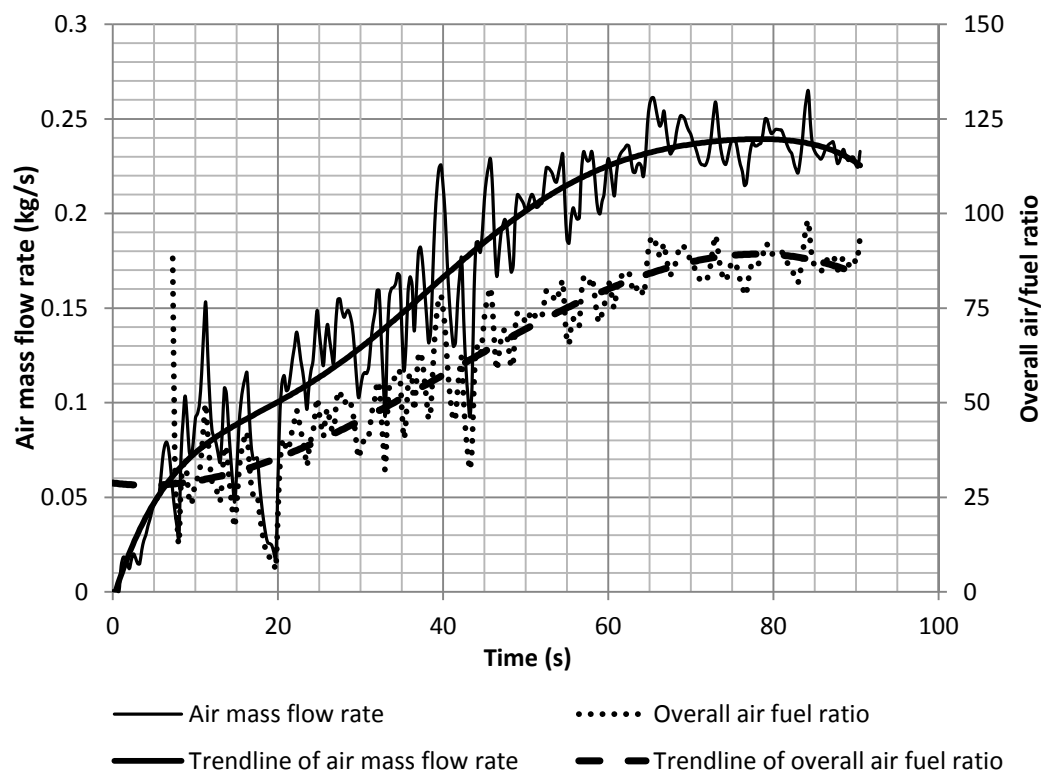


Figure 5-24: The air mass flow rate, the overall air fuel ratio and their trendlines along with time

The overall air/fuel ratio is another factor to monitor the running condition of the engine. During the starting procedure, the fuel flow rate was controlled by gradually opening the LPG cylinder valve. As shown in the figure above, the engine was running in a lean combustion condition during the starting procedure. After the engine reached the maximum speed at the 60th second, the air/fuel ratio was between 75 to 100, which was ideal for complete combustion. The LPG cylinder valve was fully open after 40 seconds and the engine could reach a stable self-sustaining condition with an air/fuel ratio of 75 to 100.

5.5.3 Main air casing temperature and lubrication system condition

The main air casing temperature can also reflect the cooling effect of the engine. Figure 5-25 illustrates the temperature along with time as well as the lubrication system condition. The valley of the air casing temperature profile around the 20th second was caused by the warm engine starting condition. The warm air trapped in the main air casing from previous test was blown away by the compressor while the combustion was still weak so that the temperature decreased before the 20th second. It then started to increase because the air was heated up again by the

combustion. The peak temperature of the air casing was only 105 °C, which was much lower than the normal operating temperature of 200 °C. This low temperature was mostly caused by the weak combustion due to the restricted LPG flow.

The lubrication system requires extra attention as well when the engine is not running at full speed of 46 000 RPM. The engine requires at least 48 kPa of the oil pressure to operate without the lack of lubrication according to the Rover manual. During the LPG running test, the oil pressure was able to reach and stabilise at approximate 70 kPa with a speed of 21 100 RPM. Therefore, the engine could be operated safely at reduced speed without the risk of lubrication failure.

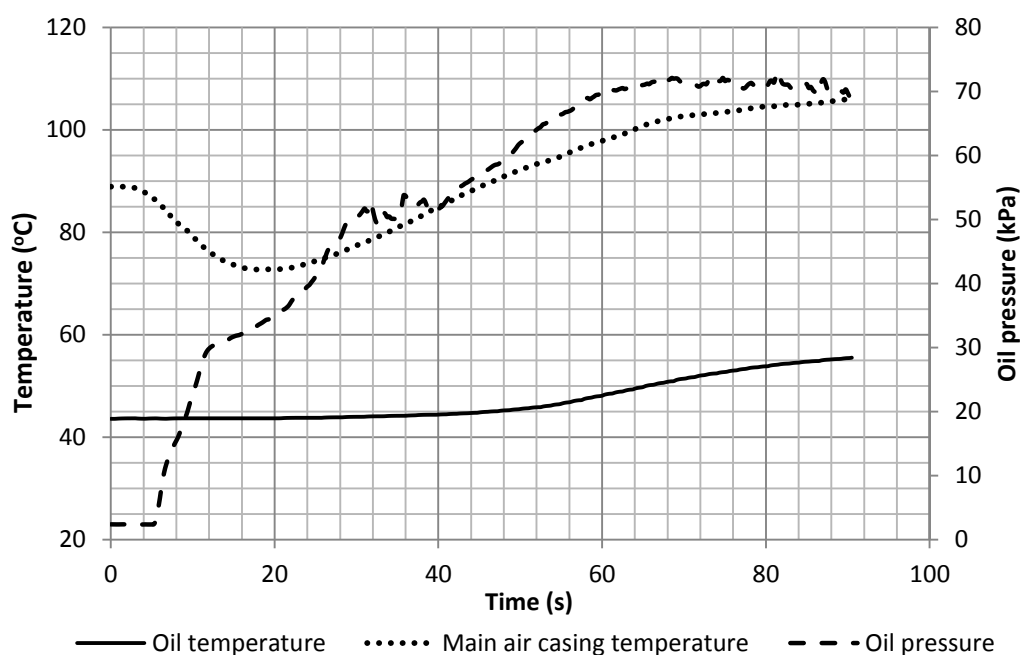


Figure 5-25: Lubrication system condition and the main air casing temperature along with the time

6 Conclusions and recommendations

A series of experimental tests have been conducted to study the Rover 1S/60 gas turbine performance and its potential for fuel system conversion. After redesigning a completely new gaseous fuel system, the engine can be successfully operated with gaseous fuel.

6.1 Conclusions

An engine test setup for the Rover 1S/60 gas turbine was successfully developed. The setup consists of the Rover gas turbine, a dynamometer, remote control system, data acquisition system and fuel supply system. The electronic control and data monitor systems including ETA and PLC were specially programmed and tuned for the gas turbine test. It is possible to conduct a gas turbine test remotely and safely while monitoring and recording all the relevant data.

During the initial engine tests, some cracks were found on the turbine blade root, and the turbine disc had to be replaced. The engine was then overhauled and all wear components were replaced. The detailed mechanism of each component was recorded for further modification.

The engine tests were conducted and firstly the exact firing-up procedure was set by analysing the results from several cranking tests. Then the engine was started and it ran up to its maximum speed of 46 000 RPM, which was also the idling speed of the engine. The data recorded during the starting procedure and idling running was carefully analysed and compared to the Rover manual. However, the results did not match the requirements set by the Rover Company. Due to the age of this particular engine, it is acceptable to have these off-limit values.

The engine was then tested to study its behaviour when it was under load. The engine was tested under several different load conditions and it showed good repeatability during all conditions. Even though the maximum continuous power output reduced from the factory rating of 45 kW to 28.4 kW, it is still acceptable, considering the age of the engine. The maximum recorded instantaneous power output was 39.7 kW, however, it was not advisable to stress the engine during continuous operation. Since many of the results were off the manufacture's limit, a new operation standard and procedure were established to suit the current condition of the engine.

To convert the gas turbine to operate with gaseous fuel, a gaseous fuel supply system was designed and implemented. The fuel supply system consists of the emergency shut-off valve, flow control device, pressure/temperature measurement device and a customised venturi flow meter. A new gaseous fuel injector was designed and tested. It was designed to restrict the gas flow so that the engine

could not over speed. The injector was modified to use different injection caps for the study of gaseous fuel combustion.

Finally, the LPG tests were conducted and the engine could be ignited smoothly by using an injection cap. The engine then ran up to the designated speed of 21 100 RPM limited by safety concerns. When the engine was supplied with gaseous fuel, the engine speed could be controlled freely, unlike the fixed speed design of the original engine. An operating procedure was established for the engine operation with LPG.

6.2 Recommendations

Although the present research work provided almost all details of the Rover 1S/60 gas turbine, there were still several uncertainties required to be studied. The current gaseous fuel supply system also requires further improvement. The recommendations for future work are listed below:

- Install a new separate module of the PLC so that more measurement ports can be used to evaluate the engine condition.
- Install an oil cooler and a cooling fan to reduce the oil temperature for continuous or more highly stressed tests.
- Study the airflow pattern inside the flame tube and design improved fuel injectors and caps.
- Design and test a new parallel combustor to study the effect of the fuel on the gas turbine.
- Improve the efficiency and the pressure ratio of the compressor and install it in the current engine.

7 References

- Abbruzzese, J., 2015. *Mashable*. [Online] (1.5) Available at: <http://mashable.com/2015/07/27/shanghai-china-stock-market/#g7d51SYRsZqU> [Accessed 10 October 2015].
- Adouane, B., 2006. *Low NO_x emissions from fuel-coupled nitrogen in gas turbine combustors*. Master thesis. University van Mosul.
- Afrox, 2007. *Product Reference Manual - Section 5 - Liquefied Petroleum Gas*. [Online] Afrox Available at: <http://www.awsgroup.co.za/data/L.P.G.pdf> [Accessed July 2015].
- Alternate Energy System, Inc., 2006. *Technical Data for Propane, Butane, and LPG Mixtures*. [Online] Alternate Energy System, Inc. Available at: http://www.altenenergy.com/downloads/pdf_public/propdatapdf.pdf [Accessed 16 Augustus 2015].
- ASME Fluid Meters Research Committee, 1981. *The ISO-ASME Orifice Coefficient Equation*.
- Bean, H.S., 1971. *Fluid Meters: Their Theory and Application*. 6th ed. New York: American Society of Mechanical Engineers.
- Bendini, R., 2015. *Exceptional measures: The Shanghai stock market crash and the future of the Chinese economy*. European Parliament.
- BS 848, 1997. *Fans for general purposes - Part 1: Performance testing using standardized airways*. BSI.
- Cape Advanced Engineering, 2008. *Rover 1S/60 gas turbine repair and testing*.
- Carpenter, J.N., Lu, F. & Whitelaw, R.F., 2015. *THE REAL VALUE OF CHINA'S STOCK MARKET*. NBER Working Paper. National Bureau of Economic Research.
- Cengel, Y.A. & Cimbala, J.M., 2010. *Fluid Mechanics Fundamentals and Applications*. Second Edition in SI Unit ed. McGraw-Hill.
- Cohen, H., Rogers, G.F.C. & Saravanamuttoo, H.I.H., 1987. *Gas turbine theory*. Third edition ed. Longman scientific & technical.
- De Zubay, E.A., 1950. Characteristics of disk-controlled flame. *Aero dig.*, pp.54-56.
- Ensola AG, 2007. *Deginitions LEL*.

- Gobbato, P., Masi, M., Toffolo, A. & Lazzaretto, A., n.d. *Numerical simulation of a hydrogen fuelled gas turbine combustor*.
- Hunt, R.J., 2011. The history of the industrial gas turbine (Part 1 the fifty years 1940-1990). *Power Engineer*, 15(2).
- Judge, A.W., 1960. Small gas turbine and free piston engines. New York: The Macmillan Company. pp.15-235.
- Judge, A.W., 1960. Small gas turbine and free piston engines. New York: The Macmillan Company. p.15.
- Kang, D.W., Kim, T.S., Hur, K.B. & Park, J.K., 2012. *The effect of firing biogas on the performance and operating characteristics of simple and recuperative cycle gas turbine combined heat and power systems*.
- Kim, D. & Park, S.W., 2010. *Forced and self-excited oscillations in a natural gas fired lean premixed combustor*.
- Lefebvre, A.H., 1983. *Gas Turbine Combustion*. Hemisphere Publishing.
- Lefebvre, A.H. & Ballal, D.R., 2010. *Gas Turbine Combustion Alternative Fuels and Emissions*. Third Edition ed. CRC Press.
- Lim, N., 2015. *The Bunsen burner*. [Online] Available at: <https://nicholaslimloveshci.wikispaces.com/The+Bunsen+burner> [Accessed 01 November 2015].
- Luiten, R.V., 2015. *Performance improvement of the Rover 1S/60 gas turbine compressor*. Master thesis. Stellenbosch: Stellenbosch University.
- Mass Flow Online, 2010. *Fuel View Manual*.
- Massachusetts Institute of Technology, 2006. *Brayton Cycle*. [Online] Available at: <http://web.mit.edu/16.unified/www/SPRING/propulsion/notes/node27.html> [Accessed 01 October 2015].
- Meher-Homji, C.B., Zachary, J. & Bromley, A.F., 2010. Gas Turbine Fuels - System Design, Combustion and Operability. *Thirty-Ninth Turbomachinery Symposium*, pp.155-86.
- Microsoft, 2007. *Choosing the best trendline for your data*. [Online] Available at: <https://support.office.com/en-gb/article/Choosing-the-best-trendline-for-your-data-1bb3c9e7-0280-45b5-9ab0-d0c93161daa8?omkt=en-GB&ui=en-US&rs=en-GB&ad=GB> [Accessed 01 October 2015].

- Olivier, A.J., 2015. *An experimental and numerical investigation of vaporizer tubes associated with micro gas turbines*. Master Thesis. Stellenbosch University.
- Pimentel, D.A., 1996. *Two-Phase Fluid Break Flow Measurements and Scaling in the Advanced Plant Experiment (APEX)*. Master Thesis. Oregon State University.
- Prinsloo, L., 2008. *The Commissioning of the Rover 1S/60 Gas Turbine*. MSC 400 Final Report. Pretoria: University of Pretoria.
- Quarta, N.J., 2012. *Simulation of a Hybridised Solar Gas Turbine System*. Master Thesis. University of the Witwatersrand.
- Rover Gas Turbine Limited, 1966. *Engine Test*. Coventry.
- Rover Gas Turbine Limited, 1972. *Overhaul Manual*. Coventry.
- Rover Gas Turbine Limited, n.d. *Rover Gas Turbine*. Product Brochure. Allday Limited.
- Rover Gas Turbine Ltd., 1966. *Rover Gas Turbines: Engine Type 1S/60 and 1S/90 Maintenance Manual*. Rover Gas Turbine Ltd.
- Rover Gas Turbine Ltd., 1966. *Rover Gas Turbines: Engine Type 1S/60 and 1S/90 Maintenance Manual*. Rover Gas Turbine Ltd.
- Satz, R.W., 1980. *The solution to the gas turbine temperature problem*.
- SCHENCK Pegasus GmGH, 1997. *Eddy-Current Dynamometer*.
- Special Metals, 2015. *NIMONIC Alloy 90*. [Online] Special Metals Available at: <http://www.specialmetals.com/assets/documents/alloys/nimonic/nimonic-alloy-90.pdf> [Accessed October 2015].
- Svenskt Gastekniskt Center AB, 2012. *Basic Data on Biogas*. Second Edition ed. Swedish Gas Center.
- White, F.M., 1994. *Fluid Mechanics*. Third Edition ed. McGraw-Hill.
- WIKA, 2015. *Electrical temperature measurement*. [Online] Available at: http://www.wika.co.za/upload/DS_TE6040_en_co_2039.pdf [Accessed 01 November 2015].
- Williams, A.F. & Lom, W.L., 1982. *Liquefied Petroleum Gases*. Second Edition ed. Ellis Horwood Limited.

Appendix A: Standard operating procedure

After conducting the initial test and analysing the engine behaviour, a new standard operating procedure was set to suit the current condition of the Rover 1S/60 gas turbine.

A.1 Standard operating procedure with kerosene

The standard operating procedure was set for the operation with kerosene. The following contents include all the procedures required to conduct a standard engine test.

A.1.1 Pre-testing procedure

Before conducting the engine test, the pre-testing procedure should be followed. It was designed to eliminate all the potential safety hazards and ensure the engine is in an operational condition.

1. Remove all the flammable materials around the gas turbine and ensure no object can be damaged by the jet blast.
2. Ensure all the components are tightened up, including the dynamometer, gas turbine, shaft guard, inlet air system, exhaust gas system and all the sensors.
3. Check the oil level and it should just below the maximum indicator.
4. Ensure the fuel is sufficient for the entire test and open the manual valve under the fuel tank.
5. Ensure the water is sufficient for the dynamometer cooling for the entire test.
6. Switch on all the electronic devices including PLC, ETA and dynamometer control.
7. Switch the dynamometer control mode to “External” and “RPM” on the control panel and press “Cal” button to calibrate the load cell.
8. Set ETA status to “online”. Check all the channels on ETA are functional.
9. Test and ensure the emergency shutdown system and remote control system are functional.
10. Open the solenoid valves before the engine and loosen the bleed screw on the fuel pump body to ensure the fuel pump is filled with liquid fuel.
11. Switch on the ventilation system.

A.1.2 Starting procedure

After conducting the pre-testing procedure, the engine can be started for the test. For the safety concerns, no one is allowed to enter the test cell during the engine test.

1. Open all the solenoid valves and ensure the mechanical remote control for the fuel sprayer shut-off valve is at close position.
2. Switch on the data recording function in ETA.
3. Switch on the spark plug and make sure the continuous “click” sound produced by the spark plug can be heard.
4. Switch on the starter motor and monitor the fuel pressure.
5. Open the sprayer shut-off valve when the fuel pressure reaches 400 kPa and ensure the ignition is successful by hearing the sound of the combustion.
6. Switch off the starter motor and spark plug at 12 000 RPM. If the starter motor was warm before the test, switch it off at 10 000 RPM.
7. Monitor the oil pressure constantly. After passing 20 000 RPM, the oil pressure must be higher than 48 kPa. If not, terminate the test immediately by close the sprayer shut-off valve.
8. The engine should run up to its maximum speed of $46\,100 \pm 300$ RPM and stabilise at this speed.

A.1.3 Operation standards

When the engine accelerates to its maximum speed, immediately check the following readings:

1. The oil pressure should be about 250 kPa and must not be less than 48 kPa.
2. The bearing seal air pressure should be between 46 000 Pa to 49 000 Pa.
3. The engine speed should be $46\,100 \pm 500$ RPM.

When the average exhaust gas temperature stabilises, check the following readings:

1. The average exhaust gas temperature should not exceed 480 °C. The temperature reading of each individual thermocouple may not exceed 500 °C.
2. The oil pressure must not be less than 48 kPa.
3. The oil temperature must not exceed 110 °C.
4. The engine speed should be $46\,100 \pm 300$ RPM.

5. The fuel pressure should be approximately 1.2 MPa and may not exceed 1.4 MPa without load.
6. The bearing seal air pressure should not exceed 51 000 Pa.
7. The compressor delivery air pressure should be approximately 150 kPa and may not less than 140 kPa.
8. The differential air pressure measured at the conical inlet should be approximately 2 400 Pa.
9. The inlet air temperature may not exceed 50 °C.
10. The dynamometer cooling water temperature must not exceed 60 °C.

A.1.4 Load test procedure

After checking the operation standards and ensuring all values are within the limits, the load test can be carried out.

1. Decrease the speed-input in ETA to a value that is 200 RPM lower than the actual driveshaft speed and wait for the decrease in the driveshaft speed. It normally takes approximate 8 seconds before the dynamometer start to apply load.
2. After the dynamometer start to apply load, change the speed-input in ETA only in small increments/decrements to the desired speed and monitor the average EGT continuously.
3. The average EGT may not exceed 560 °C at any time during the normal load test.
4. When finishing the load test, increase the speed-input in ETA in small increments to 3 100 RPM, which is higher than the maximum driveshaft speed so that the dynamometer cannot apply load to the engine.
5. Check the average EGT. It should decrease to approximate 440 °C.

A.1.5 Normal shutdown procedure

Before shutting down the engine, remove all load from the dynamometer and check that all values are within the limits according to the operation standards. Then the engine can be shut down safely.

1. Close the fuel sprayer shut-off valve.
2. When the engine has stopped completely, loosen the fuel accumulator attached to the fuel sprayer to release the pressurised fuel in the fuel line.
3. Keep the accumulator loose and briefly crank the engine to approximate 5 000 RPM to assist the engine cool down.

A.1.6 Emergency shutdown procedure

1. Press the emergency switch button.
2. Simultaneously close the fuel sprayer shut-off valve.
3. When the engine has stopped completely, release the fuel pressure by loosening the fuel accumulator.
4. Inspect the engine carefully. Do not attempt to crank or start the engine before the inspection has finished.

A.1.7 Post-testing procedure

1. Tighten the fuel accumulator.
2. Switch off all electronic devices and disconnect the battery.
3. Close the cooling water supply and the manual valve under the fuel tank.
4. Switch off the ventilation system.
5. Ensure all recorded data is saved.

A.2 Operating procedure with LPG of the initial test

The initial engine test with LPG was been conducted. The engine used a gas injector with the flow restriction function to prevent the engine over speed and the maximum engine speed was 21 100 RPM. Therefore, this procedure cannot be used as the final version for the LPG testing procedure. However, the procedure listed below can be used as a reference for the further modification work.

A.2.1 Pre-testing procedure

1. Follow the procedure listed in A.1.1, except for the procedures related to the liquid fuel system.
2. Close the LPG cylinder valve.
3. Test the remote function of the quick-action valve and the needle valve system.
4. Open the quick-action valve and switch the needle valve to the maximum position.

A.2.2 Starting procedure

1. Switch on the data recording function in ETA.
2. Open the ball valve connected to the gas injector.
3. Switch on the spark plug and make sure the continuous “click” sound produced by the spark plug can be heard.

4. Switch on the starter motor and monitor the oil pressure.
5. Gradually open the LPG cylinder valve when the engine speed reaches approximate 6 000 RPM.
6. Listen carefully to the sound of the combustion. If the ignition was failed, close the cylinder valve and repeat from Step 3.
7. Continuously but slowly open the cylinder valve. The starter motor and spark plug can be switched off when engine speed reaches 12 000 RPM.
8. Continuously open the cylinder valve to the fully open position.

A.2.3 Operation standards for the initial test with 2 mm orifice restricted gas injector

1. The engine speed should be $21\,100 \pm 300$ RPM.
2. The gas mass flow rate should be approximate 0.0028 kg/s with an air/fuel ratio of approximate 80.
3. The average EGT should be approximate 530 °C.

A.2.4 Normal shutdown procedure

1. Close the LPG cylinder valve completely.
2. Switch on the spark plug and wait until the engine has stopped completely, and then switch it off.
3. Briefly crank the engine to approximate 5 000 RPM to eliminate the possible remaining LPG.

A.2.5 Emergency shutdown procedure

1. Pull the emergency shut-off handle to close the quick-action valve.
2. Simultaneously close the cylinder valve.
3. Switch on the spark plug to assist the ignition of the remaining LPG.
4. After the engine has stopped completely, switch off the spark plug and inspect the engine.

A.2.6 Post-testing procedure

1. Follow the procedure listed in A.1.7, except for the procedures related to the liquid fuel system.
2. Keep the ventilation system on for at least 3 minutes to eliminate the possible remaining LPG and then switch it off.

Appendix B: Fuel sprayer test

The fuel sprayer of gas turbine plays a key role in the combustion process and engine control. The sprayer determines the maximum allowable fuel flow rate at a specific pressure. A fine atomization can also result in a high efficiency clean combustion, especially when using low volatility liquid fuel. On the contrary, the engine may even not be able to start with bad atomization.

According to the Rover manual, there are three types of fuel sprayers, shown as below:

- Air assisted sprayer manufactured by Rover, manual shut-off valve/solenoid operated valve
- Air assisted sprayer manufactured by Lucas, solenoid operated valve
- Non air assisted sprayer, used on early type engines

The fuel sprayer used for the test falls in the last category: Non-air assisted sprayer. This type of sprayers may vary slightly in construction, but they all have the same basic design (Rover Gas Turbine Limited, 1966). The construction of this particular sprayer is shown in figure below.

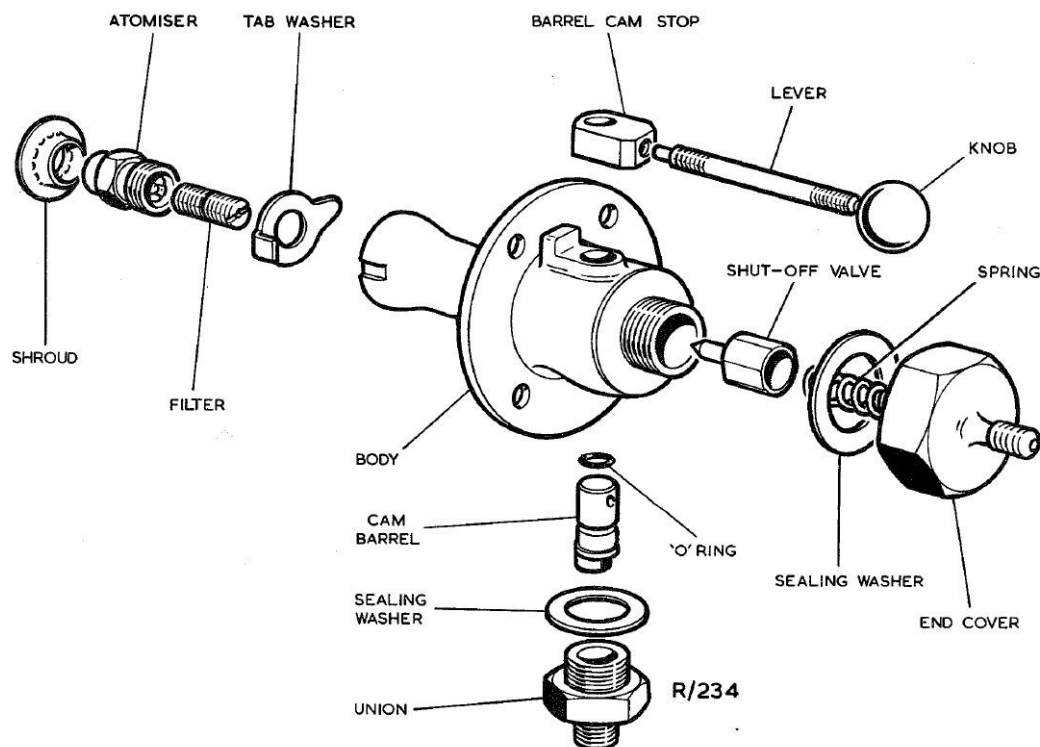


Figure B-1: Construction of the early type sprayer

The Rover manual has a detailed description for a fuel system test. However, such test requires a very sophisticated test rig and special tools which are not available at hand. To have a general view for the performance of the fuel sprayer, a simple test rig was built. The sprayer is bolted on top of a plastic bucket and the fuel was fed from a 12 V gear pump that produces fixed pressure. The average fuel flow rate is calculated by measuring weight change during a specific time.

B.1 Function test

This sprayer had never been tested on a test rig and the performance of atomization was totally unknown. It is important to know its performance under different working conditions. To have a full understanding of this particular sprayer, the test is divided into five different modes, so that each mode focuses on different operational condition. These five modes are listed below:

Table B-1: Different mode tests on studying fuel sprayer

	Shut-off valve	Accumulator	Comments
Mode 1	Fully open	Fully closed	3 repeat basic tests
Mode 2	Fully open	Open 180°	Study on effect of accumulator
Mode 3	Fully open	Open at varies positions	Study on effect of accumulator
Mode 4	Partially open	Fully closed	Study on effect of shut-off valve
Mode 5	Fully open	Fully closed	Repeatability test

The fuel shut-off valve is simply used as a valve to control the fuel flow. The accumulator can store a small amount of fuel so that it can assist the atomization when the pressure generated by the fuel pump has fluctuations. When the fuel pump starts working, it pumps the fuel into the fuel sprayer and the accumulator. The accumulator was filled by air before engine starts and now filled with fuel and compressed air. The accumulator requires a vertical position so that the compressed air is always on top of it. When the fuel pressure has an unwanted sudden drop in a short time, the compressed air in accumulator will push the fuel into atomizer to maintain a fine atomization at all times.

B.1.1 Mode 1 test

Mode 1 consists of three individual tests with same testing conditions: fully open shut-off valve and fully closed accumulator. The purpose of this mode of test is to have a general overview of the fuel sprayer under normal operating condition.

At the beginning of the test, there was a serious fuel leakage at the inlet connection. After inspection, the O-ring was replaced and the leak stopped

immediately. A matching label was marked on the accumulator for the positioning purpose. When two labels match, the accumulator was in its fully closed position. Detailed pictures are shown as below.



Figure B-2: Replacing O-ring and accumulator with position marker

When the fuel pump was connected to a 12 V lead-acid battery, the pressure varied between 6.5 bar to 7.5 bar, preventing an exact reading. Measuring the “zero weight” of empty bucket and “final weight” with fuel, divided by time gives the fuel mass flow rate. The table below shows the original test data and calculated results.

Table B-2: Mode 1 test results with fully open shut-off valve and fully closed accumulator

Duration [s]	Pressure [Bar]	Zero weight [kg]	Final weight [kg]	Mass flow rate [kg/hr]
10.26	6.5 - 7.5	0.329	0.395	23.158
10.26	6.5 - 7.5	0.328	0.395	23.509
10.6	6.5 - 7.5	0.329	0.394	22.075

According to the results listed above, the sprayer shows a very good consistency on allowable fuel flow rate under certain pressure.

B.1.2 Mode 2 test

The working condition for Mode 2 is a fully opened shut-off valve and an accumulator rotated anti-clockwise by 180°. The purpose is to study the effect of accumulator position on fuel flow rate. The accumulator uses an O-ring seal against the sprayer body when at the fully closed position. Rotating the accumulator will make the seal non-functional. The test results are listed below.

Table B-3: Mode 2 test results with fully open shut-off valve and 180° rotated accumulator

Duration [s]	Pressure [Bar]	Zero weight [kg]	Final weight [kg]	Mass flow rate [kg/hr]
10.33	2.8	0.329	0.369	13.930
12.13	2.8	0.329	0.378	14.542
12.25	2.8	0.329	0.378	14.400
12.28	2.8	0.329	0.377	14.071

By unscrewing accumulator, it opens a by-pass tunnel for fuel flow and the fuel mass flow rate will decrease through the atomizer. The excess fuel skips the sprayer and flows through the coil tube that is attached on the accumulator base. The excess fuel requires a container for storage. As one can see from the results above, the pressure is stable at 2.8 bar and the fuel mass flow rate does decrease to approximate 14 kg/hour and also with a good consistency. Even this could decrease the fuel flow rate, it cannot be used as a practical method to reduce fuel flow during engine testing.

B.1.3 Mode 3 test

As it is already known that opening the accumulator will decrease the fuel flow rate through the atomizer, it is also necessary to know at which point such an action is effective. Therefore, the accumulator is rotated anti-clockwise for 360°, 90°, 10° and fuel flow rate at each position will be tested.

Table B-4: Mode 3 test results with accumulator rotating different degrees

Duration [s]	Accumulator position [°]	Pressure [Bar]	Zero weight [kg]	Final weight [kg]	Mass flow rate [kg/hr]
12.25	360	2.8	0.329	0.378	14.400
12.21	90	2.8	0.329	0.399	14.742
12.31	10	2.8	0.330	0.377	13.745

The results of fuel mass flow rate are very similar to those from Mode 2 tests. This indicates the position of accumulator only provides two types of impact to fuel flow rate: decrease the flow rate or having no effect on the flow rate. The rotation degree has no effect on the fuel flow decrease which means once the

accumulator breaks the seal condition, the fuel flow rate will drop to a specific value and be stable.

B.1.4 Mode 4 test

The function and behaviour of the accumulator is fully known so far, but it is also important to understand how the shut-off valve works. When the valve is closed, a taper pin is pushed down against the fuel passage by a spring. Such pin and the passage can make a contact seal and a further increase in fuel pressure will help this sealing. When opening the shut-off valve, it lifts up a taper pin so that it opens a passage for fuel flow. The lifting height of the shut-off pin could affect the fuel flow rate through the passage to the atomizer. The table below shows the test results.

Table B-5: Mode 5 test results with shut-off valve at different position

Duration [s]	Shut-off valve position [°]	Pressure [Bar]	Zero weight [kg]	Final weight [kg]	Mass flow rate [kg/hr]
10.28	30	6.5 - 7.5	0.329	0.395	23.113
10.26	60	6.5 - 7.5	0.330	0.394	22.456

When the shut-off is fully open, the results are known from the Mode 1 test. From the results listed above, it can be seen that the shut-off position has no effect on the fuel flow rate. The shut-off valve is either in the fully open or fully closed position. It also shows the valve can be opened easily by just turning it by 30°. Such a characteristic is very important when designing a remote control device for a fuel shut-off valve, since the operation of the valve only requires very little movement.

B.1.5 Mode 5 test

The different tests from four modes list all the possible operation methods for the fuel sprayer. The Mode 5 test is to test the repeatability of the sprayer. The conditions of this test are the same as Mode 1. The test result is listed below.

Table B-6: Mode 5 test results with exact same condition as Mode 1

Duration [s]	Pressure [Bar]	Zero weight [kg]	Final weight [kg]	Mass flow rate [kg/hr]
10.26	6.5 - 7.5	0.330	0.393	22.105

Compared to the average fuel mass flow rate from Mode 1 test, the result from Mode 5 test has only a 3.53 % difference. It shows good repeatability of the fuel sprayer performance at a specific pressure.

B.2 Atomization test

Atomization is one of the most important factors required to operate a gas turbine efficiently. It is necessary to know how the atomizer behaves under different pressures. This particular atomizer is sensitive to pressures. When the pressure is above 2 bar (gauge pressure), the atomizer creates a 110° fine atomization. Any further increase in pressure will not change the shape of atomization. However, if the fuel pressure drops below 1 bar, the fine atomization becomes a stream of fuel and such condition is not suitable for combustion. The processed photo below shows the atomization at different pressure.

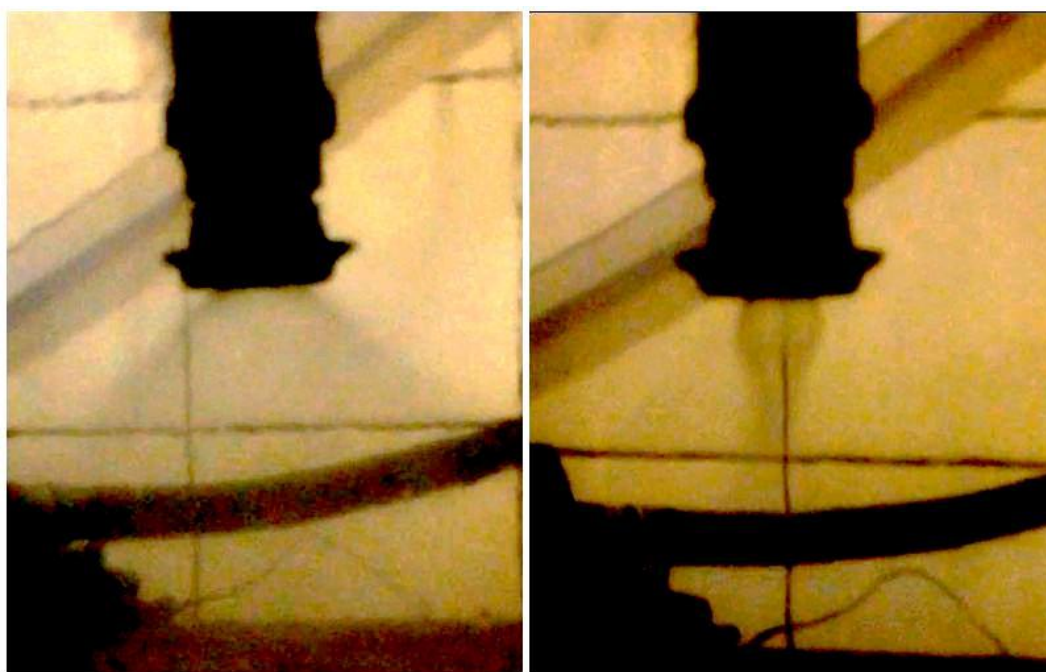


Figure B-3: Fuel atomization at high (left) and low pressure condition (right) (processed photos)

The shape of the atomization cone has a different at different operating pressures. The atomization at low pressure is unacceptable for combustion under idle working conditions. However, low fuel pressure condition cannot be avoided completely during the starting procedure, even though incomplete combustion should be prevented as much as possible.

Appendix C: Gas injector design and test

C.1 Flow restriction design of the gas injector

When converting the engine to operate with LPG, a gas injector is required to inject gaseous fuel to the combustor. For safety concerns, the injector was designed to restrict the gas flow so that the engine could not over speed. The flow restriction uses the concept of the compressible flow as discussed in Chapter 2.4. The key of the design is setting a specific orifice diameter so that the flow speed can reach the sonic speed when flowing through the orifice, thus the flow reaches the maximum flow rate.

C.1.1 Assumption for the design of restriction orifice

The restriction orifice design can only be carried out after setting the required maximum allowable gas flow rate. Since no engine tests with LPG was conducted before, the precise gaseous fuel flow rate during the engine tests is unknown. However, an assumption can be made using the air mass flow rate. The air mass flow rate can be calculated from the recorded differential pressure as discussed in Chapter 5.3.3. By assuming the air/fuel ratio of 80 for a general complete combustion, the required gaseous fuel flow rate can be calculated. The required gaseous fuel mass flow rate is shown in the figure below.

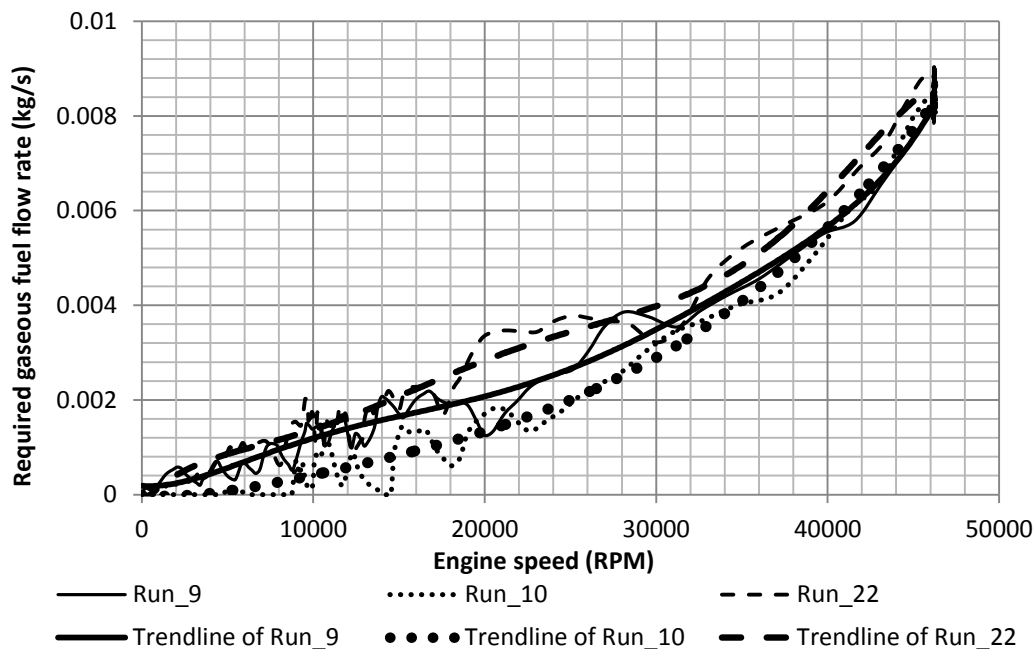


Figure C-1: Required gaseous fuel flow rate during the starting procedure

Due to the sensitivity of the differential pressure transducer used for the air mass flow rate calculation, the results had severe fluctuations. Therefore, trendlines were used to provide a better tendency of the required gaseous fuel flow rate.

For the engine tests with LPG, safety is the most important concern, especially when no LPG test was conducted on this engine before. Therefore, the maximum engine speed was set to 35 000 RPM so that there was enough safety margins for the test. According to the kerosene test results, the engine health condition at 35 000 RPM is acceptable, especially for the oil pressure. The oil pressure at 35 000 RPM was higher than the minimum requirement so that the engine would not experience the lack of lubrication. According to Figure C-1, the minimum required fuel flow rate at 35 000 RPM is approximate 0.004 kg/s among three different tests. It indicates that the engine can only reach 35 000 RPM or lower when restricting the fuel flow rate at 0.004 kg/s. Therefore, the fuel flow rate is restricted at 0.004 kg/s.

According to Equation 2-7, to calculate the diameter of the orifice, the stagnation temperature and pressure of the gas are required. Assuming the propane stagnation temperature is 288 K and the stagnation pressure is 500 kPa. Using Equation 2-7:

$$\dot{m}_{\max} = A^* P_0 \sqrt{\frac{k}{RT_0}} \left(\frac{2}{k+1} \right)^{(k+1)/[2(k-1)]} \quad (\text{C-1})$$

$$\dot{m}_{\max} = 0.004 \text{ kg/s}$$

$$P_0 = 500\,000 \text{ Pa}$$

where

$$T_0 = 288 \text{ K}$$

$$R = 188.569 \text{ J/kg} \cdot \text{K}$$

$$k = 1.127$$

The A^* can be calculated and the diameter of the orifice equals 1.935 mm. For the manufacture, the orifice diameter can be set to 2 mm and the maximum flow rate becomes 0.00427 kg/s, which is still acceptable for a safety test.

C.1.2 Restriction orifice test

For the safety concerns, it is necessary to test the flow restriction function of the gas injector before installing to the engine. Therefore, the compressed air was used to test the gas injector and propane was not advisable to use for the test since it is highly flammable. A calibrated WIKA hot wire flow sensor was used to verify the flow rate. A needle was used to control the upstream pressure and a calibrated WIKA master gauge was used to monitor the upstream pressure. For

research purpose, the restriction orifice diameter was first manufactured in 1 mm. After conducting the test with 1 mm orifice, the orifice was then expanded to 2 mm and the test was carried out. The test results are listed below.

Table C-1: Test and theory results with orifice diameter of 1 mm

Gauge pressure [kPa]	Flowmeter reading [kg/h]	Result based on theory [kg/h]
100	1.0209	1.3464
120	1.1546	1.4810
140	1.2774	1.6157
200	1.5729	2.0196
240	1.8014	2.2889
300	2.0998	2.6929
340	2.3262	2.9621
400	2.6408	3.3661
440	2.8694	3.6354
500	3.2068	4.0393
540	3.4317	4.3086
600	3.8367	4.7125

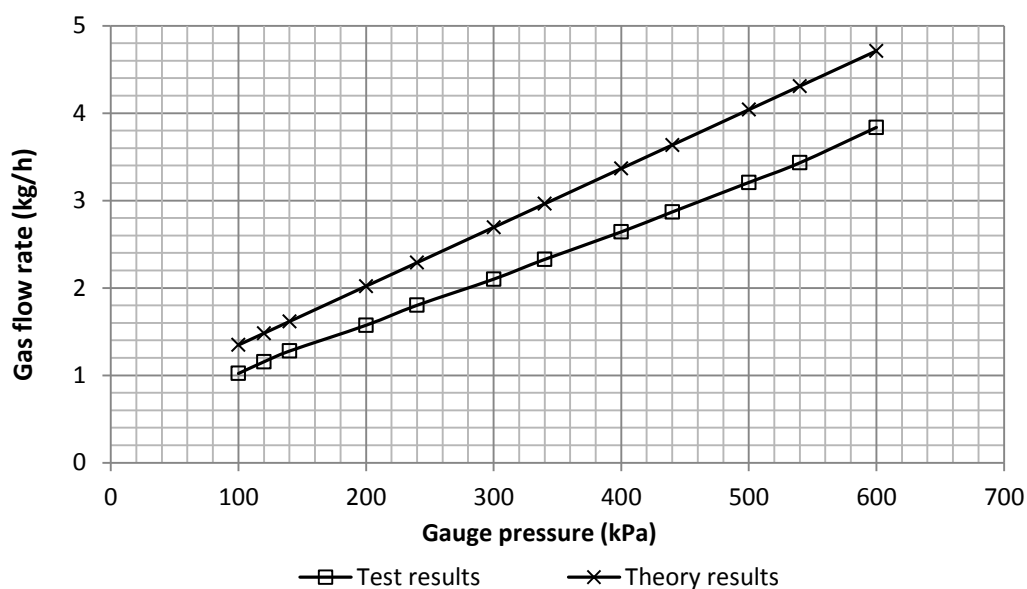
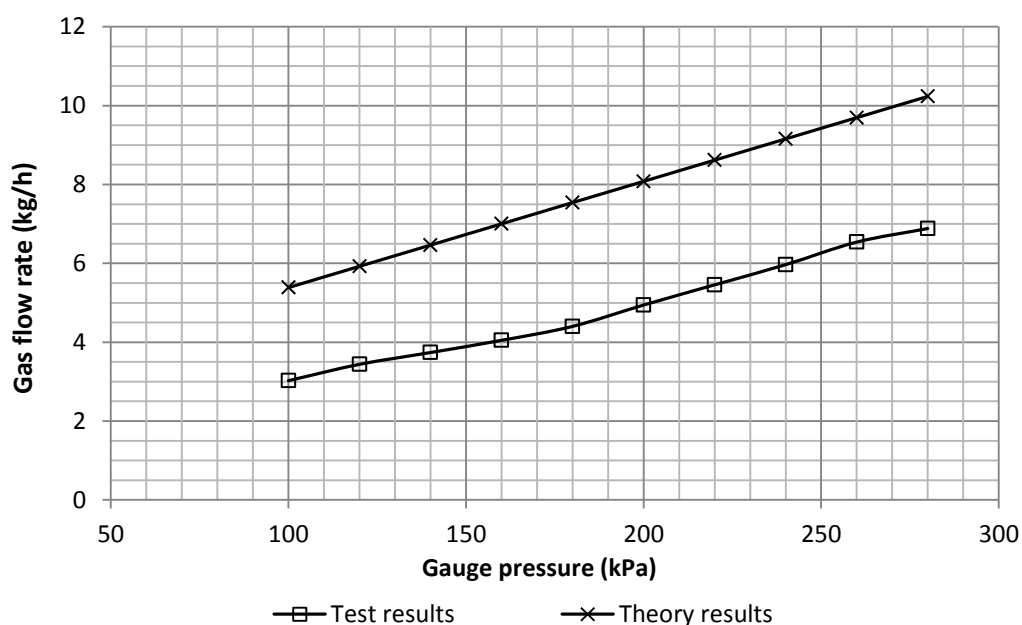


Figure C-2: Test and theory results with orifice diameter of 1 mm

Table C-2: Test and theory results with orifice diameter of 2 mm

Gauge pressure [kPa]	Flowmeter reading [kg/h]	Result based on theory [kg/h]
100	3.0252	5.3858
120	3.4390	5.9243
140	3.7382	6.4629
160	4.0476	7.0015
180	4.4011	7.5401
200	4.9428	8.0787
220	5.4551	8.6172
240	5.9667	9.1558
260	6.5385	9.6944
280	6.8825	10.2330

**Figure C-3: Test and theory results with orifice diameter of 2 mm**

The theory results were calculated by using Equation 2-7 with air properties. Unfortunately, the test with a 2 mm orifice diameter had to be terminated at the pressure of 280 kPa due to the limited range of the flow sensor. Tests with higher pressure would push the flow rate higher than the flow sensor limit, thus the sensor could be damaged permanently. The results clearly showed the actual test

results are always lower than the theoretical results. The margins between two types of results had a tendency of increase with the climbing gauge pressure. According to the results with 2 mm orifice, the actual flow rate is lower than the theoretical result by 67 % at 280 kPa. Assuming the percentage valve stays the same when the gaseous fuel stagnation pressure is 500 kPa, a 2 mm orifice would provide a propane flow rate of 0.00268 kg/s. By referring to Figure C-1, the engine speed range is from 20 000 RPM to 30 000 RPM with a flow rate of 0.00268 kg/s. Even though the assumed engine speed is lower than the designated speed, it is still acceptable for the initial engine test. The differences between theory and test results are most probably caused by imperfect manufacturing process. The gas flow rate can be increased by expending the orifice of the injector. However, it is suggested to do so only after fully understanding the engine behaviour on LPG.

C.2 Pre-mixing holes design

The gas injector was designed to have a similar function to the liquid fuel sprayer. It is necessary to study the gas flow pattern inside the combustor. The figure below illustrates the gas flow of the combustor. The black arrows indicate the ambient air and the white arrows indicate the combustion gases.

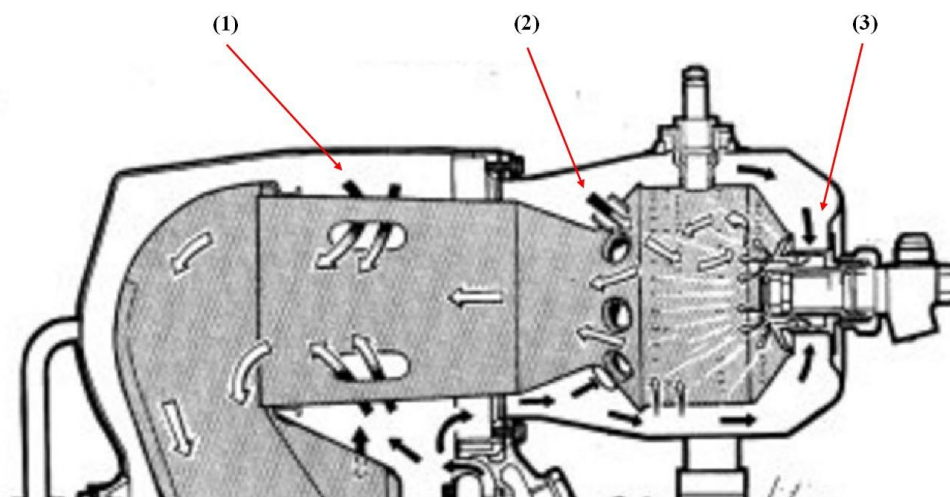


Figure C-4: Gas flow diagram of the combustor (Rover Gas Turbine Limited, 1966)

As one can find, the air has three main ways to enter the flame tube: through the dilution holes (1), through the vortex jets (2) and through the primary air holes (3). The component names can be found in Figure 3-6. The dilution holes are used for cooling down the combustion gases. The vortex jets allow the air entering the combustion zone to create a vortex flow pattern for a longer combustion time. The air passing through the primary air holes can be mixed with the atomized fuel for a complete combustion. To design a gas injector, the concept of gas burner with pre-mixing holes can be used.

Gas burner with pre-mixing holes can be found in many applications including Bunsen burner and domestic gas stove. The figure below illustrates the construction of a Bunsen burner.

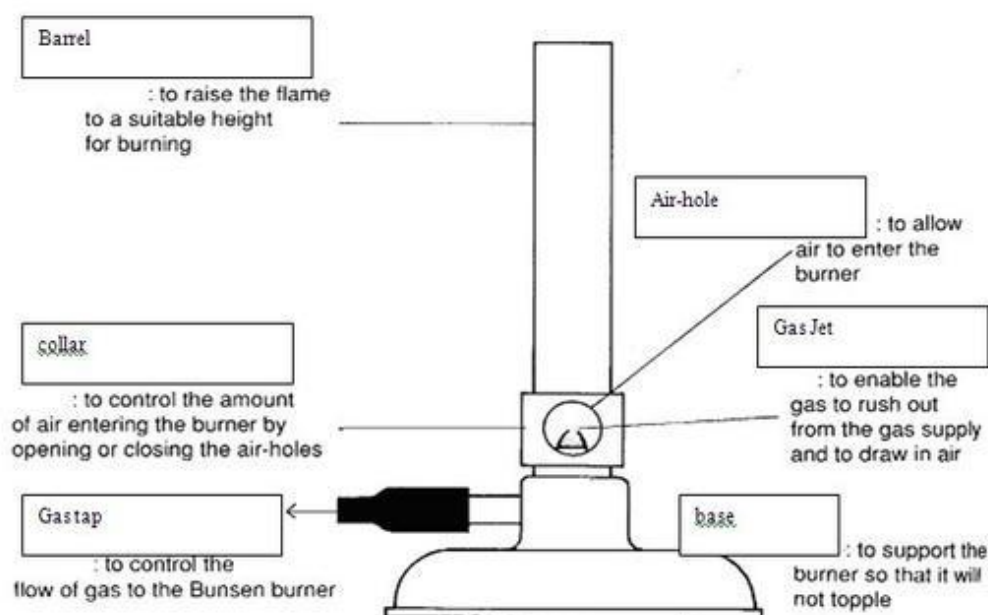


Figure C-5: Construction of a Bunsen burner (Lim, 2015)

The design and concept of the pre-mixing holes are relatively simple. The high speed flammable gas rushed out from the gas jet creates a low pressure zone and the air will be sucked into the barrel, which also known as pre-mixing tube. The air and the flammable gas mix in the barrel and then can be ignited. Because the speed of the gas is extremely high at the gas jet, the mixture can only combust after the speed of the mixture reduces to a certain level.

By comparing the Bunsen burner to the Rover gas turbine combustor, it is found that the air originally flowing through the primary air holes could be used for the pre-mixing. The flammable mixture then could enter the primary zone of the flame tube and combust rapidly without mixing with the air. Since no previous gas combustion test could be found, it was decided to use an injector with pre-mixing holes for the initial LPG test. If the initial test failed, then other designs could be carried out.

Before installing the gas injector to the engine, the injector was tested using a 5 kg LPG cylinder and the separate Rover combustor in the open air. The gas injector was connected to the LPG cylinder directly to obtain the maximum flow rate and then bolted on the combustor. The gas flow was controlled by the cylinder valve and ignited by a butane lighter. The screenshots of the test video are shown in Figure C-6.



Figure C-6: Gas injector test on the separate combustor with low flow rate (left) and high flow rate (right)

As the test was conducted under the atmospheric condition with limited gas flow, the characteristic of the combustion could not indicate it would be the same during the engine testing. The results could only be used as the guidance for the injector design. During the test, once the gas was ignited, the flame was extremely stable in the flame tube. Any sudden change in gas flow rate could not extinguish the flame. The flame length was almost the same as the length of the flame tube, which indicated that the flame would not stress the turbine system. As these results showed a good potential of the current injector design, further injector test could be carried out.

C.3 Gas injector caps design

The gas injector shown in Figure 4-10 was used for the LPG test before carrying out the injector caps design. During the test, the pre-mixed gas could not be ignited properly by the surface discharged spark plug. It was believed that the flammable pre-mixed gas was rushing out into the flame tube without having contact with the spark. When injecting LPG during the engine cranking, the mixture was blown away by the airflow coming from the compressor. When injecting LPG without cranking the engine, the flammable mixture could not be ignited until it filled most of the engine body and then the spark could ignite it. Since the engine body was filled with the flammable mixture, the ignition would cause an explosion instead of a continuous combustion.

To ignite the gas properly, it was decided to inject the gas directly to the spark plug. Therefore, three different caps were designed to fit with the current gas injector so that the manufacture work could be reduced to a minimum level. After installing cap (a) to the injector, the engine was successfully ignited and it could run up to a speed of 21 100 RPM as planned.

Appendix D: Experimental setup

The testing software, sensor calibration and rest of the testing equipment are discussed in the following contents.

D.1 Control interface

Engine test automation (ETA) was used for all the control management and data acquisition. The dynamometer can be controlled through ETA while all the parameters can be recorded and displayed on the monitor. The ETA was programmed for the alarms, automatic emergency shutdown, and calibration for all the sensors. It can also be programmed to conduct the engine test automatically. However, it cannot test the Rover gas turbine automatically because the fuel sprayer shut-off valve has to be operated manually. The Figure below shows the ETA user interfaces.

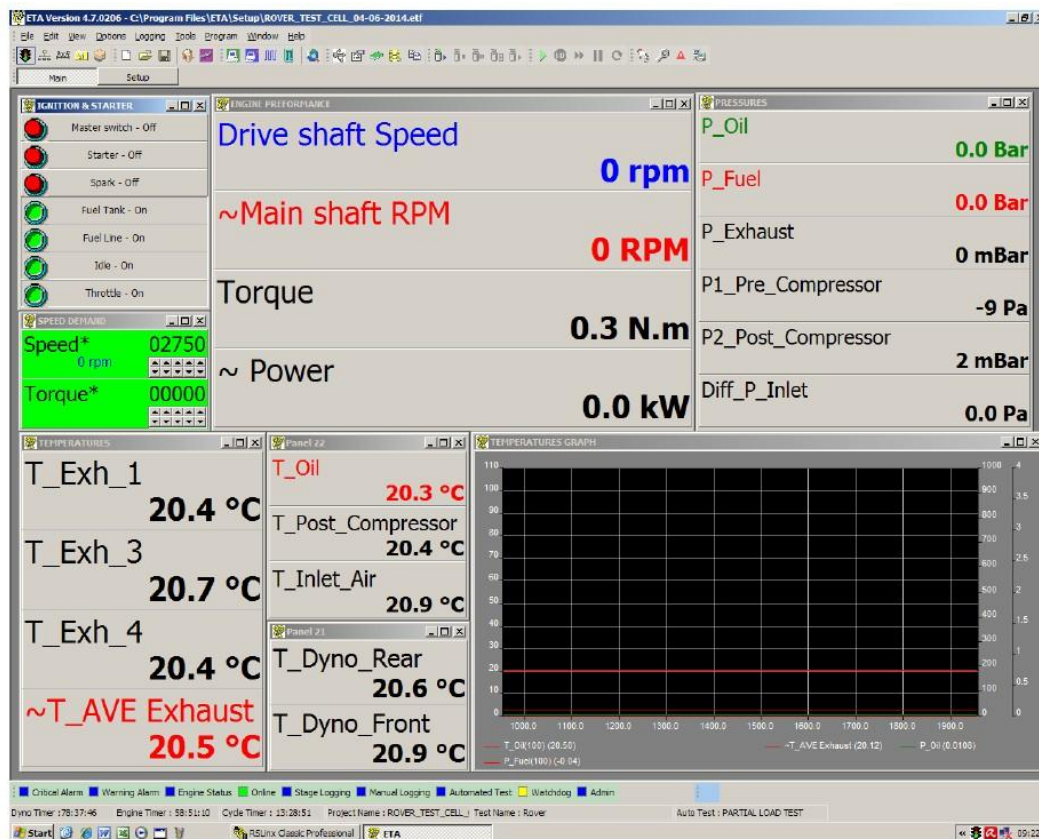


Figure D-1: ETA user interface for kerosene test

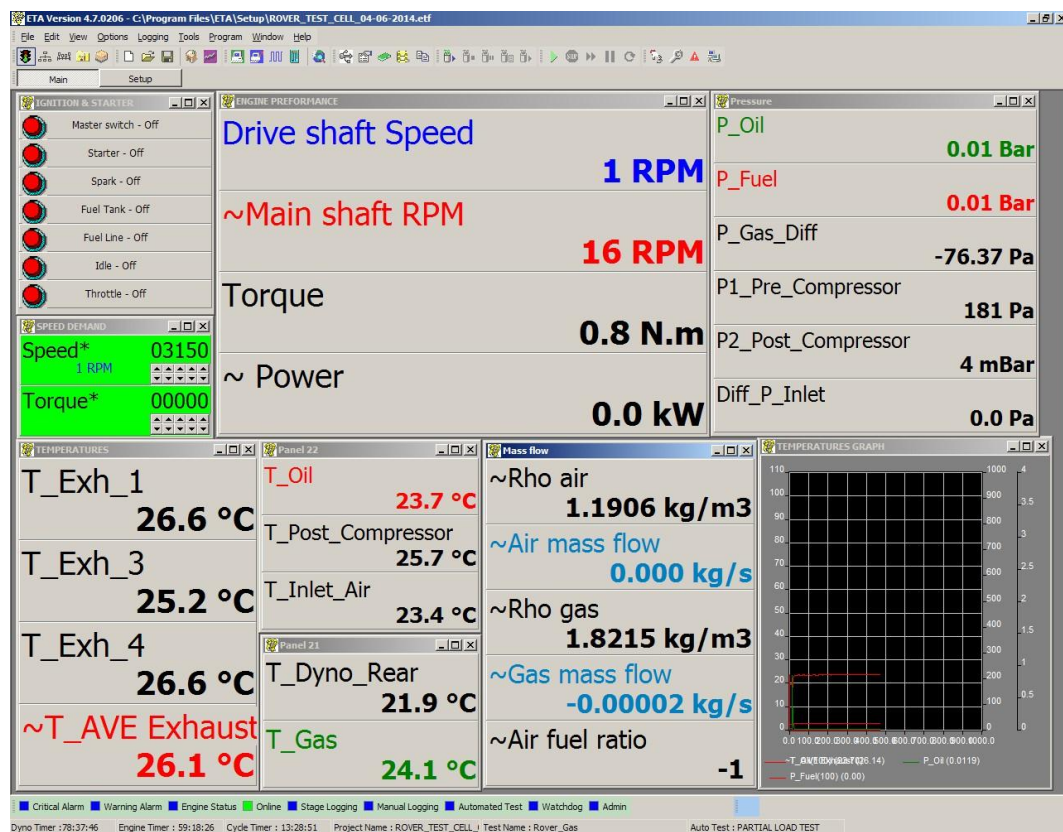


Figure D-2: ETA user interface for LPG test

The user interface in ETA can be customised; therefore, the user interface used for kerosene test is different from the one for LPG. The LPG test requires the air and gas flow rate to monitor the combustion condition and control the gas flow.

D.2 Calibration of the measurement sensors

All the sensors are directly connected to the PLC and the PLC is responsible to communicate with the ETA. The raw data generated by the sensor is calibrated by the ETA and displayed on the monitor. The ETA picks up the measurement values provided by the PLC, and then transfer the values to the final measurement readings. Figure D-3 and D-4 shows the calibration screen of the speed sensor and the air differential pressure transducer.

The load cell, pressure transducers and thermocouples all had gone through the same calibration procedure as shown in the figure. Once the calibration has been done, the measurement reading can be used directly for the study. However, it is still suggested to check the calibration regularly to maintain the reliability of the measurement results.

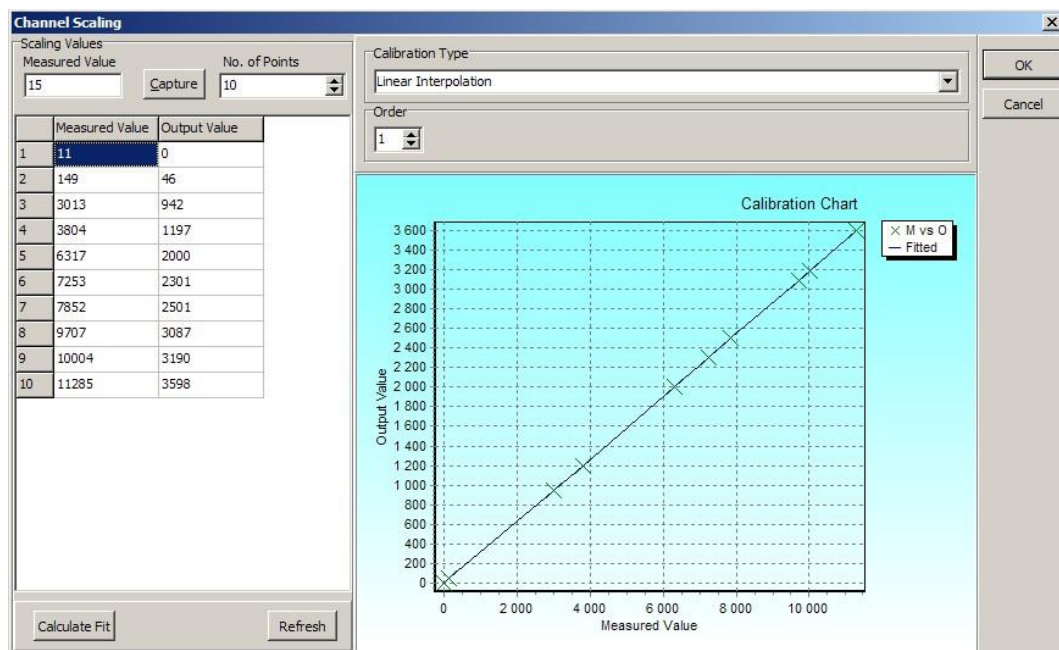


Figure D-3: Calibration of the speed sensor

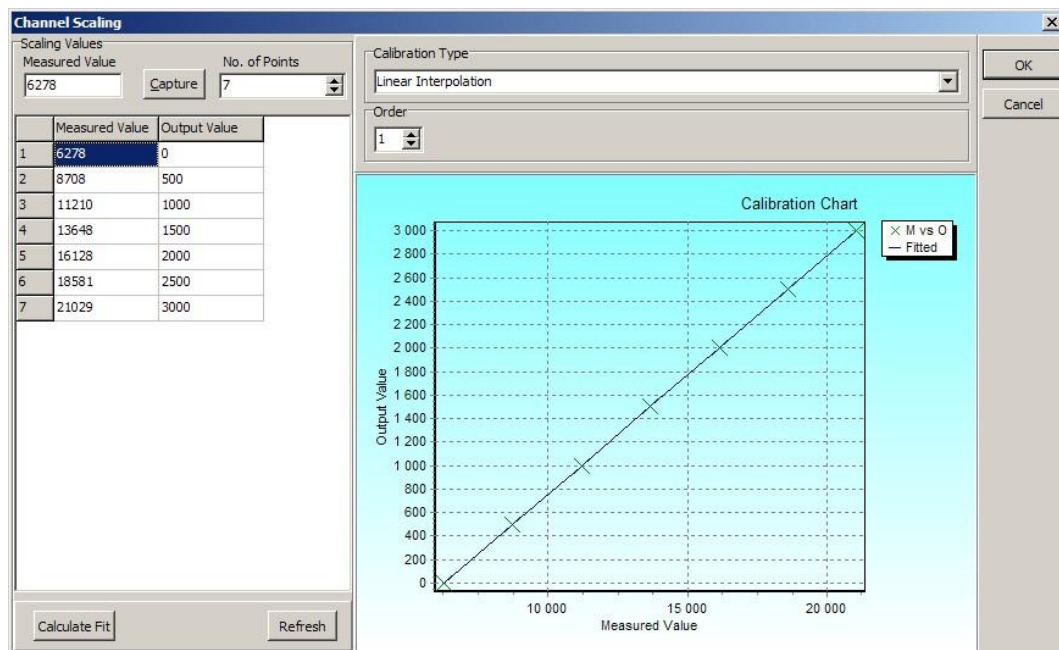


Figure D-4: Calibration of the air differential pressure transducer

D.3 Air inlet system

The air inlet system was designed for the calculation of the inlet air mass flow rate. It was designed by Prinsloo (2008) based on *British Standard BS 848 Part 1*:

Fans for general purposes (1988). The difficulty during the design was to find a balance between the size and the accuracy of the inlet system. The detailed dimensions can be found in the table and figure below.

Table D-1: The detailed dimensions of the conical inlet

Throat diameter [m]	0.11
Throat area [m ²]	0.0095
Mach number	0.1544
Mass flow rate [kg/s]	0.6
Flow velocity [m/s]	52.9
Static temperature [K]	293.16
Static pressure [Pa]	101325
Total pressure difference [Pa]	1 811.6 (< 4 000)
Reynolds number at throat	38 4819 (> 30 000)

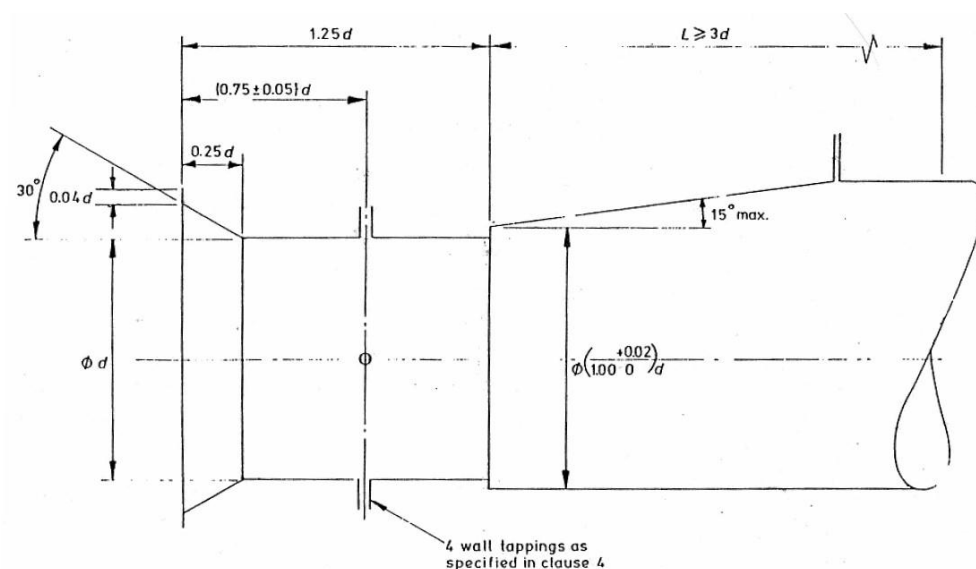


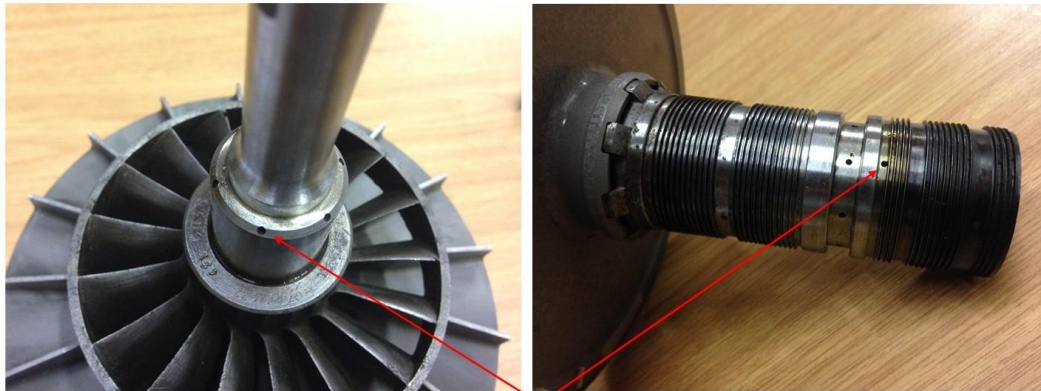
Figure D-5: Geometry of the conical inlet (BS 848, 1997)

The total pressure difference and the Reynolds number at the throat are all within the required limits. Therefore, the conical inlet system can be used for the air mass flow rate calculation and the accuracy can be guaranteed.

D.4 Lubrication system of the engine

The lubrication system plays an important role to maintain the engine in a healthy running condition. The system includes an oil pump, an oil filter, oil transfer tunnels and optional oil cooler.

There are several build-in tunnels to transfer the oil to lubricate different components. The tunnels lead to the oil spray holes, which are the exit of the pressurised oil. These holes must not be blocked at all times. During the engine overhaul, it was found that these holes could be blocked by metal debris easily. Therefore, the oil spray holes must be checked carefully during the overhaul. The figure below shows the oil spray holes on the engine main shaft.



Oil spray holes

Figure D-6: Oil spray holes on the engine main shaft

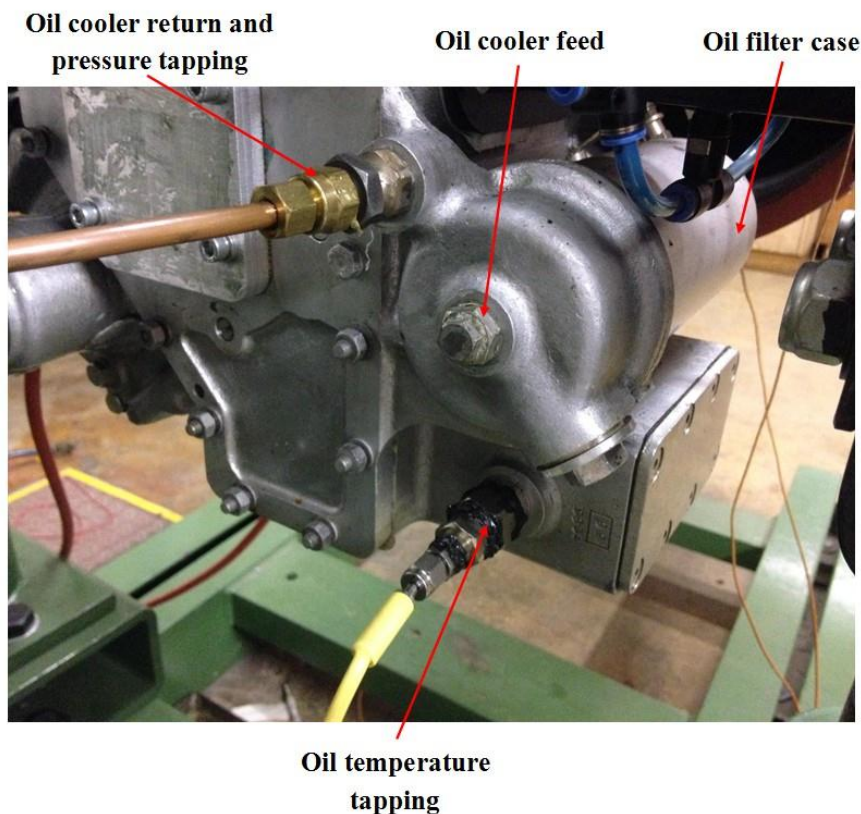


Figure D-7: Oil system connections

The length of the engine tests in this project are relatively short because there was no need to carry out the stress test and long-time continuous running test. Therefore, the oil cooler was not necessary since the test would be finished before the oil temperature reached the maximum limit of 110 °C. However, if the test continued, the oil temperature eventually would exceed the temperature limit. An external is then required if the tests with longer period are preferred. Figure D-7 illustrates the oil system connections. The photo was taken when no external oil cooler was used for the test and therefore, the oil cooler feed connector was blocked by a bolt.

D.5 Dynamometer

The details of the dynamometer behaviour will be discussed in this chapter. The dynamometer was used to apply load to the engine and measure the speed and torque. It is necessary to operate the dynamometer properly otherwise the engine could be damaged by improper operation. The dynamometer is able to be controlled in two modes: RPM (speed mode) and TRQ (torque mode). Due to the lack of throttle control on the Rover gas turbine, only RPM mode can be used. By setting a speed (lower than current shaft speed) on the control screen, the dynamometer applies load to the shaft to match this lower speed. The setting of the dynamometer control unit for engine testing is shown in Figure 4-3.

D.5.1 Dynamometer specifications

The table below shows the specifications of the Schenck W130 dynamometer used in this project.

Table D-2: Dynamometer specifications (SCHENCK Pegasus GmgbH, 1997)

Schenck W130 eddy current dynamometer	
Nominal torque	400 N
Maximum Speed	10 000 RPM
Nominal power	130 kW
Maximum coupling weight at maximum speed	2 kg
Mass of inertia	0.14 kg*m ²
Weight	270 kg
Torsion spring constant up to centre of dynamometer	0.0535 N*m/rad

D.5.2 Dynamometer cooling water temperature

The temperature of dynamometer cooling water is measured by two individual thermocouples located at two exit of cooling water. The eddy current type

dynamometer produces considerable heat when it is under load condition. Theoretically, the dynamometer will not generate heat when no load is applied. Figure D-8 shows the cooling water temperature along with time.

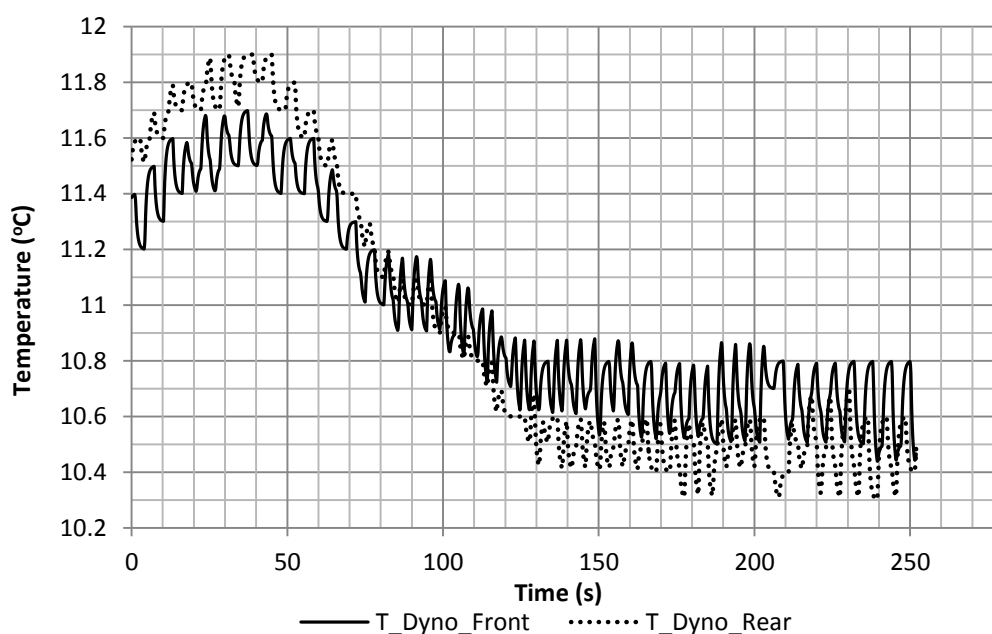


Figure D-8: Dynamometer cooling water temperature during the engine test

The values used in the figure above are original data without any post-processing. The fluctuation shows a constant cycle and within a small range of 0.2 °C. It is believed these fluctuations are caused by the deprecation of thermocouples. The water temperature becomes stable after 130 seconds. The final cooling water temperature is 10.6 °C, which is the temperature of supply water tank. During the entire test, the cooling water temperature was kept in a low range and was safe for the dynamometer operation. However, extra attention should be paid when applying load to the dynamometer.

D.5.3 Time lag for the dynamometer

When the value of driveshaft speed has changed in ETA, the dynamometer will not be responded immediately. It normally takes several seconds for the dynamometer to adjust its load. It is necessary to verify the exact response time for this particular setup so that control can be operated in advance to perform a desirable operation.

Figure D-9 and D-10 shows the speed setting in ETA and the real engine speed along with time.

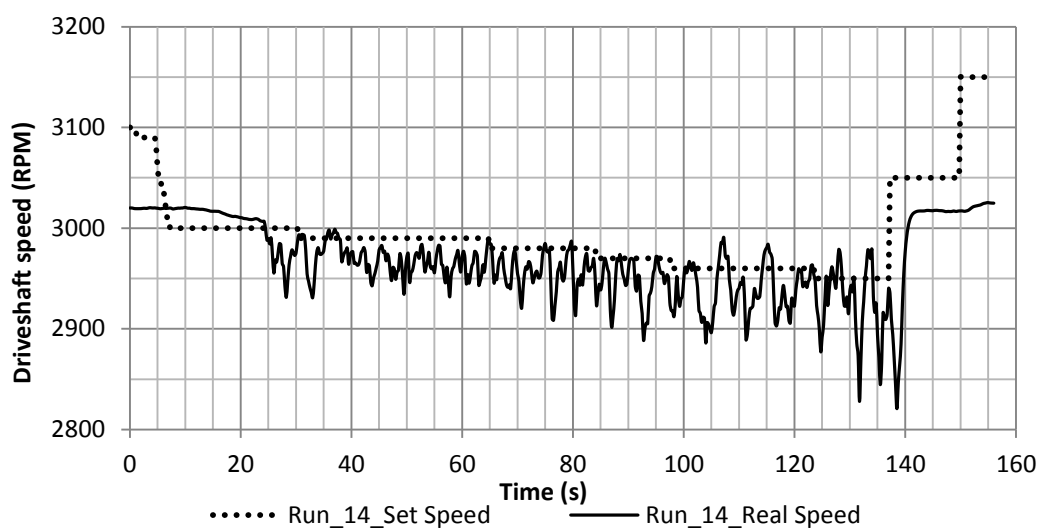


Figure D-9: Set and real driveshaft speed along with time in “Run_14”

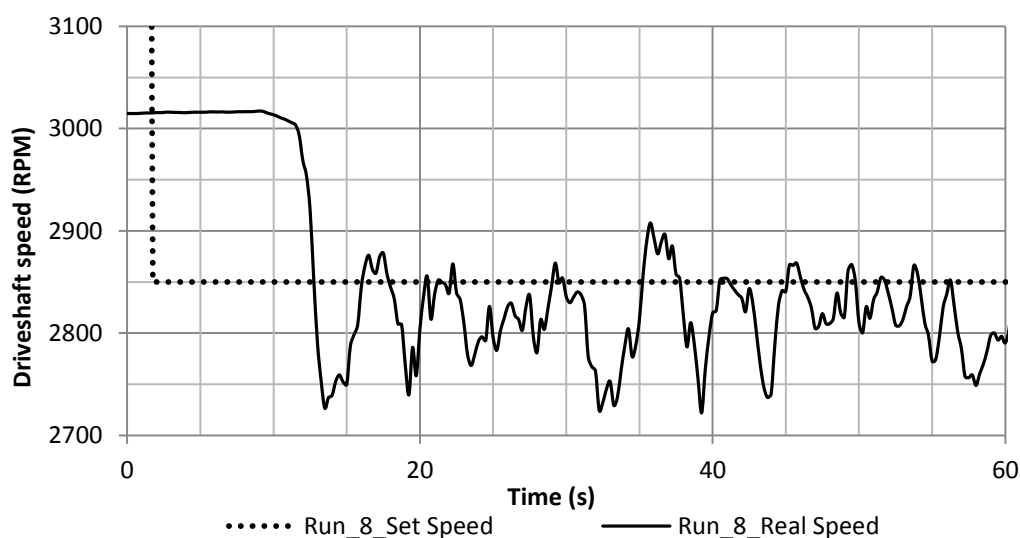


Figure D-10: Set and real driveshaft speed along with time in “Run_8”

The set speed indicates the value input for the dynamometer control. When the set speed is higher than real driveshaft speed, no load is applied to the dynamometer. When the set speed is lower than the real speed, the dynamometer control starts to apply load to slow down the engine and try to match the driveshaft speed to the input speed. The time lag is a period between two special points that one is when set speed is lower than real speed and another is dynamometer starting to apply load to the engine.

As shown in figures, the real driveshaft speed had considerable fluctuations when engine was under load. This was caused by the working principle of the dynamometer. The dynamometer constantly adjusts the load in very small scale to match the desired speed. It is a dynamic process so that the real speed has constant fluctuations.

In Figure D-9, the time that set speed was lower than real speed is at 6.75 second. At 15 second, the dynamometer started to apply load and only after 10 seconds, the real speed matches the set speed. Between 25 to 140 second, the dynamometer tried to adjust load to match the set speed. The set speed was set to a much higher value at 137 second and the load was removed at 138.5 second. These results demonstrated that the time lag for applying and removing load are different. The time lag for applying load was 8.25 seconds and removing only took 1.5 seconds in the test of “Run_14”.

For the test of “Run_8”, the time lag for applying load was 8 seconds. After speed was set in ETA, the dynamometer showed a good stability to keep the driveshaft speed as stable as possible. The most severe fluctuation happened during the test only had 127 RPM different in driveshaft speed.

From the results discussed above, the dynamometer time lag for applying load is approximately 8 seconds and the lag for removing load is approximate 1.5 seconds. When the load has been already applied to the engine, any further change in set speed will cause the dynamometer to adjust load immediately. Therefore, the operator should be prepared to set a desired speed 8 seconds in advance when firstly applying load to the engine.

D.6 Gas flowmeter

To measure the gas flow rate, a customised flowmeter was designed and manufactured. The detailed design and test results are discussed in the following contents.

The fuel injector requires the maximum pressure provided by the LPG supply system to perform well. Therefore, the venturi type flowmeter was decided to use for the mass flow calculation of the gaseous fuel because it has the minimum nonrecoverable head pressure loss. The construction of the venturi flowmeter is shown in Figure D-11.

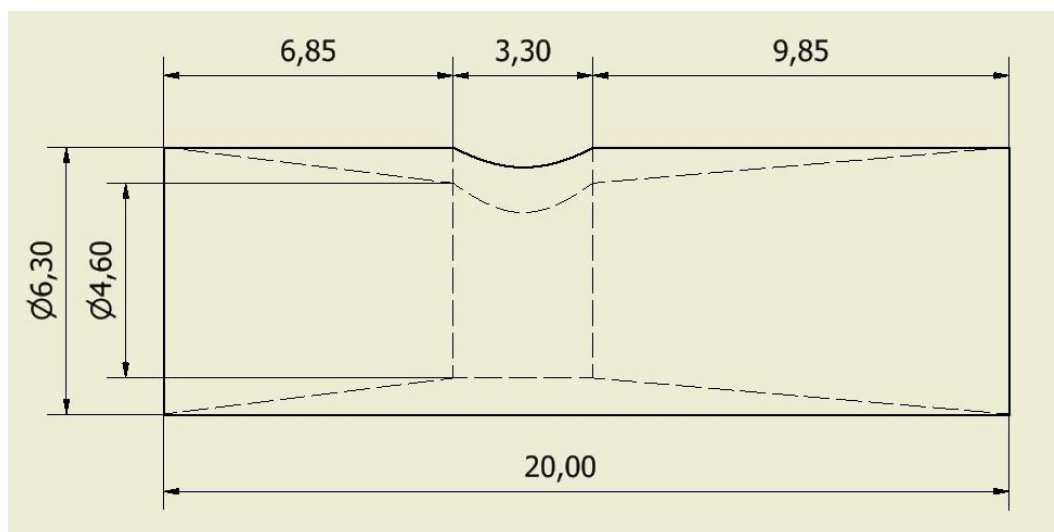


Figure D-11: Construction of the venturi flowmeter (unit in mm)

The venturi flowmeter was inserted into a T-piece as shown in Figure 4-10. A differential pressure transducer was used to measure the upstream and throat pressure. The gas volume flow rate then can be calculated by the equation below:

$$\dot{V} = A_0 C_d \sqrt{\frac{2(P_1 - P_2)}{\rho(1 - \beta^4)}} \quad (\text{D-1})$$

where

$$A_0 = \pi d^2 / 4$$

$$\beta = d / D$$

A_0 indicates the cross section area of the throat and β it is called the diameter ratio. C_d is called the discharge coefficient and it is determined experimentally. The precise value of discharge coefficient depends on the particular design and the Reynolds number. It is suggested to have an upstream Reynolds number between 10^4 and 10^7 .

A temporary test setup was built and used to determine the discharge coefficient of the flowmeter. Similar to the gas injector test, a calibrated WIKA flow sensor was used to measure the air flow. A water manometer was used to determine the differential pressure between the throat and upstream. The designed throat diameter was 4.6 mm, however, it was measured at 4.4 mm after manufactured. The test results are listed below.

Table D-3: Venturi flowmeter test results

Flowmeter reading [L/min]	Differential pressure [Pa]	Re_D	Calculated C_d
11.5	88.29	2.63E+03	0.900
20.5	245.25	4.69E+03	0.940
30.3	490.5	6.94E+03	0.904
40.2	696.51	9.21E+03	0.922
50.4	882.9	1.15E+04	0.946
60.5	1059.48	1.39E+04	0.951
70.8	1226.25	1.62E+04	0.954
80.5	1393.02	1.84E+04	0.954
90.3	1540.17	2.07E+04	0.969
100.6	1706.94	2.30E+04	0.967
110.2	1814.85	2.52E+04	0.987
120.5	2020.86	2.76E+04	0.974
130.1	2128.77	2.98E+04	0.986
140	2285.73	3.21E+04	0.987
150.1	2442.69	3.44E+04	0.985
161.3	2707.56	3.69E+04	0.970
170.1	2756.61	3.89E+04	0.988
177.8	2903.76	4.07E+04	0.983

As shown in the table above, the discharge coefficient was relatively stable when the upstream Reynolds number was more than 2.52E+04. Therefore, to obtain an accurate value of the gas flow rate, the upstream Reynolds number should be larger than 2.52E+04. For testing purpose, the discharge coefficient can set to 0.983.